



**Investigation of the auto-ubiquitination and ubiquitination potentials of
Retinoblastoma Binding Protein 6 and its binding to p53**

Taskeen Simons

Thesis submitted in fulfillment of the requirements for the degree of

Master of Science in Biotechnology

University of the Western Cape

Supervisor: Prof. David J. R. Pugh

December 2019



UNIVERSITY *of the*
WESTERN CAPE

ABSTRACT

Investigation of the auto-ubiquitination and ubiquitination potentials of Retinoblastoma Binding Protein 6 and its binding to p53

T. Simons, MSc Biotechnology Thesis, Department of Biotechnology, Faculty of Natural Sciences, University of the Western Cape.

Retinoblastoma Binding Protein 6 (RBBP6) is a 200 kDa human protein known to play an essential role in mRNA 3'-end processing, as well as functioning as an E3 ligase to catalyze ubiquitination and suppression of p53 and other cancer-associated proteins. A RBBP6 knock-out mouse model previously suggested that RBBP6 cooperates with MDM2 in poly-ubiquitinating p53, but is not able to ubiquitinate p53 without the assistance of MDM2. However, unpublished studies from our laboratory suggest that the N-terminal 335 residues of RBBP6, known as R3, are able to ubiquitinate p53 in full *in vitro* assays, and that the isolated RING finger of RBBP6 is able to catalyze ubiquitination of itself, a phenomenon known as auto-ubiquitination. It is, however, possible that other domains within RBBP6, in particular the ubiquitin-like DWNN domain situated near to the RING finger, may modulate the auto-ubiquitination and substrate-ubiquitination potentials of the complete protein. In addition, auto-ubiquitination is widely accepted as a useful proxy for substrate-ubiquitination, enabling the catalytic mechanism to be explored without the need for substrates such as p53, which is known to be unstable and difficult to work with in solution. For example, many E3 ubiquitin ligases form homo-dimers or hetero-dimers, and in some cases dimerization has been found to be essential for ubiquitination activity. Our laboratory has previously shown that the isolated RING finger domain is homodimeric in solution, and has identified single amino acid mutations that abolish the dimerization. Auto-ubiquitination may therefore provide a useful tool for investigating the importance of dimerization for ubiquitination activity.

The primary aim of this thesis was to compare the auto-ubiquitination potentials of the RING finger and larger fragments of RBBP6, in fully *in vitro* assays. The ability of poly-ubiquitin chains to catalyze degradation in the proteasome was investigated using human 26S proteasome, purified from mammalian cell lysates. The effect of homodimerisation on auto-

ubiquitination is investigated using wild type RING finger, which is partially homodimeric, as well as the N312D and K313E mutants known to abolish dimerization. Our results suggest that RBBP6 auto-ubiquitinates itself very efficiently, and that the DWNN domain has no effect on its auto-ubiquitination potential. Monomerizing the RING finger does not abolish its ability to auto-ubiquitinate itself, although it is possible that it reduces it, and may also reduce the efficiency with which the poly-ubiquitination catalyses degradation in the proteasome. Finally, a fully *in vitro* assay showed that the RING finger of RBBP6 is able to ubiquitinate p53 as efficiently as the RING finger of MDM2, and that there is evidence to suggest that the two RING fingers act cooperatively in ubiquitinating p53.

In a parallel investigation, the possibility of a direct interaction between R3 and p53 was investigated using Far Western blot and GST pull-down assays. Our data confirms that the R2 fragment of RBBP6, comprising the zinc knuckle domain and the RING finger, interacts robustly with residues 95–393 of p53, a region which includes the DNA Binding Domain. This represents a novel interaction between these two proteins, distinct from the previously-identified binding site for p53, which is located within the poorly-conserved C-terminal tail of RBBP6. As such, it lays the foundation for future studies aimed at determining the structure of the complex and identifying null mutants, which may aid in future investigation of the function of the protein *in vivo*.

Key words: RBBP6, p53, ubiquitination, proteasome, protein-protein interaction, immunoprecipitation, Western blot, site-directed mutagenesis, cancer

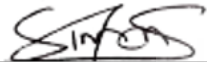
DECLARATION

I declare that “**Investigation of the auto-ubiquitination and ubiquitination potentials of Retinoblastoma Binding Protein 6 and its binding to p53**” is my own work that has not been submitted for any degree or examination in any other university, and that all the sources I have used or quoted have been indicated or acknowledged by complete references.

Taskeen Simons

Date: 20 December 2019

Signed:



UNIVERSITY *of the*
WESTERN CAPE

ACKNOWLEDGEMENTS

I would like to thank Prof David Pugh for affording me the opportunity to complete my MSc Research Project under his supervision. I would like to express my sincere gratitude for his invaluable support over the course of my research project.

I would like to thank Dr Andrew Faro, my co-supervisor, for always being there to point me in the right direction. Thank you for your advice, guidance and unwavering support. It did not go unnoticed. Thank you for the time and effort you put into assisting me whenever I need it. Most importantly, Thank you for all the moral support.

I would like to thank all my peers of the Cancer Structural Biology Research group and the Biotechnology Department at UWC for all the support, friendship and fellowship. Among them I would like to give special thanks to Mrs Tephney Mahomed, Mr Mhlahli Mlaza, Ms Zaida Parsons and Mrs Mishka Sedres for providing me with some of the most important resources needed to complete this project. Thank you for providing me with constructs, proteins, growing cells in tissue culture and, most importantly, for everything you taught me. Words cannot describe how grateful I am for your friendship, assistance and support. Thank you for the constant motivation when I thought that this process would never end.

Po-An, words cannot describe how grateful I am for all the support you have given me over the past few years. Thank you for providing me with some of the proteins needed to conduct my experiments. Thank you for helping me get this far. Without the constant pep talks I am almost certain I would have given up a long time ago, especially during the write-up process. Thank you for keeping me company during the countless hours spent in the lab whether it be during the week or on a weekend. Thank you for helping me whenever I need help. Thank you for all your help during the hardest and most trying time of my life, when I could barely walk let alone take a breath. If it wasn't for you pushing me around in a chair when it took me months to recover from pneumonia, I surely would never have completed my lab work. Most importantly, thank you for being the friend that you are.

My family, thank you for allowing me the opportunity to pursue my studies. While I know you did not always understand, you nevertheless supported me unconditionally. Thank you for making sure I never gave up. My parents, Mr and Mrs Simons, thank you for everything. I cannot quantify how grateful I am for everything. My husband, Nabeel Ariefdien, thank you

for your support and encouragement. Thank you for the countless nights that you sat up with me while I tried to complete my write-up. I know it wasn't always easy.

I would also like to praise the Almighty for without him, none of this would be possible. My countless prayers have been answered not only in my academic life but in my personal life as well.

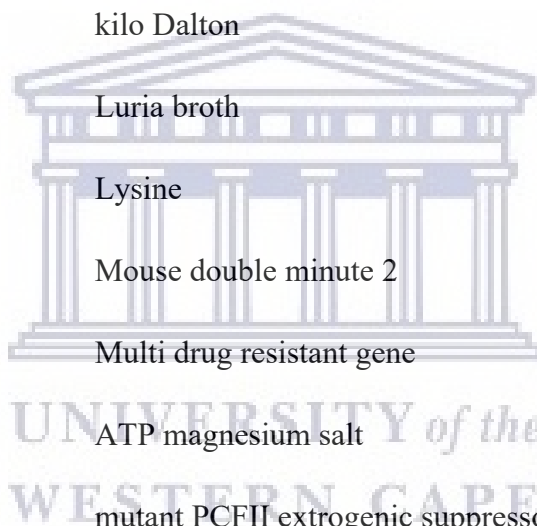
Finally, I would like to thank the National Research Foundation of South Africa for providing the necessary financial support to pursue my studies.



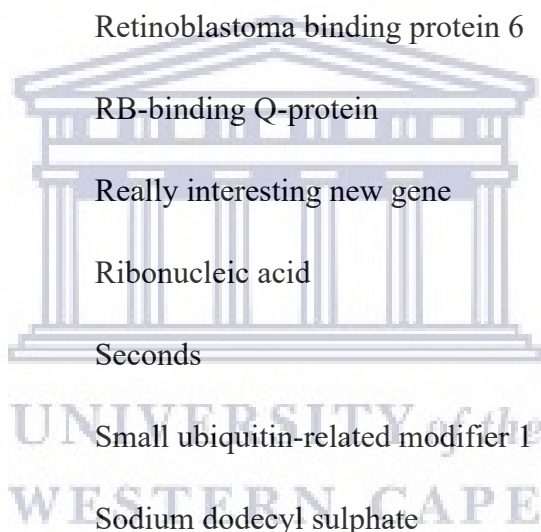
LIST OF ABBREVIATIONS

Amp	Ampicillin
APS	Ammonium persulphate
ATP	Adenosine tri-phosphate
Bp	Base pair
BSA	Bovine Serum Albumin
CFI	Cleavage factor 1
CFII	Cleavage stimulatory factor
CstF	Cleavage Stimulatory factor
C-terminus	Carboxyl Terminus
Cys	Cysteine
DNA	Deoxyribonucleic acid
dNTP	2'-deoxynucleoside 5'-triphosphate
DTT	1,4-dithio-DL-threitol
DWNN	Domain with no name
E1	Ubiquitin-activating enzyme
E2	Ubiquitin conjugating enzyme
E3	Ubiquitin ligase
EDTA	Ethylene diamine tetra acetic acid
FLAG	DYKDDDK immune tag
GST	Glutathione S-Transferase

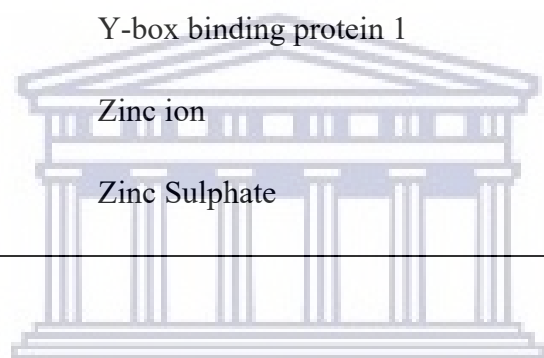
HECT	Homologous to E6-AP carboxyl terminus
HA	Hemagglutinin
HDM2	Human Double Minute 2
His or H	Histidine
Hsp70	Heat shock protein 70
IPTG	Isopropyl-1-thio-D-galactoside
Kan	Kanamycin
Kb	kilo base
kDa	kilo Dalton
LB	Luria broth
Lys or K	Lysine
MDM2	Mouse double minute 2
MDR1	Multi drug resistant gene
Mg-ATP	ATP magnesium salt
Mpe1	mutant PCFII extrogenic suppressor 1
mRNA	messenger RNA
MW	Molecular weight
NaN ₃	Sodium azide
NEDD8	Neural Precursor Cell-expressed Developmentally Down-regulated 8
Ng	Nanogram
N-terminus	Amino terminal
p53	protein 53 kDa



P2P-R	proliferation potential protein-related
PACT	p53-Associated Cellular Protein-Testes derived
PAGE	Polyacrylamide Gel Electrophoresis
PBS	Phosphate buffer saline
PCR	Polymerase chain reaction
PDB	Protein database
PVDF	Polyvinylidene difluoride
pRb	Retinoblastoma protein
RBBP6	Retinoblastoma binding protein 6
RBQ-1	RB-binding Q-protein
RING	Really interesting new gene
RNA	Ribonucleic acid
s	Seconds
SUMO-1	Small ubiquitin-related modifier 1
SDS	Sodium dodecyl sulphate
SR	Serine/Arginine
Tris	2-amino-2-hydroxymethylpropane-1, 3-diol
TEMED	<i>N, N, N', N'</i> -tetramethylethylenediamine
Ub	Ubiquitin
UBL	Ubiquitin-like
UBP	Ubiquitin-domain protein
Ubc	Ubiquitin conjugating enzymes



UBA	Ubiquitin associated domain
UBC	Ubiquitin-conjugating catalytic domain
UBL	Ubiquitin like protein
ULM	Ubiquitin like modifiers
UPP	Ubiquitin proteasome pathway
UV	Ultra Violet
μl	Microliter
Y2H	Yeast-2-Hybrid
YB-1	Y-box binding protein 1
Zn^{2+}	Zinc ion
ZnSO_4	Zinc Sulphate



UNIVERSITY *of the*
WESTERN CAPE

-

TABLE OF CONTENTS

ABSTRACT	i
DECLARATION.....	iii
ACKNOWLEDGEMENTS.....	iv
LIST OF ABBREVIATIONS.....	vi
LIST OF FIGURES	xiii
LIST OF TABLES	xv
CHAPTER 1: LITERATURE REVIEW	1
1.1 Introduction.....	1
1.2 Retinoblastoma Binding Protein 6 (RBBP6).....	4
1.3 Domain organisation of RBBP6.....	6
1.3.1 DWNN domain	6
1.3.2 Zinc finger domain.....	7
1.3.3 RING finger domain	7
1.4 The involvement of RBBP6 in cancer.....	8
1.5 The role of RBBP6 in mRNA processing.....	9
1.6 RBBP6 interaction partners.....	10
1.6.1 zBTB38.....	10
1.6.2 Y-Box Binding Protein 1 YB-1.....	10
1.6.3 Hsp70.....	11
1.6.4 pRb	11
1.6.5 p53	11
1.7 The Ubiquitin Proteasome Pathway	18
1.7.1 Ubiquitin activating Enzyme (E1).....	21
1.7.2 Ubiquitin conjugating Enzyme (E2).....	21
1.7.3 Ubiquitin Ligases (E3s)	22
1.8 Ubiquitin-like proteins	24
1.8.1 SUMO-1	25
1.8.2 NEDD8	25
1.8.3 DWNN.....	25
1.9 Aims and objectives of this thesis	27
CHAPTER 2: MATERIALS AND METHODS.....	29
2.1 Antibodies used.....	29

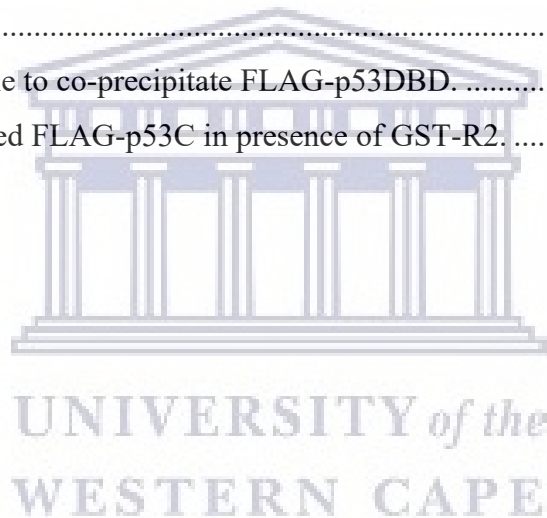
2.1.1	Primary Antibodies	29
2.1.2	Secondary Antibodies	29
2.2	Bacterial Culture	29
2.2.1	Preparation of competent E. coli cells for transformation	29
2.2.2	Bacterial transformations	30
2.3	Cloning.....	30
2.3.1	Specifications of cloning vector.....	30
2.3.2	PCR amplifications	33
2.3.4	Restriction digest and DNA ligation	35
2.3.5	Screening of putative clones	36
2.3.6	Agarose gel electrophoresis	36
2.3.7	Determination of DNA concentration	36
2.4	Expression and purification of recombinant proteins	37
2.4.1	Protein expression.....	37
2.4.2	Protein purification	37
2.5	Preparation of mammalian cell lysates.....	38
2.6	In vitro auto-ubiquitination and ubiquitination assays.....	39
2.7	GST pull-down assays.....	40
2.8	Purification of proteasome out of human cell lysates	41
2.9	Analysis of proteins using SDS-PAGE	41
2.10	Western blot analysis.....	42
2.11	Far Western Analysis	42
CHAPTER 3: Investigation of the auto-ubiquitination potential of fragments of Retinoblastoma Binding Protein 6		43
3.1	Introduction.....	43
3.2	Investigation of the auto-ubiquitination potentials of RBBP6 fragments <i>in vitro</i>	45
3.2.1	Recombinant expression of R3, RING and monomeric mutants RING _{K313E} and RING _{N312D}	45
3.2.2	Generation of the pGEX-R2-6His expression construct.....	52
3.2.3	Recombinant expression of pGEX-R2-6His	52
3.2.4	Bacterial expression and purification of associated ubiquitination enzymes.....	56
3.3	Investigation of the auto-ubiquitination potentials of fragments of RBBP6 and the RING monomeric mutants	56
3.3.1	Auto-ubiquitination of the isolated RING finger and monomerising mutants..	56

3.3.2	Auto-ubiquitination of the R3 fragment of RBBP6.....	63
3.3.3	Auto-ubiquitination of R2	66
3.4	Ubiquitination of p53QM by a combination of GST-RBBP6 RING and GST-MDM2 RING.....	69
CHAPTER 4: <i>In vitro</i> investigation of the interaction between p53 and the N-terminus of RBBP6.....		
		73
4.1	Introduction.....	73
4.2	Recombinant expression of FLAG-p53QM and Far Western analysis	73
4.3	Far Western analysis	74
4.4	GST pull-down assays.....	76
4.5	Cloning of p53N for interaction studies	78
4.5.1	Generation of an expression construct for FLAG-p53ΔN using deletion mutagenesis.....	81
4.5.2	Generation of an expression construct for FLAG-p53DBD and FLAG-p53C	87
4.6	GST-pull-down assays to localise interaction of N-terminus of RBBP6 within p53.....	93
Chapter 5: Conclusions and future outlook.....		
		96
5.1	RBBP6 auto-ubiquitinates itself efficiently in vitro	96
5.2	The RING finger of RBBP6 ubiquitinates p53	98
5.3	p53 interacts directly with the N-terminus of RBBP6	98
BIBLIOGRAPHY		
		101
APPENDICES.....		
		113

LIST OF FIGURES

Figure 1.1 Domain organization of full length human RBBP6.....	5
Figure 1.2: p53 regulates numerous downstream processes.....	12
Figure 1.3: Schematic representation of the domains of p53 protein.....	13
Figure 1.4: p53 and MDM2 negative feedback loop.....	15
Figure 1.5: An illustration of the ubiquitin-proteasome pathway..	19
Figure 1.6: An illustration of the functional process of ubiquitin on a substrate.	21
Figure 1.7: The structure of the DWNN domain is highly similar to that of ubiquitin.....	27
Figure 2.1: Restriction map of pGEX-6P-2 including the multiple cloning cassette	31
Figure 2.2: Restriction map of pET28b, including the multiple cloning cassette	32
Figure 2.3: Schematic diagram of the deletion mutagenesis protocol used.	35
Figure 3.1: Recombinant expression and purification of GST-RING.....	48
Figure 3.1: Recombinant expression and purification of GST-R3-6His.....	49
Figure 3.3: Recombinant expression and purification of GST-RING _{K313E}	50
Figure 3.4: Recombinant expression and purification of GST-RING _{N312D}	51
Figure 3.5: Cloning of pGEX-R2-6xHis..	54
Figure 3.6: Recombinant expression and purification of GST-R2-6His.	55
Figure 3.7: Auto-ubiquitination and proteasomal degradation of the isolated RING finger from RBBP6.	59
Figure 3.8: Auto-ubiquitination and proteasomal degradation of the RING _{K313E} monomeric mutant	61
Figure 3.9: Auto-ubiquitination and proteasomal degradation of the RING _{N312D} monomeric mutant.	62
Figure 3.10: Auto-ubiquitination and proteasomal degradation of the R3 fragment of RBBP.	64
Figure 3.11: Auto-ubiquitination and proteasomal degradation of the R2 fragment of RBBP.	68
Figure 3.12: In vitro p53 ubiquitination by a combination of GST-RBBP6 RING and GST-MDM2 RING.	71
Figure 4.1: Expression and purification of FLAG-p53QM using nickel ion affinity.....	74

Figure 4.2: Far Western analysis of FLAG-p53QM with N-terminal fragments of RBBP6. .	76
Figure 4.3: Co-precipitation of FLAG-p53QM with GST-R2.	77
Figure 4.4: Molecular cloning of pet28b-FLAG-p53N.	80
Figure 4.5: Co-precipitation of FLAG-p53N is not co-precipitated by GST-R2.	81
Figure 4.6: Schematic representation of the deletion mutagenesis strategy.	84
Figure 4.7: Deletion mutagenesis of pet28a-FLAG-p53ΔN.	85
Figure 4.8: Expression and purification of FLAG-p53ΔN using nickel ion affinity chromatography.	86
Figure 4.9: FLAG-p53ΔN is co-precipitated by GST-R2.	87
Figure 4.10: Generation of pET28a-FLAG-p53DBD.	89
Figure 4.11: Deletion mutagenesis of pet28-FLAG-p53C.	91
Figure 4.12: Expression and purification of FLAG-p53DBD and FLAG p53C using nickel ion affinity.	92
Figure 4.13: GST-R2 is able to co-precipitate FLAG-p53DBD.	94
Figure 4.14: Co-precipitated FLAG-p53C in presence of GST-R2.	95



LIST OF TABLES

Table 2.1: General setup for <i>in vitro</i> auto-ubiquitination assay	39
Table 2.2: General setup for <i>in vitro</i> p53 ubiquitination assay	40
Table 3.1: Oligonucleotide primers for amplification of R2-6His.	52
Table 4.1: Oligonucleotide primers for restriction endonuclease-mediated cloning of p53 constructs.....	79
Table 4.2: Sequence specific oligonucleotides for the generation of p53 deletion mutagenesis constructs.....	83



UNIVERSITY *of the*
WESTERN CAPE



UNIVERSITY *of the*
WESTERN CAPE

CHAPTER 1: LITERATURE REVIEW

1.1 Introduction

Retinoblastoma Binding Protein 6 (RBBP6) is a 200 kDa multi-domain nuclear protein, which has been implicated in mRNA processing, cell cycle control and apoptosis (Mbita *et al.*, 2012). RBBP6 is one of a small group of proteins reported to interact with both tumour suppressor proteins pRb and p53 (Simons *et al.*, 1997 and Witte & Scott., 1997).

RBBP6 contains a RING domain and has E3 ubiquitin ligase activity, and has been reported to promote the ubiquitination and degradation of p53 in conjunction with MDM2, in terms of which it can be characterised as an oncoprotein and a suppressor of p53 (Li *et al.*, 2007). More recently, strong evidence has been presented to show that RBBP6 plays an essential role in the molecular complex that determines the site of 3'-end polyadenylation of mRNA transcripts in both humans and yeast, through which it potentially promotes the expression of a large number of pro-cancerous genes (Di Giammartino *et al.*, 2014 and Lee & Moore., 2014).

A gene orthologous to human RBBP6 has been found in all eukaryotic genomes sequenced to date, but not in any prokaryotic genomes. In most cases it is present at single copy number. All eukaryotic genomes express at least one transcript including conserved regions corresponding to a DWNN domain at the N-terminus, followed by a zinc knuckle and a RING finger domain; in lower eukaryotes that accounts for the entire gene, whereas higher eukaryotes encode long, poorly-conserved, C-terminal extensions.

A range of different isoforms are produced by alternative splicing and possibly alternative promoters; in humans these include the full length 1792-amino acid protein, known as isoform 1, as well as the highly truncated isoform 3, which consists of the N-terminal 101-amino acids of isoform 1, comprising predominantly of the DWNN domain, followed by a 17-amino acid motif not found in any other isoform (Pugh *et al.*, 2006). The structure of the human DWNN domain has been determined in humans (Pugh *et al.*, 2006) and yeast (Hill *et al.*, 2019) and found to adopt an ubiquitin-like structure.

In addition to its ubiquitin-like structure, in higher eukaryotes the DWNN domain contains a conserved di-glycine motif at precisely the same position as that found in ubiquitin. In ubiquitin the di-glycine serves as the point of cleavage and conjugation to the substrate lysine, and its

presence in RBBP6 strongly suggests that the DWNN domain may become covalently attached to proteins in a manner similar to ubiquitination, a process which we refer to as “DWNNylation”. If so, then we may expect that if the di-glycine motif is not present, DWNNylation will not be able to happen. Preliminary data from our laboratory suggested that if a fragment of RBBP6 terminating immediately after the di-glycine motif, designated DWNN-GG, was added to mammalian cell lysate, and the lysate was subsequently probed by western blot with antibodies recognizing the DWNN domain, a ladder of bands was identified that was not present when the DWNN domain was omitted. An explanation of this results is that the DWNN domain is being covalently attached to high molecular weight proteins in the lysate. We aimed to test this result by repeating it with DWNN-GG with the addition of an N-terminal FLAG tag, FLAG-DWNN-GG, and with the addition of a construct terminating immediately before the di-glycine; since the DWNN domain terminates with the amino-acids -Proline-Isoleucine-Glycine-Glycine, or -PIGG in 1-letter notation, this construct was designated FLAG-DWNN-PI.

The presence of the RING finger domain, as well as the ubiquitin-like DWNN domain, suggests that RBBP6 may play a role in ubiquitination. This has been confirmed in the cases of Y-Box Binding Protein 1 (YB-1) (Chibi *et al.*, 2008) and zBTB38 (Miotto *et al.*, 2014). In 2007 a knock-out mouse study conducted by Li and co-workers indicated that RBBP6 enhances MDM2-mediated ubiquitination of p53, but does not itself have ubiquitination activity. This led them to propose that RBBP6 plays the role of a molecular scaffold, bringing MDM2 and p53 together on the p53-binding domain previously identified near the C-terminus of RBBP6 (Simons *et al.*, 1997 and Li *et al.*, 2007). The study concluded that RBBP6 functions by activating the ubiquitination activity of MDM2, rather than having ubiquitination activity of its own.

Ubiquitination involves the attachment of the 7 kDa ubiquitin protein to target proteins, through the formation of an iso-peptide bond between the backbone carboxyl group of ubiquitin and the ϵ -amino group of a lysine on the target protein. It serves numerous functions, the most well-established of which is to direct the target protein for degradation in the 26S proteasome (Hershko *et al.*, 1998). Ubiquitination involves the action of three different enzymes, namely an ubiquitin activating enzyme (E1), an ubiquitin conjugating enzyme (E2), and an ubiquitin ligating enzyme (E3). The primary role of the E3 is to recruit both the substrate protein, through its substrate binding domain, and the ubiquitin-conjugated E2, through a domain which binds specifically to E2 enzymes. In the majority of E3 enzymes the E2 binding role is played by a RING finger domain, such as that found in RBBP6.

Many RING fingers and RING finger-containing E3s form homo-dimers or hetero-dimers in solution, and in some cases dimerization has been shown to be essential for ubiquitination or auto-ubiquitination. A frequently-cited example is the RING finger of the breast cancer-associated BRCA1 protein, which is functional only when it is conjugated to the RING finger of BARD1 (Hashizume *et al.*, 2001 and Xia *et al.*, 2003). BARD1 has no ubiquitination activity of its own. Another example is MDMX, a RING-finger-containing protein very similar to MDM2. MDMX forms a hetero-dimer with MDM2 and enhances the ubiquitination potential of MDM2, but has no ubiquitination activity of its own. But unlike MDM2, MDMX does not form homo-dimers (Wade *et al.*, 2013).

Auto-ubiquitination is the process whereby an E3 protein catalyzes ubiquitination or poly-ubiquitination of itself. Most, if not all, proteins capable of catalyzing ubiquitination of other proteins are also capable of auto-ubiquitination. Auto-ubiquitination has been routinely used as an indicator of ubiquitination activity, especially in cases where substrate proteins are not known. Auto-ubiquitination serves as a means of self-suppression of the protein; MDM2, for example, keeps its levels low partially by auto-ubiquitination and subsequent proteasomal degradation (Stommel & Wahl., 2004). Parkin, an E3 ligase which plays a central role in Parkinson's Disease, has an N-terminal ubiquitin-like domain which has been shown to regulate its auto-ubiquitination activity by blocking access to the RING finger domain responsible for its auto-ubiquitination activity (Chaugule *et al.*, 2011).

The question therefore arises whether RBBP6 is able to auto-ubiquitinate itself. Since it has been reported to catalyze ubiquitination of YB-1 (Chibi *et al.*, 2008) and zBTB38 (Miotto *et al.*, 2014), both *in vitro* and *in vivo*, it seemed likely that RBBP6 should also be able to auto-ubiquitinate itself. Unpublished data generated in our laboratory suggested that the isolated RING finger domain of RBBP6 is able to auto-ubiquitinate itself (Matodzi Portia Maumela, MSc thesis, University of the Western Cape, 2016). It suggested, furthermore, that two mutant forms of the RING finger, which are monomeric in solution, auto-ubiquitinate themselves less efficiently than the wild type RING finger does.

The isolated RING finger used in the previous study is known to be partially monomeric and partially homo-dimeric; longer fragments of RBBP6, such as the R2 fragment, which contains the zinc knuckle domain in addition to the RING finger, or the R3 fragment, which contains the DWNN domain in addition to the zinc finger and the RING finger, appeared to form stronger homo-dimers than the isolated RING finger (Matodzi Portia Maumela, MSc thesis,

University of the Western Cape, 2016). If so, then our data leads to the expectation that the R2 fragment will be able to auto-ubiquitinate itself more efficiently than the isolated RING finger. And if, as in the case of Parkin, the ubiquitin-like DWNN domain interferes with the ubiquitination activity of the RING finger, then the auto-ubiquitination activity of the R3 fragment may differ from that of the R2 fragment.

1.2 Retinoblastoma Binding Protein 6 (RBBP6)

RBBP6 orthologues are found in all eukaryotic genomes, in many cases at single copy number, but neither in prokaryotes nor in archaea. The single human RBBP6 gene is located on chromosome 16; it gives rise to at least four major transcripts, by alternative splicing and alternative promoters. The four transcripts encode proteins of 1792, 1758, 118 and 952 amino acid residues respectively, called isoforms 1-4 (Genbank: NP_008841, Genbank: NP_061173, Genbank: NP_116015) (Pugh *et al.*, 2006 and Mbita *et al.*, 2012). Isoform 1, the full length protein, is encoded by 18 exons: isoform 2 is identical to isoform 1, with the omission of exon 17. Isoform 3 is encoded by exons 1-3 and is the result of transcription from an alternative promoter (Pugh *et al.*, 2006); it consists of the first 100 codons of isoform 1, followed by 18 amino acids not found in any other isoform. Being expressed from an alternative promoter, its expression has been reported to be regulated independently of isoform 1 (Mbita *et al.*, 2011).

The domain organisation of RBBP6 in eukaryotic organisms can be seen in Figure 1.1. At the N-terminus are found the DWNN domain (in yellow), which adopts an ubiquitin-like fold, followed by a zinc knuckle (in red) and the RING finger domain (in blue). These three domains are found in all lower eukaryotes, and are hypothesised to make up the core catalytic region of the protein (Di Giammartino *et al.*, 2014). Higher eukaryotes contain long C-terminal extensions which enable more complex functions, such as the SR domain, suspected to play a role in mRNA splicing, and the p53- and pRb-binding domains.

Isoform 3 is made up almost entirely of the DWNN domain (residues 1-80 of 118), followed by what appears to be an unstructured tail. Although the function of isoform 3 is not yet understood, a study conducted by Mbita and co-workers in 2011 showed that isoform 3 of RBBP6 is independently regulated from isoform 1 and is deregulated in a number of cancers, thereby potentially playing a role in cell cycle regulation (Mbita *et al.*, 2011). A study by Di Giammartino and co-workers reported in 2014 that the DWNN domain of isoform 3 regulated

mRNA processing splicing by competing with the DWNN domain of isoform 1 (Di Giammartino *et al.*, 2014). To date, no studies have been conducted specifically on isoforms 2 and 4 and therefore their functions within the cell remain unclear.

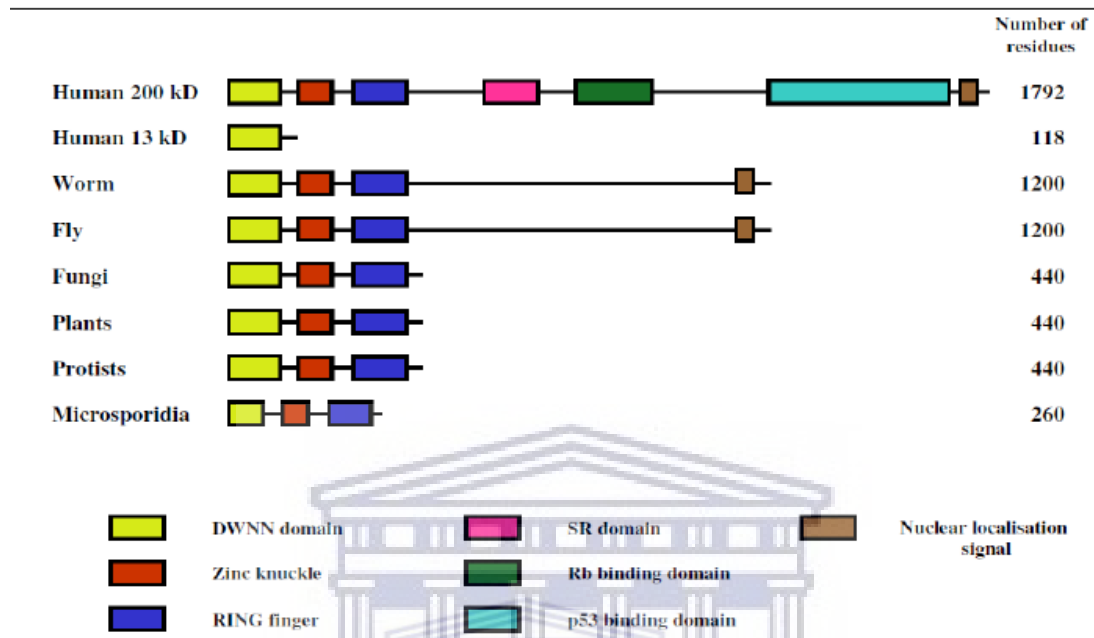


Figure 1.1 Domain organization of full length human RBBP6. All homologues of RBBP6 contain an N-terminal DWNN domain, zinc finger, SR domain, RING finger, Rb-binding domain and the p53 binding domain.

RBBP6 was originally cloned and characterized independently by three different groups. A study conducted by Sakai and co-workers (Sakai *et al.*, 1995) screened a human small cell lung carcinoma (H69c) library using pRb as a probe. The study identified a 140 kDa protein later found to correspond to residues 150-1146 of RBBP6, and designated “Rb Binding Protein Q-1” (RBQ-1), which was shown to selectively bind to hypo-phosphorylated Rb but not to hyper-phosphorylated pRb. This led the authors to propose that it functions oncogenically by repressing the tumour suppressive effects of hypo-phosphorylated pRb. The study also showed that the subsequent binding to Rb was inhibited by the E1A adenovirus protein, suggesting that RBQ-1 binds to the physiologically important pocket region of pRb (Sakai *et al.*, 1995)

A study conducted by Simons and co-workers (Simons *et al.*, 1997) used a similar approach, but with wild-type p53 as a probe on a murine testis expression library. They identified a cDNA which encodes a novel nuclear protein, designated “p53 associated cellular protein, testes-derived” (PACT), which was later found to correspond to residues 207-1792 of RBBP6. PACT was found to interact with wild-type p53 in addition to pRb; however, it was unable to bind to

transcriptionally inactive mutants such as R273H. Additionally, PACT was shown to localize to nuclear speckles (Simons *et al.*, 1997).

Proliferation Potential Protein-Related (P2P-R), a murine protein highly homologous to PACT, was identified by Witte and Scott (Witte and Scott, 1997) through the screening of a 3T3 cDNA λ gt11 expression library, using two monoclonal antibodies which specifically detect heterogeneous nuclear ribonucleoproteins (hnRNPs). The study identified a protein later found to correspond to residues 199-1972 of RBBP6. Expression of P2P-R is significantly reduced during terminal differentiation. Evidence was presented to show that the P2P-R cDNA product contains an Rb binding domain which binds to the pocket domain of Rb (Witte & Scott., 1997).

1.3 Domain organisation of RBBP6

1.3.1 DWNN domain

The DWNN domain is found exclusively in RBBP6 family proteins, many of which are annotated in the databases as “DWNN domain-containing proteins”. While there is little similarity between the two domains at sequence level, the DWNN domain is classed as an ubiquitin-like protein due to the similarity of its 3-dimensional structure to that of ubiquitin (Pugh *et al.*, 2006). The DWNN domain was initially identified through genetic screening aimed at targeting novel components of the antigen processing and presentation pathway via major histocompatibility class molecules (MHC class I) (Mbita *et al.*, 2012). In addition to forming part of the full length RBBP6 protein, also known as isoform 1, the DWNN domain also forms part of isoform 3, which is expressed in vertebrates as a single 13 kDa protein. The first 101 amino acids of isoform 3 are also found also in isoform 1, but they are followed by a 17-amino acid sequence, VCKNTISHFFYTLLLPL, found only in isoform 3 (Pugh *et al.*, 2006).

The presence of both the DWNN domain and the RING finger domain, combined with the fact that the DWNN domain is also independently expressed as a 13 kDa protein, raises the possibility that the DWNN domain may become covalently attached to other protein in a manner similar to that of ubiquitin. The presence of a conserved di-glycine (-GG) motif in the same position as found in ubiquitin-like modifiers, lends weight to that hypothesis.

1.3.2 Zinc finger domain

Zinc knuckles are small protein motifs which fold around a single zinc ion (Matthews *et al.*, 2002). Four conserved cysteine or histidine residues coordinate the zinc ion. In CCHC-type zinc finger domains, commonly referred to as the “zinc knuckles”, the zinc ion is coordinated by a cysteine, a cysteine, a histidine and a cysteine, in order along the amino acid sequence. They are found in abundance in higher eukaryotic organisms in proteins carrying out functions such as transcription, translation, DNA replication and repair as well as cellular proliferation and apoptosis (Sri Krishna *et al.*, 2003 and Vo *et al.*, 2001). Zinc knuckles have also been found in proteins involved in mRNA processing, as well as in viral proteins (Bae *et al.*, 2003). Zinc fingers are known to bind to both DNA and RNA, as well as being involved in protein-protein interactions (Matthews *et al.*, 2000). A study conducted by Cordier and co-workers in 2009 reported that zinc fingers have the ability to bind ubiquitin (Cordier *et al.*, 2009).

1.3.3 RING finger domain

The RING finger domain is the third conserved domain in RBBP6. RING fingers are a characteristic feature of E3 ubiquitin ligases, where they serve as binding sites for the Ub-conjugated E2 (Deshaies & Joazeiro., 2009). A RING finger is a cysteine rich domain in which 8 cysteine or histidine residues coordinate two zinc ions in a cross-braced arrangement, in which the first and third Cys/His pairs coordinate the first zinc ion and the second and fourth pairs coordinate the second zinc ion (Hanzawa *et al.*, 2001 and Capili *et al.*, 2004). The secondary structure of the RING finger domain is comprised of a single three stranded anti-parallel β -sheet and an α -helix, which are connected by loops (Kellenberger *et al.*, 2005). The ability of the RING finger domain to fold independently is as a result of the ability to coordinate the two zinc ions which stabilizes the structure of the RING finger domain (Pickart., 2001).

The RING finger of RBBP6 can also be classified as a U-box domain protein, on the basis of a conserved pattern of the hydrophobic residues (Chibi *et al.*, 2008; Aravind *et al.*, 2000). U-box domains adopt the same fold as RING fingers, but, unlike RING fingers, do not require zinc ions to stabilise them, relying instead on hydrogen bonds and hydrophobic contacts. The fact that the RBBP6 RING finger is so similar to a U-box is intriguing, but whether it has any biological significance is still open to investigation.

In *Drosophila melanogaster* (fruit fly) the above three structured domains—namely the zinc, RING finger domains and DWNN domain—have been named the “DWNN catalytic module”

(DCM) (Antunes *et al.*, 2008), on the assumption that it contains the core ubiquitination activity of the full RBBP6 protein. In humans, the same fragment is known as R3 (in this work), or as RBBP6-N (Di Giammartino *et al.*, 2014). *In vitro*, bacterially-expressed human R3 has been shown to mediate ubiquitin ligase activity of Y-Box Binding Protein-1 (YB-1) and of zBTB38 (Chibi *et al.*, 2008; Miotto *et al.*, 2014).

1.4 The involvement of RBBP6 in cancer

Numerous studies have established that RBBP6 is up-regulated in a range of different cancers. A study conducted in 2013 by Chen and co-workers found a correlation between overexpressed RBBP6 and mutant p53 in colon cancer (Chen *et al.*, 2013). The study showed that patients who had tumours with an accumulation of mutant p53 and RBBP6 had a poor survival rate. (Chen *et al.*, 2013). This study revealed that RBBP6, as well as p53, could be useful predictors of prognosis in cancer (Chen *et al.*, 2013).

A study conducted in 2011 by Motadi and co-workers reported that RBBP6 suppresses apoptosis and up-regulates cellular proliferation in lung cancer (Motadi *et al.*, 2011). Yoshitake and co-workers found that correlated with tumour progression in oesophageal and cervical cancer. They established that RBBP6 is not over-expressed in normal oesophageal epithelial cells, however, only in oesophageal cancer cells. The study concluded that RBBP6 may therefore be a model immunotherapy target for patients with oesophageal cancer (Yoshitake *et al.*, 2004).

RBBP6 is also over-expressed in gastric cancer. Morisaki and co-workers used a proteomics-based approach (mass spectrometry) in an attempt to identify novel biomarkers for use in the diagnoses of gastric cancers. After analysis of 300 different gastric cancers RBBP6, along with eight other proteins, was found to be overexpressed compared to the parent cells. Of these, RBBP6 was considered to have the greatest promise as a potential biomarker and a therapeutic target for gastric cancer (Morisaki *et al.*, 2014).

Recently, RBBP6 was found to play a role not only cancer but in diabetes and Ebola as well. A study conducted in 2012 by Zhao and co-workers showed that RBBP6 possibly plays a role in the survival of the beta cells in diabetes. The paper describes which genes are activated or turned off once the beta cells are exposed to GLP-1, a human hormone which promotes the growth and survival of insulin-producing beta cells. The study found that of the genes present

on the microarray chips, the top 5 include RBBP6, which is upregulated by 3.1 fold. Although RBBP6 was not screened by real time PCR, 5 of the genes were and the values obtained were consistent with those of the microarray data. On the assumption that RBBP6 acts in an anti-apoptotic manner by suppression p53, the upregulation of RBBP6 was taken as evidence of the anti-apoptotic activity of GLP-1 (Zhao *et al.*, 2012).

A study conducted in 2018 by Batra and co-workers showed a possible role of RBBP6 in the Ebola Virus (EBOV). The study used affinity tag-purification mass spectrometry (AP-MS) to generate an EBOV-host protein-protein interaction map. The study found 194 high confidence interactions between Ebola proteins and human proteins, including between the Ebola viral transcription regulator, VP30, and RBBP6. A crystal structure and computational analysis of the VP30-RBBP6 protein complex showed that RBBP6 mimics the binding of the viral nucleoprotein (NP) binding to the same interface on VP30. The study showed that exogenous expression of RBBP6 inhibits Ebola replication (Batra *et al.*, 2018).

1.5 **The role of RBBP6 in mRNA processing**

Mutant PCFII Extrogenic suppressor 1, also known as Mpe1, is the *Saccharomyces cerevisiae* (yeast) orthologue of human RBBP6. Mpe1 is a 440 amino acid protein which, like RBBP6, contains the DWNN domain, zinc domain as well as the RING finger domain (Vo *et al.*, 2001). A study conducted in 2001 by Vo and co-workers reported that Mpe1 is crucial for mRNA processing. The study also established that Mpe1 is a critical component of the cleavage and polyadenylation factor complex (CPF) (Vo *et al.*, 2001). Vo and co-workers concluded that Mpe1 is vital for specific cleavage and poly-adenylation of pre-mRNA, by promoting the formation of a complex of CF1 with the cleavage and polyadenylation complex.

3'-end cleavage and polyadenylation are vital steps in the synthesis of functional mRNA. The core 3'-end processing machinery is a complex comprising 4 subunits, namely cleavage and polyadenylation specificity factor (CPSF), cleavage stimulatory factor (CstF), cleavage factor I (CFI) and cleavage factor II (CFII). RBBP6 forms part of the cleavage and polyadenylation factor complex in yeast as well as the pre-mRNA 3'-end processing complex in humans (Vo *et al.*, 2001 and Shi *et al.*, 2009). A study in 2014 by Di Giammartino and co-workers established the involvement of RBBP6 in the regulation of the human polyadenylation machinery. The study also showed that isoform 3 of RBBP6, which contains only the DWNN domain,

negatively regulates 3'-end processing by competing with the DWNN domain of full length RBBP6 for binding to CstF, thereby establishing isoforms 1 and 3 as regulators of 3'-end processing (Di Giammartino *et al.*, 2014).

1.6 RBBP6 interaction partners

1.6.1 zBTB38

RBBP6 has been reported to play a role in the regulation of transcriptional repressor zBTB38 and the subsequent prevention of DNA damage (Miotto *et al.*, 2014). RBBP6 ubiquitinates and destabilizes ZBTB38, whereas ZBTB38 negatively regulates transcription and the levels of MCM10 replication protein on chromatin (Miotto *et al.*, 2014). A study conducted by Miotto and co-workers in 2014 reported that cells which lack RBBP6 experience reduced replication fork progression, as well as an increase in damage at common fragile sites as a result of the accumulation of ZBTB38 and the downregulation of MCM10 (Miotto *et al.*, 2014). RBBP6 regulates genomic replication and CFS stability by downregulating ZBTB38. In the absence of RBBP6, DNA replication slows down and the CFS become lost from the genome due to ZBTB38 accumulation, which subsequently leads to the downregulation of MCM10. MCM10 is a replication factor that is a direct target of transcriptional repression by ZBTB38. Its downregulation is responsible for the replication abnormalities, which occur in the absence of RBBP6 (Miotto *et al.*, 2014).

1.6.2 Y-Box Binding Protein 1 (YB-1)

YB-1, also known as DNA binding Protein B (dbpB), is a multifunctional protein involved in mRNA metabolism as well as transactivation of the expression of a number of pro-survival genes, which include c-Myc, cyclin A and MDR1 (Davies *et al.*, 2011). YB-1 belongs to the cold shock domain superfamily due to the presence of the highly conserved cold shock domain (Horn *et al.*, 2007). YB-1 is regulated by ubiquitin-mediated proteasomal degradation, catalysed by RBBP6 and F-box protein 33, which are E3 ligases (Chibi *et al.*, 2008 and Lutz *et al.*, 2006).

Expression of YB-1 in the nucleus is correlated with tumorigenesis and poor prognosis in clinical cancer. YB-1 upregulates expression of the multi-drug resistance gene (MDR1). The gene for MDR1 is overexpressed in numerous cancer cells and confers resistance to

chemotherapeutic agents during treatment (Davies *et al.*, 2011). Chemotherapeutic agents such as Cisplatin causes YB-1 to induce the expression of MDR1 by means of an increased binding to a Y-box element within the promoter of MDR1 (Asakuno *et al.*, 1994 and Ohga *et al.*, 1998).

1.6.3 Hsp70

Heat shock proteins 70 are essential in numerous protein folding processes. The activity of Hsp appears to be dependent on the ability of Hsp to interact with the hydrophobic parts of proteins in an ATP-dependent manner. A number of U-box proteins are known to interact with chaperones or co-chaperones. The most noticeable being the C-terminus of Hsp70 interacting protein which interacts with Hsp70 as well as Hsp90 respectively, by means of its tetra peptide domain in order to ubiquitinate unfolded proteins represented by Hsp70. RBBP6 has been reported to interact with Hsp70 thereby implicating it in protein quality control (Kappo *et al.*, 2012).

1.6.4 pRb

pRb is a tumour suppressor protein, encoded for by the Rb tumour suppressor gene. The Rb gene encodes a nuclear-phosphoprotein of 105kDa. The Rb gene has been found to be defective in the pathogenesis of retinoblastomas. pRb undergoes phosphorylation as it advances through the cell cycle.

A vital function of pRb is the regulation of the G1 to S phase transition within the cell cycle. pRb also prevents the premature G1/S phase transition through its interaction with transcription factor E2F. E2F is essential for the activation of the S phase genes. Phosphorylation of pRb is highly regulated by the action of cyclin dependent kinases (CDK's) (Adams *et al.*, 2001). pRb has to be phosphorylated by the G1/S phase CDK complexes in order for the cell cycle to advance normally. The C-terminal domain of pRb is necessary for the recruitment of the CDK's (Adams *et al.*, 2001).

1.6.5 p53

p53 has been dubbed “Guardian of the genome” (Efeyan & Serrano, 2007) due to its key role in coordinating the response of the cell to genotoxic stress as can be seen in Figure 1.2 below. p53 is a tumour suppressor protein, which functions primarily as a transcription factor for a number of genes which are vital for apoptosis, senescence and cell cycle arrest.

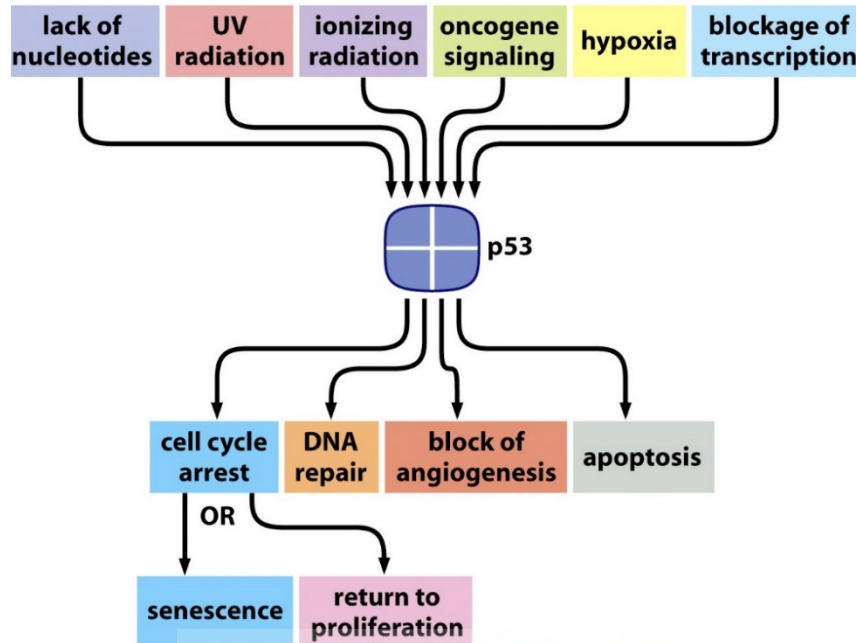


Figure 1.2: p53 regulates numerous downstream processes. p53 is activated in response to various stress signals. The activated p53 increases the transcription of the target genes which carry out the p53 effector functions. (Adapted from Weinberg, R. 2007).

The gene coding for p53 is found on the short arm of chromosome 17 and encodes a protein of 393 residues. Despite its name, the molecular weight of p53 is 43 kDa rather than 53 kDa, but it is so named because it migrates at an effective molecular weight of 53 kDa on SDS-PAGE gels. p53 forms a homo-tetramer in solution, mediated by a tetramerization domain, which is alternatively referred to as the oligomerization domain in Figure 1.3. Each subunit contains an N-terminal transactivation domain, a DNA binding (core domain), a tetramerization domain as well as a C-terminal regulatory domain (Ho *et al.*, 2006). The proline-rich domain found near the N-terminus of p53 contributes to the pro-apoptotic functions of p53 (Weinberg, R., 2007) and the C-terminal regulatory domain is post-translationally modified by phosphorylation, acetylation, sumoylation and ubiquitination (Bai & Zhu, 2006 and Rodriguez *et al.*, 2000). The MDM2-mediated ubiquitination of the C-terminus of p53 is the primary mechanism for the down-regulation and subsequent degradation of p53 by the 26S proteasome (Brooks *et al.*, 2006). The N-terminal transactivation domain is the site of post-translational modification by numerous proteins and transcription factors. The DNA binding core domain of p53 has an affinity for binding a sequence motif composed of the sequence Pu-Pu-Pu-C-A/t-T/a-G-Py-Py-Py repeated twice in tandem, where Pu indicates the purine nucleotides A or G and Py indicates the pyrimidine nucleotides C or T; A/T represents a site at which A occurs more often than T;

and T/a represents a site at which T occurs more often than A, which is present within the promoters of target genes whose expression is induced by p53 (Weinberg, R., 2007).



Figure 1.3: Schematic representation of the domains of p53 protein. Human p53 is a 393-residue protein that can be roughly divided into an N-terminal region (residues 1-94), a DNA Binding Domain (residues 95-292) and a C-terminal region (residues 293-393)". (Adapted from Kumari *et al.*, 2014)"

p53 was originally identified in a study conducted by Chang and co-worker (1979), in which they observed that antibodies against the large T antigen from animals bearing tumours produced by SV40 transformed cells co-precipitated a protein with apparent molecular weight 53 kDa. They subsequently showed that p53 acts cooperatively with the Ras oncogene to transform cells in culture, which led them to classify p53 as an oncogene. However, it was subsequently revealed that the p53 used in this study, which had been isolated from a mouse tumour, carried a transforming mutation. When replaced with wild type, p53 was found to act antagonistically towards large T antigen (Chang *et al.*, 1979).

An independent study conducted by De Leo and co-workers in 1979, also identified p53 by its high levels of expression in chemically induced tumours (DeLeo *et al.*, 1979).

1.6.5.1 Mutations affecting p53

p53 is one of the most frequently mutated genes in human cancer and is found to be either mutated, deleted or mis-regulated in the vast majority of cancer cases. More than 90% of all p53 mutations found in clinic occur within the DNA binding domain of p53 and reduce the transcriptional activity of p53 (Weinberg, R., 2007 and Brown *et al.*, 2009).

Cancer-associated mutations of p53 can be divided into two groups, DNA contact mutations and conformational mutations (structural contact mutations). Conformational mutations affect the amino acids which are required in order to maintain the structure and stability of p53 and typically exerts a dominant negative effect (Brown *et al.*, 2009; Weinberg, R., 2007; Liu *et al.*, 2010). Conformational mutations are found in the H1 helix and the L3 loop. DNA contact mutations are found near the protein-DNA interface and interfere directly with the binding of p53 to DNA. Cho and co-workers identified 6 'hotspot' mutations—Arg-248, Arg-273, Arg-

175, Arg-282, Arg-249 and Gly-245—which are all involved in the p53-DNA binding interface (Yunje *et al.*, 1994). Arg-175, Arg-282, Arg-249 and Gly-245 are involved in stabilising the structure of the DNA binding surface of p53. Arg248 makes contact at the minor groove while Arg 273 contacts a phosphate on the backbone of DNA (Yunje *et al.*, 1994).

The DNA binding domain of p53 is only marginally stable under normal physiological conditions. A study conducted by Nikolova and co-workers in 1998 compared the amino acid sequences of p53 homologues from 23 species in order to increase the stability of p53 for use in gene therapy (Nikolova *et al.*, 1998). They used four separate mutations, namely M133L, V203A, N239Y and N268D and were able to increase the stability of human p53 at 25 °C from 7.5-8.5 kcal/mol to 11.3 kcal/mol. These mutations were made within the DNA binding domain of p53 without affecting the ability of the p53-DNA binding domain to bind DNA (Nikolova *et al.*, 1998). In 2004 the crystal structure of the “quadruple mutant p53” was determined, which established that the structure of the mutated p53 was unchanged from that of wild-type p53 (Joergher *et al.*, 2004).

Additionally, mutations within the N-terminal domain of p53 affect the stability of p53 by means of modulating the effects of post-translational modifications such as ubiquitination and phosphorylation. Furthermore, zinc has also been shown to be essential in the proper folding of the DNA binding domain of p53 and resultantly mutations which affect the zinc binding domain are frequently encountered in human cancers (Hoe *et al.*, 2014).

1.6.5.2 Regulation of p53

p53 is a tumour suppressor protein which prevents the outgrowth of abnormal cells by inducing processes such as cell cycle arrest, DNA repair or apoptosis. p53 ensures the integrity of the genome by protecting it from the adverse effects of DNA damage.

The regulation of p53 is a vital process involving numerous post-translation modifications including ubiquitination, phosphorylation, acetylation and methylation. In healthy cells, p53 is barely detectable, contrastingly in abnormal or stressed cells, an accumulation of p53 is detected. MDM2, an E3 ubiquitin ligase, highly regulates the levels of p53 by means of MDM2-mediated ubiquitination and the subsequent degradation by the 26S proteasome. Contrastingly, the phosphorylation of the N-terminal transactivation domain of p53 by Chk2 leads to the protection of p53 from MDM2-mediated ubiquitination (Hock & Vousden., 2014 and Pant & Loranzo., 2014).

MDM2 regulates the function of p53 in 3 different ways: 1) by blocking its transactivation activity, 2) by catalysing the degradation of p53 by the 26S proteasome and 3) by transporting p53 out of the nucleus.

MDM2 blocks the transactivation activity of p53 by binding to a hydrophobic cleft in the N-terminal transactivation domain of p53, thereby concealing a p53 α -helix in the hydrophobic cleft of MDM2 and thereby preventing the N-terminal transactivation domain from interacting with the transcription machinery (Harms & Chen., 2006). Furthermore, MDM2 acts as an E3 ubiquitin ligase, catalysing the ubiquitination of p53 and leading to degradation of p53 in the 26S proteasome (Haupt *et al.*, 1997; Li *et al.* 2007). Additionally, MDM2 contains a nuclear export signal which allows for p53 to be directly co-transported into the cytoplasm.

MDM2 therefore creates a negative feedback loop whereby the cellular levels of p53, as well as of MDM2, are kept low (Li *et al.* 2003 and Hunziker *et al.* 2010) as depicted in Figure 1.4 below.

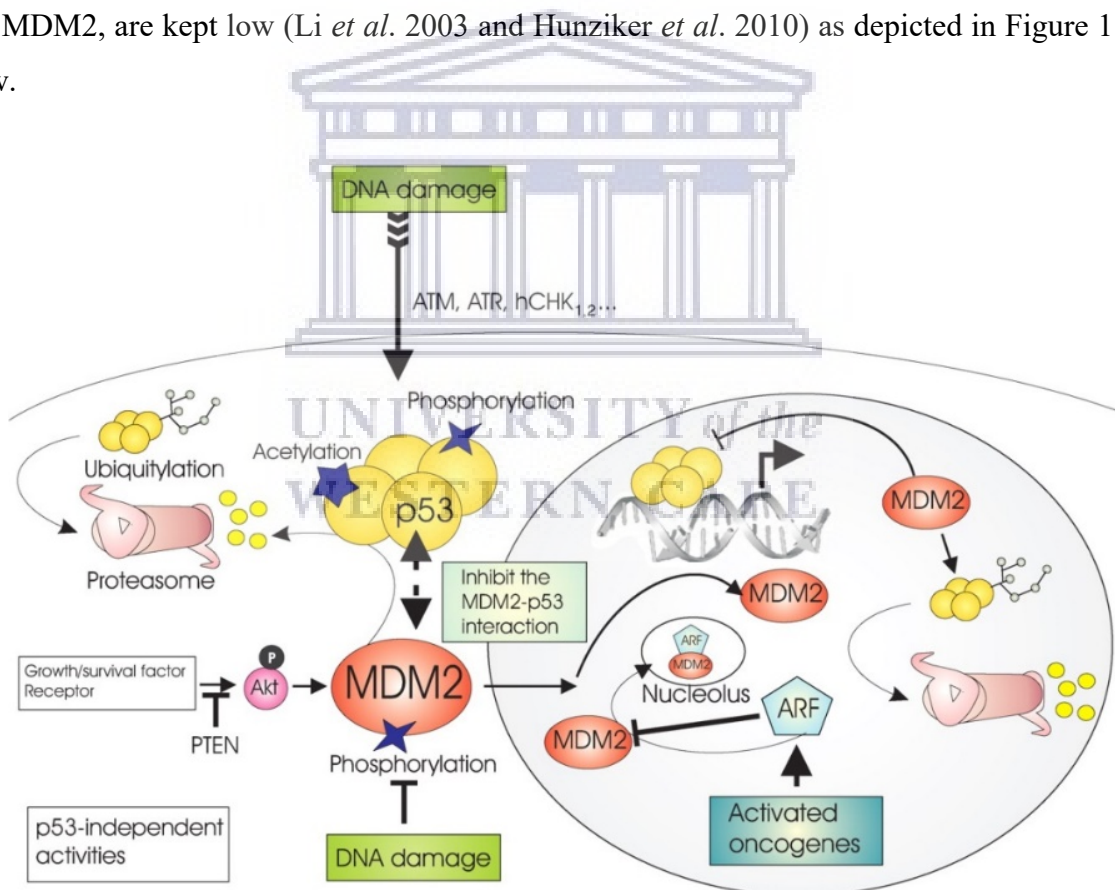


Figure 1.4: p53 and MDM2 negative feedback loop. MDM2 itself is a target of p53's transcriptional activity. Hence, MDM2 is highly expressed when p53 is highly expressed. p53 participates in a negative feedback loop with MDM2 thereby driving its own degradation. Adapted from (Moll *et al.*, 2003)

In contrast, human cancer cells carry mutant p53 alleles often express an excess of p53, compared to barely detectable levels in normal cells. A majority of mutations that affect p53 results in p53 losing its function as a transcription factor. Consequently, p53 is unable to induce the expression of MDM2 and thereby escapes proteasomal degradation and accumulates to high levels. Hence, numerous human cancer cells often contain high levels of inert p53 (Weinberg, R., 2007).

MDM2-mediated ubiquitination of p53 can be reversed by the de-ubiquitinating enzyme herpesvirus-associated ubiquitin-specific protease (HAUSP), which prevents p53 from degradation by the proteasome (Brooks *et al.*, 2006). MDM2 can catalyse its own ubiquitination and degradation (Michael *et al.*, 2003).

Additional proteins which regulate the function of p53 have been identified, including MDMX, p19^{ARF}, cop1 and pirh2, cyclin G, CIP1, BAX. MDMX forms a hetero-dimer with MDM2 as it has no ubiquitin ligase activity and therefore works cooperatively with MDM2 to enhance p53 ubiquitination. On the other hand, ARF inhibits the ability of MDM2 to ubiquitinate p53 (Stommel *et al.*, 2005).

In 2007, a study conducted by Li and co-workers reported that PACT, the murine orthologue of human RBBP6, plays a role in embryonic growth and development in mice. The study showed that following knockout of PACT, heterozygous knockout (PACT^{+/-}) mice were found to be fertile, but PACT^{-/-} embryos died after 7.5 days and the embryos were small and developmentally retarded. As a consequence of the high levels of p53 and apoptotic cells within the mice, Li and co-workers suspected that p53 played a role in the lethal genotype. When Li and co-workers performed the same PACT knockout in p53^{-/-} mice, the p53^{-/-}PACT^{-/-} mice survived longer (up to embryonic day 11.5), although they were smaller in comparison to the wild-type mice. This led to the conclusion that PACT plays a role in the suppression of p53 during embryonic development.

The over-expression of exogenous PACT in mammalian cells resulted in an increase in the levels of MDM2-mediated ubiquitination of p53 and a subsequent decrease in the transcriptional activity of p53. The study went on to show that the overexpression of PACT alone did not result in a decrease in the levels of p53, whereas when both PACT and MDM2 were simultaneously over-expressed it led to a decrease in the levels of p53. The degradation of p53 was abolished when PACT was over-expressed in the absence of the RING finger even when MDM2 and PACT were simultaneously over-expressed. Based on these findings they

concluded that PACT facilitates the MDM2-mediated ubiquitination of p53 however is unable to ubiquitinate it on its own which lead to the hypothesis that RBBP6 potentially acts as a scaffolding protein thereby bringing MDM2 and p53 together in order to facilitate ubiquitination and in turn possibly playing the role of an E4 ubiquitin ligase (Li *et al.*, 2007).

p53 levels can be controlled by upstream regulator p19^{ARF} (mice) and p14^{ARF} (humans). ARF is able to bind to MDM2 in the nucleoplasm of cells and drags MDM2 into the nucleolus after which MDM2 is no longer able to target p53 for degradation by the 26S proteasome. Therefore, increased levels of ARF causes increased levels of p53 (Weinberg, R., 2007).

Honda and co-workers identified MDM2 as the first E3 ubiquitin ligase to catalyse the degradation of p53 by the 26S proteasome *in vitro* (Honda *et al.*, 1997). Yet questions still arose regarding the ability of MDM2 to catalyse the poly-ubiquitination of p53 in fully *in vitro* assays. Thereafter, MDMX was identified as an inactive E3 ligase and a partner to activate MDM2 and catalyse p53 ubiquitination. Unlike MDM2, MDMX which is a structural homologue of MDM2 has no E3 ligase activity. Since both MDM2 and MDMX form homo-dimers in solution through their RING finger domains, it was shown that both MDM2 and MDMX also form hetero-dimers through their RING finger domains. The MDM2/MDMX hetero-dimeric complex was found to have more poly-ubiquitination activity than MDM2 has on its own (Wang *et al.*, 2011) The combination of MDM2/MDMX has subsequently been shown to also catalyse poly-ubiquitination of p53 with the ubiquitin-like protein Nedd8, denoted Neddylation.

The primary site for p53 ubiquitination is the C-terminus of p53. The C-terminal regulatory domain of p53 undergoes numerous post-translational modifications, predominantly the acetylation of lysine residues. Lysine's K370, K372, K373, K381, K382 and K386 seem to be the sites for ubiquitination. Rodriguez and co-workers conducted a study which involved the mutation of individual lysine residues to arginine residues in which no effect on the stability of p53 was observed when individual lysine's were mutated to arginine. However, when 6 lysine residues were simultaneously mutated to arginine, MDM2-mediated p53 ubiquitination did not occur (Rodriguez *et al.*, 2000). An additional post-translational modification of p53 includes sumoylation of K386 which promotes the transcriptional activity of p53 (Moll *et al.*, 2003).

1.7 The Ubiquitin Proteasome Pathway

Ubiquitin is an 8.5 kDa, 76 amino acid protein which is highly conserved in evolution (Yeh *et al.*, 2000). It contains a di-glycine motif at position 76, which plays a vital role in its conjugation to side chain-amino groups of lysine residues on target proteins, a process known as ubiquitination.

Ubiquitination is a highly specific, ATP dependent post-translational modification which is involved in the regulation of the function and activity of cellular proteins. Ubiquitination is a cellular process in which ubiquitin molecules are covalently attached to cellular proteins (Kerscher, *et al.*, 2006). Ubiquitination serves numerous functions within the cell, including DNA repair and signalling pathways, quality control and endocytosis (Kim *et al.*, 2007; Chen, 2005). The most well-characterised function of ubiquitination is the targeting of proteins for degradation by the 26S proteasome, whereby ubiquitin is attached to the target protein to form a poly-ubiquitin chain (lysine48-linked) which is recognised by the receptors on the proteasome (Young *et al.* 1998).

The ubiquitin pathway occurs via two steps: (a) The attachment of multiple ubiquitin moieties to the target protein, (b) the degradation of the ubiquitin tagged target protein by the 26S proteasome (Figure 1.5). Ubiquitination is achieved by a combined action of 3 enzymes, namely ubiquitin-activating enzyme E1, ubiquitin-conjugating enzyme E2 and a substrate specific ubiquitin protein ligase E3 (Kerscher *et al.*, 2006). It is believed that other conjugation factors known as E4 ligases may also be required for poly-ubiquitination of protein substrates, however their role is still in dispute (Grossman *et al.*, 2003).

In the first step of ubiquitination, the E1 activates ubiquitin by cleaving immediately after the di-glycine motif, forming a high-energy thioester bond between the C-terminus of ubiquitin and the side-chain SH group of the catalytic cysteine of the E1. Ubiquitin is then transferred from the E1 to the E2 where it forms a thioester bond with the side-chain SH group of the catalytic cysteine of the E2. The ubiquitin conjugated E2 is then recruited to the substrate by the E3 where it is transferred to the side-chain amino group of a lysine in the substrate (Kerscher *et al.*, 2006). The ubiquitin proteasome system (UPS) is illustrated schematically in the Figure 1.5 below.

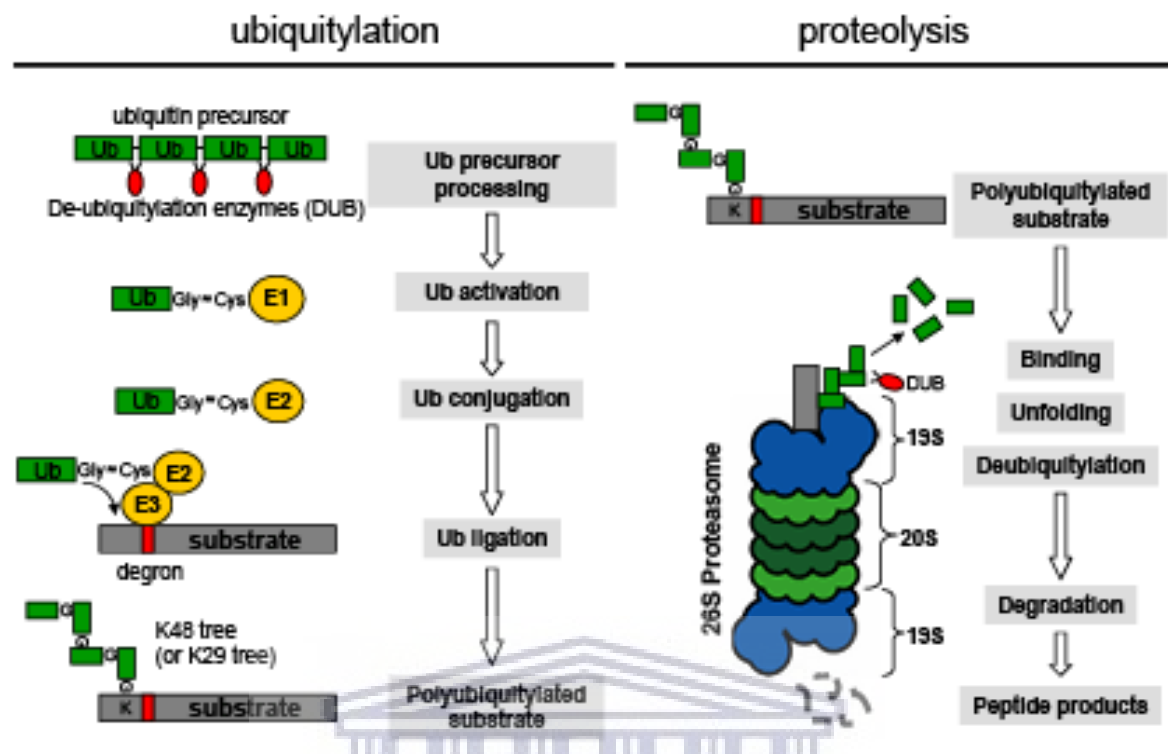


Figure 1.5: An illustration of the ubiquitin-proteasome pathway. Ubiquitination of substrate proteins is achieved by an intricate system consisting of E1 enzymes, E2 enzymes and E3 enzymes. In the last step ubiquitin is either directly transferred from E2 to the protein substrate or through an E3 with the formation of a thiol ester bond between E2 and E3. Ubiquitin is recycled when the cycle is complete.

The 26S proteasome is comprised of two parts, namely the 19S regulatory particle and the 20S core particle. The 20S core particle is barrel shaped and is composed of 14 α - and 14 β -subunits which are arranged in 4 rings of 7 subunits in a $\alpha_7\beta_7\beta_7\alpha_7$ configuration. The 20S core particle contains all the proteolytic activity and the proteolytic active sites are located on the β -subunits 1, 2 and 5 respectively. These active sites have three types of activity namely, chymotryptic which cleaves after hydrophobic side-chains, tryptic which cleaves after positively charged side chains and post-glutamyl which cleaves after negatively charged side chains.

The 19S regulatory particle is composed of 19 subunits, including 6 related ATPase subunits and 4 non-ATPase subunits. The lid of the 19S regulatory particle contains 9 non-ATPase subunits and regulates access in an ATP dependent manner (Nandi *et al.*, 2006). The 19S regulatory particle is responsible for recognising the lysine-48 linked poly-ubiquitin chains, unfolding the targeted protein and feeding it into the 20S core particle for degradation (Belzile

et al., 2010; Kao *et al.*, 2012). The function of the 26S proteasome is to mediate the degradation of lysine48-linked poly-ubiquitin chains.

Ubiquitination is a reversible reaction. De-ubiquitination enzymes also known as DUBs, are present in cells and regulate the levels of ubiquitination as well as facilitating the removal of ubiquitin tags from proteins for recycling before degradation in the 26S proteasome (Woelk *et al.*, 2007).

Further ubiquitin moieties can be added in order to form poly-ubiquitin chains. Therefore, the specific lysine residue used in the formation of the poly-ubiquitin chain determines the fate of the protein. Ubiquitin contains 7 lysine residues at positions 6, 11, 27, 29, 33, 48 and 63 respectively which form the attachment points for additional ubiquitin molecules. Mono-ubiquitination is the attachment of a single ubiquitin moiety to a target protein and is involved in processes such as endocytosis, DNA repair, nuclear export, endosomal sorting, histone regulation, virus budding and cytoplasmic translocation (Brooks *et al.*, 2004). Multiple mono-ubiquitination is the attachment of a single ubiquitin to more than one lysine residue and is involved in receptor internalization as well as endocytosis (Sorokin *et al.*, 2009).

The attachment of four or more ubiquitin moieties to a single lysine residue on a target protein is called poly-ubiquitination. Poly-ubiquitination involves internal isopeptide bonds between the C-terminus of each ubiquitin and the side chain amino group of one of the 7 lysine's on the next ubiquitin moiety (Windheim *et al.*, 2008). Lysine48 linked poly-ubiquitin chain promotes the recruitment of the target protein to the 26S proteasome and its subsequent degradation in the presence of ATP (Ciehanover and Stanhill, 2014). Lysine63 linked poly-ubiquitin chains are involved in the activation of transcription factors, endocytosis, regulation of protein function, protein-protein interactions, activation of protein kinases as well as signalling DNA repair (Chen *et al.*, 2005 and Nathan *et al.*, 2013). The different fates of ubiquitination on a substrate is seen in Figure 1.6 below.

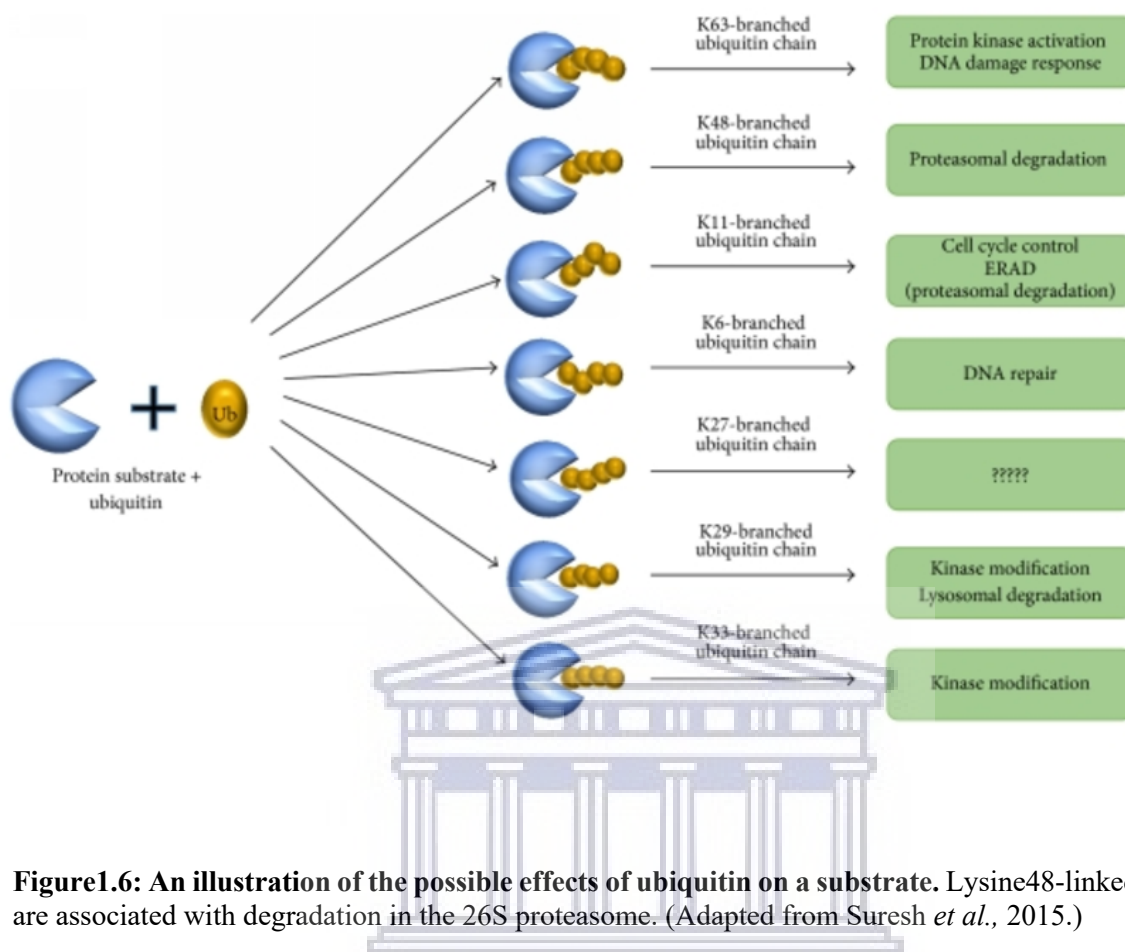


Figure 1.6: An illustration of the possible effects of ubiquitin on a substrate. Lysine48-linked chains are associated with degradation in the 26S proteasome. (Adapted from Suresh *et al.*, 2015.)

1.7.1 Ubiquitin activating Enzyme (E1)

The initial step in ubiquitination is carried out by ubiquitin activating enzyme E1, a 110kDa enzyme which uses ATP to activate ubiquitin. The E1 activates ubiquitin by forming a high energy thioester bond between the C-terminus of ubiquitin and the side chain SH group of the catalytic cysteine of the E1 (Pickart., 2001). There are only two E1's in humans namely, Uba6 and Ube1 (Jin *et al.*, 2007).

1.7.2 Ubiquitin conjugating Enzyme (E2)

A total of 35 E2 enzymes has been found in humans (Metzger *et al.*, 2014), with other species having between 16 and 35 (van Wijk *et al.*, 2010). The presence of the conserved ubiquitin-conjugating catalytic domain (UBC) is a characteristic feature of all E2's. The UBC is comprised of 15-200 amino acids and interacts with the E1 (Arai *et al.*, 2006; Burroughs *et al.*, 2008). E2s are classified into three classes, namely class I, class II, class III. Class I contains

only the catalytic domain whereas class II is comprised of C-terminal extensions. Class III is comprised of additional N-terminal sequences (Winn *et al.*, 2004).

1.7.3 Ubiquitin Ligases (E3s)

Ubiquitin ligases, also known as E3s, play a vital role in determining the specificity of the substrate (Pringa *et al.*, 2001). E3s are substrate-specific and therefore there has to be the same number of E3s as there are substrates to be modified (Semple *et al.* 2003). E3s are closely associated with RING finger containing proteins, wherein their function is to recognise and recruit the substrate protein to the ubiquitin-conjugated E2. E3s must therefore contain a substrate binding domain as well as an E2 binding domain. Numerous E3 ligases have been shown to have the ability to ubiquitinate themselves in a process known as auto-ubiquitination. BCA2 is an E3 ubiquitin ligase that is able to auto-ubiquitinate itself based on its RING domain (Amemiya *et al.*, 2008).

There are four classes of E3 ubiquitin ligases, namely HECT (homologous to E6-AP C-Terminus) domain, RING (Really Interesting New Gene) domain, U-box domain and N-end Rule ligases.

The HECT domain is a homologous C-terminal region which is comprised of 350 amino acids. There are 30 HECT ligases which have been identified in humans (de Bie *et al.*, 2011). HECT type E3s differs from RING type E3 ligases in that the formation of a thioester intermediate with ubiquitin is distinctive to HECT E3s (Joazeiro and Weissman., 2007; Metzger *et al.*, 2014). Consequently, the substrate and the E2 do not interact with the E3 simultaneously.

A family of HECT domain proteins known as WW domains recognises a specific sequence PPxY as well as other proline-rich motifs. The WW domains comprises proteins with numerous functions including, NEDD4 and E6-AP. NEDD4 mediates ubiquitination as well as the downregulation of an epithelial cell sodium channel (Huang *et al.*, 2000). E6 associate protein (E6-AP), a HECT domain E3 ligase, was found to interact with the E6 protein of HPV (human papillomavirus) thereby form a dimer which targeted p53 for degradation by the 26S proteasome (Huang *et al.*, 2000; Narisawa-Saito *et al.*, 2007).

Around 600 RING-type E3s have been identified in humans (de Bie *et al.*, 2011). RING-type E3s act as adaptor molecules by binding simultaneously to the E2 and to the substrate, thereby facilitating the transfer of ubiquitin from the E2 to the substrate (Joazeiro *et al.*, 2000 and Metzger *et al.*, 2014). RING-type E3s has been shown to play a vital role in numerous

processes. Well-known examples are BRCA1, in which mutations are closely associated with breast cancer, and MDM2 which is a major regulator of p53 (Honda *et al.*, 1997).

The U-box motif was first identified in yeast protein ubiquitin fusion degradation protein 2 (UFD2), and thereafter shown to be present in other eukaryotic proteins as well (Pringa *et al.*, 2001). U-box containing E3 ubiquitin ligases contains a U-box domain which comprises approximately 70 amino acid residues and is found in a number of proteins ranging from humans to yeast. U-box E3s has an identical structure to that of RING fingers however it does not need zinc in order to fold. In the U-box domain, the zinc ions are replaced by a set of hydrophobic residues interconnected by salt bridges and hydrogen bonds which subsequently stabilizes the U-box domain (Andersen *et al.*, 2004). The RING finger domain and the U-box domain were found to be involved in the ubiquitin-proteasome pathway. However, the removal of the U-box or the mutation of the amino acid residues abolishes the ubiquitination activity of a large number of u-box E3's. U-box E3's catalyse the poly-ubiquitination of target proteins by targeting the lysine residues of ubiquitin other than lysine48 (Joazeiro *et al.*, 2000).

These U-box E3 ligases are also considered as a characteristic of E4 ubiquitin ligases which enables the formation of ubiquitin chains during ubiquitination which subsequently stabilizes the structure of the protein (Cyr *et al.* 2002).

The N-end rule E3 ligases bind N-end rule protein substrates that have basic or bulky hydrophobic N-terminal amino acid residues (Baboshina *et al.*, 2001). A significant portion of eukaryotic protein degradation occurs through the N-end rule pathway. The N-end rule recognition pathway is highly conserved in eukaryotic evolution (Mogk *et al.*, 2007).

While a number of E3 ligases are monomers, some have been found to be homo-dimers or hetero-dimers (Nikolay *et al.* 2004). Dimerization is physiologically important because mutations on amino acids which disrupts the formation of the dimer, abolishes the activity of the E3. Although, the formation of dimers is a common occurrence, numerous RING finger domains can form hetero-dimers, sometimes preferentially with an inactive partner (Metzger *et al.*, 2014). such as MDM2-MDMX hetero-dimer and the BRCA1-BRCA2 hetero-dimer. Mutated RING finger domains are unable to promote that transfer of ubiquitin, suggesting that the dimerization of the RING finger domain is essential to increase the concentration of the E2 enzymes and subsequently promote catalytic processes such as ubiquitination (Liew *et al.*, 2010).

An example is Parkin, a RING-in-between-RING (RBR) protein, which is implicated in Parkinson's disease and has structural similarities to RBBP6. Parkin contains an N-terminal ubiquitin-like domain, a 60 amino acid linker followed by RING0, a zinc finger unique to Parkin and three additional zinc domains which are characteristic of the RBR family proteins (Trempe *et al.*, 2013). A study by Chaugule and co-workers showed that the ubiquitin-like domain regulates the ubiquitination activity of Parkin whereby the domain folds over and blocks access to the RING finger domain (Chaugule *et al.*, 2011).

A study by Kappo and co-workers in 2012 determined the structure of the RBBP6 RING domain using nuclear magnetic resonance spectroscopy (NMR) and showed that the RING forms a homo-dimer along the same interface as that found in numerous other RING finger domains (Kappo *et al.*, 2012). Kappo and co-workers identified two mutations which monomerize the RING finger, namely N312D and K313E (Kappo *et al.*, 2012). This was confirmed when K313 was mutated to K313E; NMR analysis showed that this mutation completely abolished the homo-dimer and subsequently disrupts the ubiquitin binding interface.

A study conducted in 2016 by Densham and co-workers identified an ubiquitin-priming surface on the BRCA1/BARD1 hetero-dimer (Densham *et al.*, 2016). On BARD1, which is thought to play only a scaffolding role in ubiquitination, the mutation R99E did not disrupt the hetero-dimer but reduced the ubiquitination of the substrate. Ubiquitination was rescued by mutating D32 on ubiquitin to D32R, which subsequently showed a close interaction of R99E on BARD1. Densham and co-workers also showed that when K313 is present, the ubiquitin binding site is present and could potentially play a role in contacting D32 (Densham *et al.*, 2016).

A study conducted in 2010 by Liew and co-workers showed that disruption of the RNF4 homo-dimer significantly reduces auto-ubiquitination (Liew *et al.*, 2010). The S155A mutation does not abolish the homo-dimer and therefore RNF4 retains most of its auto-ubiquitination potential whereas the S155E mutation abolishes the homo-dimers and subsequently RNF4 loses most of its auto-ubiquitination potential.

1.8 Ubiquitin-like proteins

Ubiquitin-like proteins, often referred to as Ubls, are post-translationally attached to substrate proteins by enzymatic reactions analogous to ubiquitination. Ubiquitin-like proteins include

proteins that function in a similar way to ubiquitin, as well as those that possess domains that are unrelated in sequence to ubiquitin but adopts an ubiquitin-like fold (Jentsch *et al.*, 2000). Ubiquitin-like modifiers typically share the di-glycine motif at the C-terminus of ubiquitin, which serves as the recognition site for a protease which cleaves after the di-glycine, thus initiating conjugation. Some Ubls, like Nedd8, share a high sequence similarity with ubiquitin, while others, such as SUMO, do not. Isoform 3 of RBBP6 is an example of an ubiquitin-like protein.

1.8.1 SUMO-1

SUMO-1 (Small Ubiquitin-like Modifier) occurs in all eukaryotic organisms. The human SUMO gene encodes for three SUMO proteins namely, SUMO-1, SUMO-2 and SUMO-3 respectively (Su *et al.*, 2002). Human SUMO-1 is comprised of 101 amino acid residues and has a long and flexible N-terminus that extends from the ubiquitin-like core. SUMO-1 has Gln69 instead of the lys48 found in ubiquitin. SUMO-1 shares 18 % sequence homology with ubiquitin. “Sumoylation” which is the conjugation of SUMO to substrate proteins, occurs in a similar way to that of ubiquitination. The sumo protein conjugation pathway consists of SUMO-E1, Ubc 9(E2) and a small number of E3s including the PIAS family. Like ubiquitin, sumoylation is a reversible process. The sumoylation of p53 activates the transcriptional activity of p53 (Muller *et al.*, 2000).

1.8.2 NEDD8

Neural Precursor cell-expressed, developmentally downregulated (NEDD8) is an ubiquitin-like protein which shares 58 % sequence similarity with ubiquitin and conjugates to target proteins in a process analogous to that of ubiquitin. Like ubiquitin, NEDD8 conjugation pathway has an E1 (UBE1C), an E2 (UBE2M) as well as E3 ligases (Rabut *et al.*, 2008). Also like ubiquitination, the conjugation of NEDD8 to target proteins is reversible (Deshaies *et al.*, 2010)

1.8.3 DWNN domain

The DWNN domain is an 80-amino acid found exclusively at the N-terminus of members of the RBBP6 protein family. The structure of the human DWNN domain has been determined by NMR spectroscopy (Pugh *et al.*, 2006) and that of the yeast orthologue by X-ray crystallography (Hill *et al.* 2019). A superposition of the structures of the DWNN domain and ubiquitin is shown in Fig 1.7 (A), and a sequence alignment, based on the structure, in panel

(B). The structure is classified as a “ β -grasp “, featuring an α -helix packing against a five-stranded β -sheet made up of strands. Most notable in the sequence alignment is the conservation of the di-glycine motif near the C-terminus, which is found in exactly the same structural position as in ubiquitin, at the C-terminal edge of the structural region. In ubiquitin this motif serves as the recognition site for the protease which cleaves the backbone in preparation for it being iso-peptide bonded to the lysine ϵ -amino group of a substrate lysine. The di-glycine is exactly conserved across vertebrates, but not invertebrates. The presence of the motif is perhaps the strongest motivation for thinking that the DWNN domain may become attached to other proteins in a process analogous to ubiquitination, which we have named DWNNylation (Pugh *et al.*, 2006). However, the fact that the GG motif is not conserved beyond vertebrates, whereas the core functions of RBBP6 appear to be well conserved across all eukaryotes, argue against it being an essential part of the function of the RBBP6 family. Nevertheless, the presence of the RING finger domain in the immediate vicinity of the DWNN domain is very intriguing.

Attachment of the DWNN domain from isoform 1 to other proteins would require proteolytic separation of the DWNN domain from the rest of the protein, which has not been observed in other ubiquitin-like proteins. However, the DWNN domain is also expressed independently as a 13 kDa protein, namely isoform 3, which consists almost entirely of the DWNN domain (residues 1-81). The rest of the protein (residues 81-118), also called the C-terminal tail, is made up of 20 amino acids present also in isoform 1, followed by 17 amino acids not found in isoform 1, which are added by the alternative promoter. The C-terminal appears to be largely unstructured. Isoform 3 would appear to be a far more likely candidate for an ubiquitin-like protein; it would require the removal of just the short C-terminal tail, which is similar to what is seen in other UBLs.

Preliminary and unpublished data from our laboratory has provided evidence for the attachment of the DWNN domain to higher molecular weight complexes. Addition of the bacterially-expressed DWNN domain, terminating immediately after the di-glycine motif, to mammalian cell lysate resulted in the appearance of ladders of higher molecular weight bands, after western blotting with antibodies raised against the DWNN domain. These bands are not present in the absence of lysate, suggesting that they may represent DWNN covalently attached to cell proteins. On the other hand, it is also possible that the lysate contains something which causes the DWNN domain to form homo-oligomers, which are what was being observed. One way to resolve this issue would be to repeat the investigation using the DWNN domain without the di-

glycine motif on the C-terminus. If the di-glycine motif is required for DWNNylation, then the higher MW species should not be present when the di-glycine motif is not.

Repeat of the above DWNNylation result was the original aim of this thesis. However, due to lack of promising results it was not pursued. The results generated have therefore been relegated to an appendix.

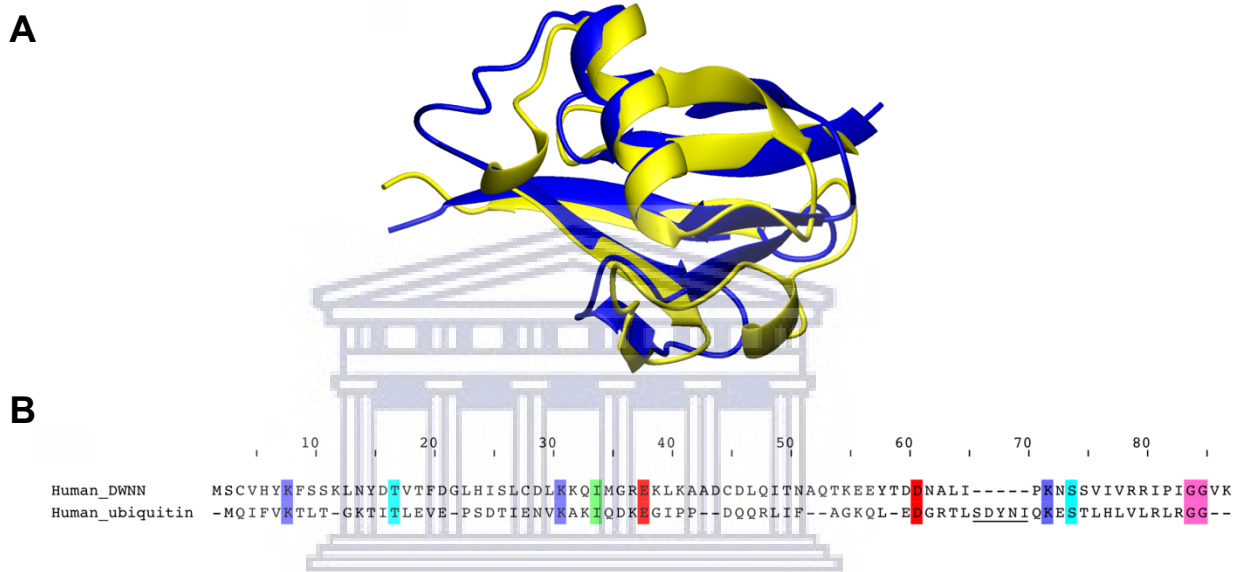


Figure 1.7: The DWNN domain adopts an ubiquitin-like fold. (A) The structure of the DWNN domain is shown in blue, superimposed on the structure of ubiquitin in yellow. (B) The C-terminal di-glycine motif, which plays a critical role in the ubiquitin reaction, occurs in precisely the same position in the DWNN domain. The di-glycine is exactly conserved across vertebrates. (Adapted from Pugh *et al*, 2006.)

1.9 Aims and objectives of this thesis

Retinoblastoma Binding Protein 6 (RBBP6) has been reported to play an essential role in suppressing p53 in developing embryos, by facilitating its poly-ubiquitination by MDM2. However, it has been suggested that it plays an auxiliary role, perhaps as a scaffold protein, bringing p53 and MDM2 together, rather than playing a direct role in catalysing the ubiquitination reaction. This conclusion is supported by the fact that the previously identified site of interaction with p53 is located near the C-terminus of RBBP6, far from the RING finger domain that is expected to be the site of ubiquitination activity. Nevertheless, unpublished data from our laboratory suggests that the N-terminal fragment of RBBP6 is able to ubiquitinate p53 without the help of MDM2.

Auto-ubiquitination, or self-ubiquitination of an E3 by itself, has been used in many investigations as a proxy for substrate ubiquitination. The first aim of this thesis was therefore to investigate whether RBBP6 is able to auto-ubiquitinate itself *in vitro*. If so, it would lend support to our hypothesis that RBBP6 can ubiquitinate p53 without the need for MDM2. It would also provide a mechanism by which RBBP6 may catalyse its own degradation in the proteasome, which may explain the low levels of the RBBP6 protein found in most cell types.

Furthermore, if RBBP6 does auto-ubiquitinate itself, it would provide a convenient platform for testing whether dimerization of RBBP6 is required for its auto-ubiquitination activity. The isolated RING finger of RBBP6 forms weak homo-dimers in solution. Unpublished data from our laboratory suggests that the RING finger is able to auto-ubiquitinate itself *in vitro*, but monomeric mutants of the RING finger are nevertheless able to auto-ubiquitinate themselves, although possibly less efficiently. The second aim of this work was therefore to reproduce these results, to compare the auto-ubiquitination potentials of the isolated RING finger and the monomeric mutants.

Unpublished data from our laboratory shows that longer fragments from the N-terminus of RBBP6 form stronger homo-dimers than the isolated RING finger. The third aim of this work was therefore to compare the auto-ubiquitination potentials of these longer fragments with that of the isolated RING finger, in order to test whether the stronger homo-dimers lead to stronger auto-ubiquitination. An associated aim was to test a hypothesis, based on the E3 Parkin, that the N-terminal DWNN domain may modify the auto-ubiquitination potential of RBBP6 by interfering with the RING finger domain.

A parallel project involved investigating whether a direct interaction exists between p53 and the N-terminus of RBBP6 *in vitro*. It has previously been reported that p53 interacts with a region near the C-terminus of RBBP6. Nevertheless, preliminary data from our laboratory suggest that a fragment consisting of the first 335 residues of RBBP6, which we have named R3, and which does not include the C-terminal p53-binding site, is able to ubiquitinate p53 without the assistance of MDM2. This suggests that there should be another p53 interaction site within the N-terminal region. We therefore aimed to investigate whether R2 interacts with p53 *in vitro*. This would be done first using the techniques of Far Western blotting and then using GST pull-down assays.

CHAPTER 2: MATERIALS AND METHODS

2.1 Antibodies used

2.1.1 Primary Antibodies

Anti-HA:

Commercial goat polyclonal raised against the HA-antigen (YPYDVPDYA), Cat. No: A00168-40 (Genscript Inc., Piscataway, NJ 08854, USA).

Anti-FLAG:

Commercial mouse monoclonal antibody raised against the FLAG-antigen (DYKDDDK), Cat. No: A00187-100 (Genscript Inc., Piscataway, NJ 08854, USA).

2.1.2 Secondary Antibodies

Rabbit anti-goat

Commercial polyclonal antibody, Horseradish Peroxidase-conjugated, Cat No: E-AB-1004 (Elabscience Biotechnology, USA)

Goat anti-mouse

Commercial polyclonal antibody Horseradish Peroxidase-conjugated, Cat No: E-AB-1001 (Elabscience Biotechnology, USA)

2.2 Bacterial Culture

2.2.1 Preparation of competent *E. coli* cells for transformation

Escherichia coli (*E. coli*) XL10 GOLD cells were streaked out on a nutrient agar plate and incubated overnight at 37 °C. A single colony was selected and inoculated into 50 ml of TYM broth and grown overnight with vigorous shaking at 37 °C. The overnight culture was then scaled-up to 500 ml of TYM broth and grown under the same conditions until the optical density at 550 nm (OD₅₅₀) was in the range of 0.4 to 0.6. The cells were rapidly chilled with constant swirling in ice water, transferred to a 500 ml centrifuge bottle and harvested by centrifugation for 10 min at 4300 rcf using a pre-cooled Beckman JA-10 rotor. After discarding

the supernatant, the cells were re-suspended in 100 ml ice cold Tfb1 and allowed to incubate at 0 °C for 30 min. The cells were harvested by centrifugation at 4300 rcf for 8 min, after which the supernatant was discarded and the pellet was re-suspended in 30 ml ice cold Tfb2. The cells were flash frozen in liquid nitrogen as 50 µl aliquots and stored at -80 °C.

2.2.2 Bacterial transformations

50 µl competent cells (prepared as described in Section 2.2.1) were thawed on ice and added to 50-100 ng of plasmid DNA, gently mixed and incubated on ice for 15 min. The cells were heat shocked at 42 °C for 90 s and placed on ice for 5 min. Following incubation on ice, 500 µl of pre-warmed LB broth was added and the transformation mixture incubated at 37 °C, with shaking, for 1 hr, to allow for the expression of the antibiotic resistance marker. The transformed cells were plated onto nutrient agar plates containing the appropriate antibiotic and incubated overnight at 37 °C, or inoculated into the required volume of LB containing the appropriate antibiotic and incubated at 37 °C with shaking overnight.

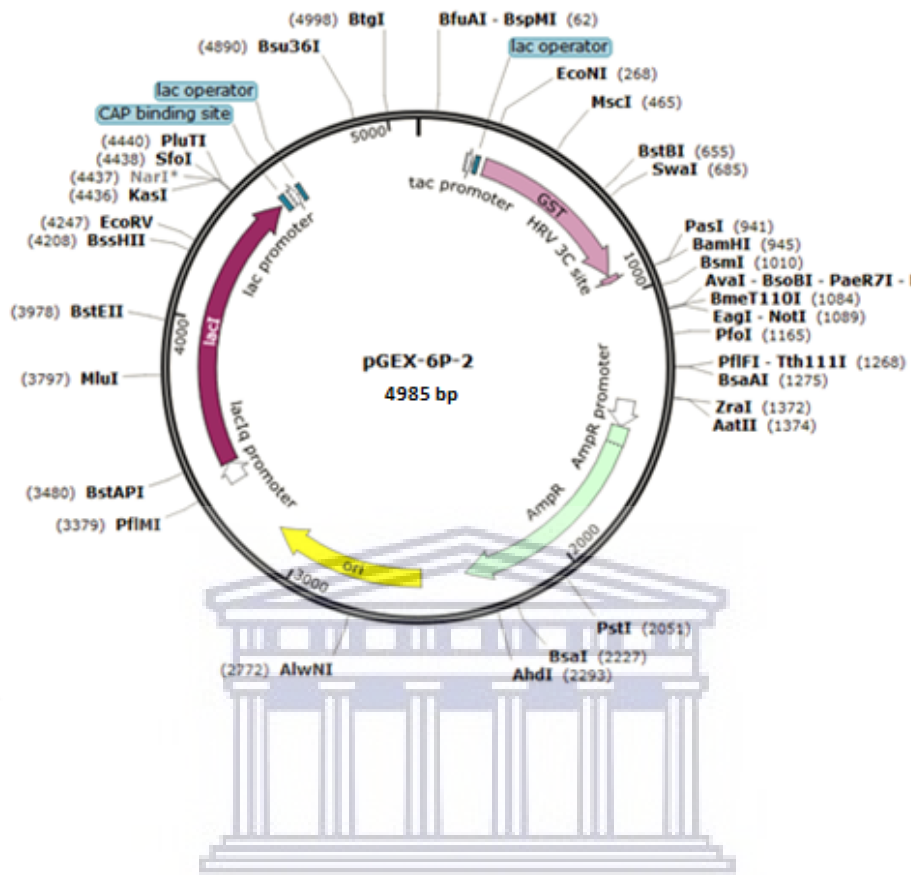
2.3 Cloning

2.3.1 Specifications of cloning vector

pGEX-6P-2 is a bacterial expression vector with a size of 4.9 kb, which expresses the target protein as a fusion to the C-terminus of Glutathione-S-transferase (GST) from *Schistosoma japonica*. GST aids in purification of recombinant proteins from *E. coli* native proteins and increases the solubility of the fusion protein. A recognition sequence for 3C protease from human rhinovirus located between GST and the MCC facilitates post-translation removal of GST from the fusion protein. The vector incorporates an IPTG-inducible *tac* promoter to drive high levels of expression. The vector confers ampicillin resistance to transformed bacterial cells.

pET28b is a 5368-bp bacterial expression vector which expresses target proteins under control of the *T7lac* promoter. Selection is provided by the kanamycin resistance gene. When used in DE3 lysogens such as *E. coli* BL21, IPTG drives expression of T7 RNA polymerase which, in turn, drives expression from the T7 promoter. The choice of restriction sites used in this work leads to the incorporation of a 6xHis-tag at the N-terminus.

A



B

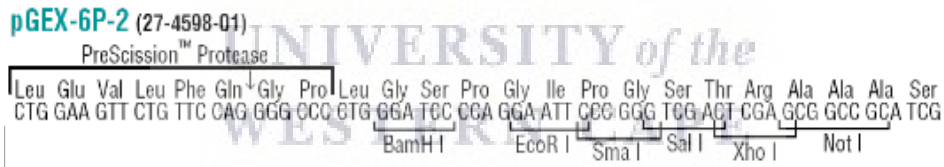
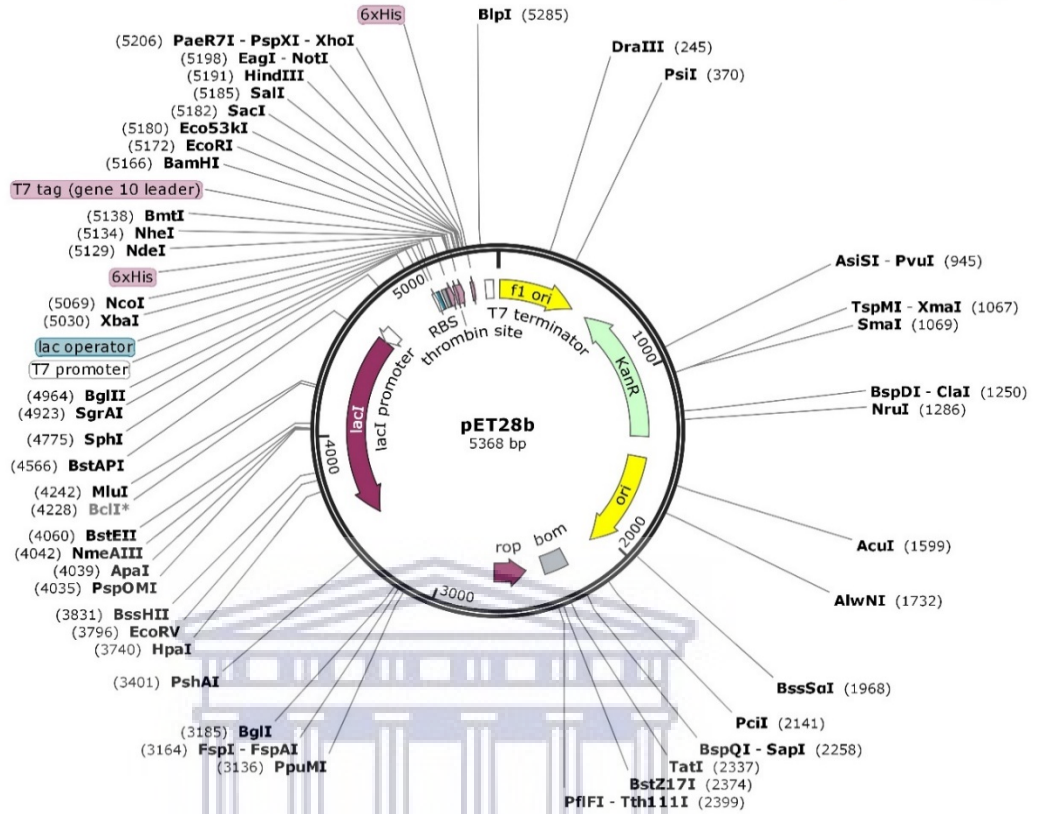


Figure 2.1: Restriction map of pGEX-6P-2. (A) The pGEX-6P-2 vector is a bacterial expression vector that drives the expression of recombinant proteins from a *tac* promoter, fused to the C-terminus of GST. (B) The linker between GST and the target protein encodes a 3C protease site, which facilitates removal of the GST moiety following affinity purification. (Figure generated using SnapGene Viewer v. 4.3.1, GSL Biotech).

A



B

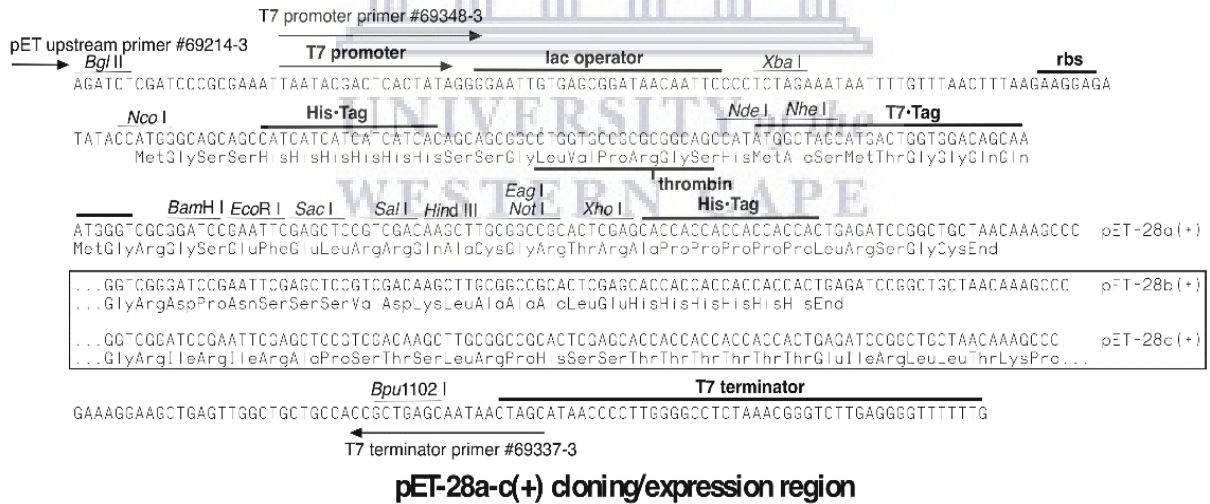


Figure 2.2: Restriction map of pET28b. (A) The pET28b vector is a bacterial expression vector that drives the expression of recombinant proteins from a T7 promoter. (B) Cloning into the MCC (between the NdeI and XhoI sites) incorporates a 6His tag at the N-terminus of the protein. Incorporating a stop codon at the end of the insert ensured that the C-terminal 6His tag is not incorporated into the C-terminus. (Figure generated using SnapGene Viewer v. 4.3.1, GSL Biotech).

2.3.2 PCR amplifications

All PCR reactions were made up to a final volume of 50 μ l with nuclease-free water, unless otherwise stated. Primers for amplification of inserts were designed to incorporate specific restriction sites based on the DNA sequence of interest and the multiple cloning cassette of the vector to be used. A standard PCR reaction was composed of 50 ng template DNA, 1X Q5 PCR Mastermix and 1 μ l of 50 ng primer set.

The amplification reactions were carried out using the following parameters:

<u>Initial denaturation</u>	<u>95 °C for 5 min</u>
<u>Denaturation</u>	<u>95 °C for 1 min</u>
<u>Annealing:</u>	<u>T_m – 5 °C for 1 min</u>
<u>Elongation:</u>	<u>72 °C for 1 min/Kb</u>
<u>Final elongation</u>	<u>72 °C for 1 min/Kb</u>

25 cycles

The standard method for carrying out mutations on DNA constructs, as implemented in the QuikChange kit, employ completely overlapping primers and therefore do not allow for exponential amplification of the target DNA, leading to inefficient generation of the desired mutants. The version used here, adapted from Liu and Naismith (Liu and Naismith, 2008), employs non-overlapping primers, which allow for exponential amplification and greatly improved efficiency.

Primers are designed to overlap at their 5'-ends, with non-overlapping 3'-ends, so that extension takes place away from the overlapping region, leading to replication of the entire circular template. As a result of the 3'-end non-overlapping region, the amplicon from one round of extension is able to serve as template for the next round, using the opposite primer, leading to exponential amplification. The absence of the non-overlapping regions is responsible for the non-exponential nature of QuikChange. At the end of the procedure, linear copies of the target plasmid are produced, containing any mutations incorporated into the primers; crucially,

a copy of the 5'-overlapping region is found at each end of the amplicon. Following transfection into a RecA⁺ strain of *E. coli*, homologous recombination of the identical flanking regions leads to circularization, leading to retention of only one copy of the overlapping region. Primers can be designed so that the melting temperature of the 5'-overlapping regions (T_{mo}) is lower than the melting temperatures of the 3'-non-overlapping regions (T_{mno}). Choosing the annealing temperature between T_{mo} and T_{mno} ensures that the 3'-non-overlapping regions of the primers will be able to anneal to the template, but the 5'-overlapping regions will not be able to anneal to each other, thereby suppressing primer-dimers.

PCR amplifications for deletion mutagenesis were carried out using the Q5 High-Fidelity 2X Master Mix (New England Biolabs, Ipswich, Massachusetts, USA). The reaction was composed of 1X Q5 master mix, 50 – 100 ng of template DNA, and 1.25 μ l of 125 ng primer set in a 25 μ l reaction.

The amplification reaction was carried out using the following parameters:

<u>Initial denaturation</u>	<u>95 °C for 1 min</u>	} 25 cycles
<u>Denaturation</u>	<u>95 °C for 30 sec</u>	
<u>Annealing</u>	<u>$T_{no} - 5$ °C for 2 min</u>	
<u>Elongation</u>	<u>72 °C for 1min/Kb</u>	
<u>Final elongation</u>	<u>72°C for 1min/Kb</u>	

An identical reaction, but leaving out the primers, was carried out to serve as a no-amplification control. This contains the same amount of template as the experiment, but no mutated amplicon, and will therefore allow the number colonies resulting from unmutated parental DNA to be assessed.

Following the amplification, 1 μ l of DpnI was added to 10 μ l each of the experimental and the no-amplification controls. DpnI is a 4-base cutter which targets methylated DNA, such as the template, which was produced in a methylation-competent strain of *E. coli*, but not

unmethylated DNA, such as the amplicon, which was produced in a methylation-incompetent reaction; it therefore suppresses the background emanating from unmutated parentals. 10 μ l each of the experimental and the no-amplification controls were kept aside to serve as no-DpnI controls. Following digestion, the DNA was transformed into *E. coli* as described in Section 2.2.2.

The experimental set-up is depicted in Figure 2.3 below.

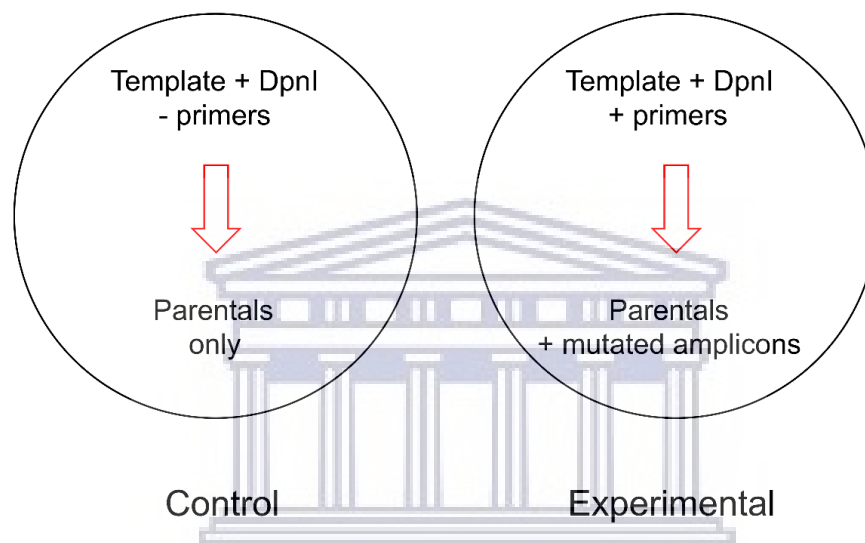


Figure 2.3: Schematic diagram of the deletion mutagenesis protocol. Following amplification, mutants were selected for by digesting the amplicons with DpnI in order to destroy methylated template DNA.

2.3.4 Restriction digest and DNA ligation

Typically, 1 μ g of DNA was digested according to manufacturer's instructions (all restriction enzymes were supplied by New England Biolabs). The digested DNA fragments were subjected to agarose gel electrophoresis for confirmation of restriction digestion, followed by subsequent purification using the GeneJet gel extraction kit (ThermoFisher Scientific, Waltham, MA USA) according to manufacturer's instructions. The purified DNA was quantified using a Nano-Drop spectrometer (ThermoFisher Scientific, Waltham, MA USA) and ligated at room temperature for a period ranging from 1 to 4 hrs.

The ligation reactions were carried out using 25 ng of vector DNA with the appropriate insert to vector ratio, calculated using the equation below:

$$\text{ng of insert required} = \frac{(\text{ng of vector})(\text{Kb size of insert})}{(\text{Kb size of vector})} \times \text{insert vector ratio}$$

After ligation, *E. coli* XL10 Gold cells were transformed with 10 µl of the ligation reaction mixture, of which 100 µl was plated onto LB plates with the appropriate antibiotic selection marker and grown at 37 °C for 16 hrs to obtain single colonies for screening purposes. Transformations were carried out as described in Section 2.2.2.

2.3.5 Screening of putative clones

Colonies were selected for screening of putative clones from the experimental plates. No colonies were observed on the vector only control plate. Overnight cultures were made of the selected colonies by sub-culturing colonies in 25 ml of LB with the appropriate antibiotic and growing overnight at 37 °C with shaking. DNA was extracted using the GeneJet plasmid mini-prep kit (ThermoFisher Scientific, Waltham, MA USA) or the Zymopure Plasmid Miniprep Kit (Zymo Research, USA) and quantified with a Nano Drop spectrometer (Thermo Scientific). The purified DNA was digested with the respective restriction enzymes to produce the DNA fragments of interest, subjected to DNA agarose gel electrophoresis, which provided preliminary confirmation of successful cloning based on the size of insert obtained. Direct sequencing by Inqaba Biotechnical Industries (Hatfield, South Africa) confirmed that the sequences were exactly as expected. The respective constructs were named according to the protein domains which the specific DNA construct encoded for.

2.3.6 Agarose gel electrophoresis

DNA fragments were analyzed by agarose electrophoresis using a 1 % agarose gel containing 1:1000 dilution of EZ-Vision in-gel DNA stain (VWR Life Science, Leicester United Kingdom). O'Gene Ruler 1Kb DNA ladder (ThermoFisher Scientific, Waltham, MA USA) were loaded alongside the DNA samples on the gels. DNA agarose gels were run at 90 V for 75 minutes after which they were visualized and imaged using a transilluminator connected to a UV-camera DC120.

2.3.7 Determination of DNA concentration

DNA concentrations were measured by measuring the absorbance at 280 nm using a NanoDrop ND-1000 spectrophotometer (NanoDrop Technologies, Wilmington DE, United States).

2.4 Expression and purification of recombinant proteins

2.4.1 Protein expression

Expression constructs were transformed into *E. coli* BL21 Codon Plus as described in Section 2.2.2 and plated onto LB agar containing the appropriate antibiotic. Colonies were selected and inoculated in 20-30 ml LB broth with appropriate antibiotics and grown overnight at 37 °C with shaking to serve as starter cultures. Starter cultures were scaled up to a final volume of 1L LB with appropriate antibiotics and grown to an optical density at 600 nm (OD₆₀₀) of 0.4-0.6. Prior to induction, 200 µM ZnSO₄ was added to zinc binding proteins to encourage native folding. Protein expression was carried out by adding varying concentrations of IPTG dependent on the protein being expressed. Proteins were induced for 4-16 hrs at 37 °C with shaking. Following induction, cells were harvested by centrifugation at 4300 *rcf* for 20 min. Cell pellets were re-suspended in cell lysis buffer and stored at -20 °C until further use.

2.4.2 Protein purification

2.4.2.1 Protein extraction

Cell pellets containing heterologous proteins were thawed on ice. Cells were lysed by sonicating the pellets for 5 x 30 seconds pulses with 30 seconds incubation on ice between pulses, using a Soniprep 150-Plus ultrasonic Disintegrator (MSE, London, UK). Sonicated pellets were centrifuged at 4300 rpm for 30 minutes to produce a clarified lysate.

2.4.2.2 Affinity purification of fusion proteins from bacterial lysates

A self-packed glutathione-agarose affinity column was prepared by adding 5-10 ml of glutathione agarose resin (Agarose Bead Technologies, Madrid, Spain) into a 1.5 cm diameter BIORAD Econo column and allowed to pack under gravity. The column was cleaned by allowing the agarose beads to incubate in 8 M urea at 37 °C for 30 min, where after it was equilibrated using 3 column volumes (CV) of PBS buffer. The clarified protein lysate was loaded onto the column and the flow through collected. The column was washed with 3 CV wash buffer (1x PBS containing 5 mM β-mercaptoethanol), after which the proteins were eluted with 3 CV of elution buffer (1x PBS containing 20 mM reduced glutathione and 5 mM β-mercaptoethanol). The final elution was carried out using 1M NaCl. Columns were stored in 1XPBS, with 0.2 % NaN₃ to discourage bacterial growth.

2.4.2.3 Dialysis and cleavage of recombinant proteins with 3C protease

3C protease from human rhinovirus was produced in-house by a co-worker as a GST-fusion protein, at a concentration of approximately 1mg/ml. Fractions containing GST fusion proteins were combined and transferred to a 3.5 kDa MWCO Snakeskin™ dialysis tubing (ThermoFisher Scientific, Waltham, MA USA) containing 1 ml 3C protease. The dialysis tubing containing the protein of interest was incubated in 2L cleavage buffer (1x PBS containing 5 mM β -mercaptoethanol) at 4 °C overnight with stirring. Cleaved GST was separated from the target protein by returning the sample to the glutathione agarose column; the target protein was recovered by flow through, whereas GST, uncleaved fusion protein and GST-3C were retained by the column and recovered by elution.

2.4.2.4 Nickel ion affinity chromatography

A Ni-NTA column, used for the purification of His-tagged proteins, was prepared according to manufacturers' instructions and allowed to pack by gravity. The column was prepared by allowing the Ni-NTA beads to incubate in 8 M urea at 37 °C for 30 min. The column was allowed to flow and 3 CV of 1M NaCl was added onto the column and allowed to flow through. This was followed by the addition of 3 CV of cleansing buffer 1 and cleansing buffer 2 respectively with 3 CV of dH₂O washes in between. The column was equilibrated with 3 CV of 1x PBS. The clarified protein lysate was loaded onto the column and the flow through was collected. The column was washed with 3 CV of wash buffer (1x PBS containing 20 mM Imidazole) after which the proteins were eluted with 3 CV of elution buffer (1x PBS containing 100-400 mM Imidazole). Columns were stored in 1x PBS with 0.2 % NaN₃. Fractions were analyzed by SDS-PAGE, as described in Section 2.9 below.

2.5 Preparation of mammalian cell lysates

The media from a flask of A549 or HeLa cells was discarded, and the cells washed twice with 1x PBS by gently swirling the flask. Cell lysis buffer (1 mM DTT, 1x PBS, Triton-X, and protease inhibitor cocktail, 100 μ g/ml Lysozyme, 100 μ M zinc sulphate) was added to the flask and allowed to incubate on ice for 5 minutes. The flask was scraped in order to free adhered cells, which were then transferred to a 15 ml Greiner tube. The cells were sonicated 3x for 15s each, with 15s on ice after each pulse. The cells were then centrifuged at 17000 xg for 10 minutes, after which the supernatant was removed and protein concentration determined as

described in Section 2.5. 10 % glycerol was added to the supernatant, which was then stored at -20 °C for future use.

2.6 *In vitro* auto-ubiquitination and ubiquitination assays

In vitro ubiquitination assays were set up using recombinantly expressed proteins, using the reagents set out in Table 1. Ubiquitination buffer was made up of 0.5 mM ZnSO₄, 5 % glycerol, 10 mM Mg-ATP, 1 mM DTT, 50 mM MgCl₂ in 1X PBS). General *in vitro* ubiquitination assays are shown in Table 1. Reactions were carried out at 37 °C, with shaking, for 2-16 hours.

Table 1: General setup for *in vitro* auto-ubiquitination assay

Reagents	Reaction – MgATP	Reaction
His-E1	400 Nm	400 nM
E2 (Ubch 5b+c)	2 Mm	2 mM
E3	10 µg	10 µM
HA-ubiquitin	1 Mm	1 mM
Mg-ATP	-----	5 mM
Ubiquitination buffer	Added to final volume of 200 µl	Added to final volume of 200 µl

MG132, a proteasome inhibitor, was added to the proteasome to allow it to pre-incubate in order to give it time to inhibit proteasome activity. Proteasome without MG132 and proteasome pre-incubated with MG132 were added to the respective auto-ubiquitination reactions after the reaction had already taken place; i.e. after higher molecular weight species were already present. After incubation, proteins were precipitated with acetone at a concentration of 80 % for 1 hour, followed by resuspension in 2x sample buffer and subjected to SDS PAGE for immunoblotting.

Table 2: General setup for *in vitro* p53 ubiquitination assay

Reagents	Reaction – MgATP	Reaction
His-E1	400 Nm	400 nM
E2 (UbcH 5b+c)	2 Mm	2 mM
E3 (MDM2/R2)	10 μ M	10 μ M
Substrate (p53)	5 μ M	5 μ M
HA-ubiquitin	1 Mm	1 mM
Mg-ATP	-----	5 mM
Ubiquitination buffer	Added to final volume of 200 μ l	Added to final volume of 200 μ l

2.7 GST pull-down assays

GST-pull-down assays are used to investigate whether precipitation of one protein (the “bait”) can co-precipitate another (the “prey”), thereby demonstrating a physical interaction between them. GST-tagged protein (bait) was incubated with 20 μ l Glutathione agarose resin at 4 °C with rolling. After 1 hour, prey protein, with no attached GST tag, was added and allowed to incubate at 4 °C with rolling for 2-3 hours. Thereafter, the reaction samples were centrifuged at 10 000 rpm for 5 minutes and the supernatant discarded. Proteins bound to the agarose were washed with 1xPBS followed by 3x washes with 0.5 M NaCl, followed by 3x washes with SDS. Finally, the beads were resuspended in 20 μ l 2x sample buffer, boiled at 95 °C for 10 minutes and then subjected to SDS-PAGE, as described in Section 2.9. Western blotting, using antibodies raised against the prey protein, was carried out to detect whether prey protein had been co-precipitated along with the bait. A negative control was included in which the GST-tagged bait protein was replaced with GST alone, in order to show that prey protein was not co-precipitated in the absence of the bait protein.

2.8 Purification of proteasome out of human cell lysates

MCP21 hybridoma cells expressing antibodies targeting the α 2-subunit of the human proteasome were purchased from Sigma-Aldrich (Sigma-Aldrich, Missouri, USA). A co-worker in the laboratory cultured the hybridoma cells and harvested the serum from them. The α -proteasome antibody was coupled to Affi-gel Beads, as per the manufacturer's instructions (Bio-Rad, Hercules, California). The procedure was as follows: 500 μ l of Affi-gel beads were washed twice with an equal volume of ice-cold distilled water, centrifuged at 4300 *g* for 10 minutes and the supernatant discarded. The beads were then incubated with 1M ethanolamine for 1 hour at 4 °C with rolling. 100 μ g of anti-proteasome antibody-containing serum was added and allowed to incubate at 4 °C overnight with rolling. The antibody-coupled Affi-gel beads were then centrifuged at 4300 *rcf* for 10 minutes and the supernatant discarded. 1 M Tris pH 8.0 was added to the beads in order to prevent any other proteins from binding, followed by 3x washes with 1x PBS. Antibody-coupled Affi-gel beads were stored in 2ml 1x PBS containing 0.02% NaN₃.

Cultured HeLa cells were kindly provided by a co-worker in the laboratory. The cells were lysed as described in Section 2.4.2.1, after which 2.5 mM Mg-ATP was added to 100 μ g cell lysate and incubated with 100 μ l antibody-coupled Affi-gel beads overnight at 4 °C with rolling. The beads were centrifuged at 4300 *rcf* for 10 minutes at 4 °C followed by 3x PBS washes. Following the washes, the proteasome-coupled beads were resuspended in 200 μ l buffer with 5 mM Mg-ATP and stored at 4 °C for further use.

2.9 Analysis of proteins using SDS-PAGE

Protein samples were separated on 16 % SDS-PAGE gels, which were prepared as follows:

Resolving gel: 4 ml 40 % acrylamide:bis-acrylamide stock (Merck, Darmstadt, Germany), 2.63 ml 1.5 M Tris pH 8.8, 50 μ l 10 % ammonium persulphate (Merck, Darmstadt, Germany), 105 μ l 10 % SDS, 10 μ l TEMED (Sigma Aldrich, Missouri, USA) and 3.2 ml distilled water.

Stacking gel: 0.5 μ l 40 % 37:5:1 polyacrylamide, 25 μ l 10 % APS, 50 μ l 10 % SDS, 1.25 ml 1 M Tris pH 6.8, 10 μ l TEMED and 3.17 ml distilled water. The gels were cast in Mini-PROTEAN® Tetra handcast systems (BioRAD, Hercules, California USA).

Samples for SDS-PAGE electrophoresis were prepared by adding an equal volume of 2x sample buffer to the protein sample, followed by boiling at 95 °C for 10 minutes. 20 μ l of each

sample was loaded onto the SDS-PAGE gel. The samples were separated by electrophoresis using the Bio-Rad Mini-Protean system, at a voltage of 200 V.

Proteins were visualized by staining the gel with Coomassie (Sigma Aldrich, Missouri, USA) for 5 minutes on an orbital shaker followed by destaining in water overnight. Alternatively, the gel was processed for Western Blotting as described in Section 2.10.

2.10 **Western blot analysis**

Following separation on SDS-PAGE gels, proteins were transferred to a PVDF membrane using a Transblot Turbo Transfer device (BioRAD, Hercules CA, USA). Filter paper and membrane were first incubated in ice cold transfer buffer for 10 minutes. SDS-PAGE gels were then placed onto the PVDF membrane with 4 pieces of blotting paper on either side of the membrane. Following transfer, the membrane was incubated in 1 % casein for 1 hour in order to block non-specific binding of proteins. After blocking, the membrane was rinsed with 1x PBST followed by incubation in primary antibody for a minimum of 1 hour, after which the membrane was washed 3x with 1xPBST. This was followed by incubation with secondary antibody for 1 hour after which any unbound antibody was washed off with three 1x PBST washes. Western Blots were visualized by incubating the PVDF membrane with Clarity Western ECL substrate (BioRAD, Hercules CA, USA) and imaged using a BioSpectrum® UVP Imaging System (UVP, Upland CA, USA).

2.11 **Far Western Analysis**

Far Western blot analysis is an alternative to pull-down or immunoprecipitation assays for detecting protein-protein interactions. Whereas in the latter the interaction between the bait and prey proteins is carried out in solution, and detection of co-precipitated prey is visualized using Western Blot, in a Far Western Blot a number of bait proteins are separated on SDS-PAGE and then transferred to a membrane, which is then incubated with the bait. The membrane is then probed-using Western Blot using antibodies targeting the prey protein. If the bait and prey interact, a band will be observed at the MW of the bait protein.

In this case, untagged RBBP6 fragments were separated on the gel, which was then incubated with FLAG-tagged fragments of p53. Immunodetection was carried out using anti-FLAG antibodies.

CHAPTER 3: Investigation of the auto-ubiquitination potential of fragments of Retinoblastoma Binding Protein 6

3.1 Introduction

The RING finger motif is typically found in E3 ubiquitin ligases, which catalyze the ubiquitination of substrate proteins. The role of the RING finger is to recruit the ubiquitin-conjugated E2 enzyme to the substrate, which in turn is recruited by a substrate-specific binding motif. The presence of a RING finger domain in RBBP6 suggests strongly that it may function as an E3 ubiquitin ligase. A study conducted in 2007 by Li and co-workers, in knockout mice, showed that homozygous knock-out of the RBBP6 gene led to embryonic death due to overexpression of p53 and widespread ectopic apoptosis. The same study reported a direct interaction between MDM2 and RBBP6, the most important suppressor of p53 (Li *et al.*, 2007). However, the conclusion of the study was that RBBP6 functions by activating the ubiquitination activity of MDM2, rather than by having ubiquitination activity of its own. Li and co-workers proposed that RBBP6 plays the role of a non-enzymatic scaffolding protein, providing a surface on which p53 and MDM2 may interact.

Since then, RBBP6 has been shown to have its own ubiquitination activity, both *in vitro* and *in vivo*, against two proteins: the mRNA-associated Y-Box Binding Protein-1 (YB-1) and the DNA repair-associated protein zBTB38. Furthermore, preliminary results from our laboratory suggest that RBBP6 is able to catalyze ubiquitination of p53 without the assistance of MDM2, in contradiction of the conclusions of Li and co-workers.

In order to lend support to our findings that RBBP6 does have its own ubiquitination activity, in this thesis we decided to look more closely at its auto-ubiquitination potential. Preliminary results generated in our laboratory have suggested that the isolated RING finger of RBBP6 is able to catalyze its own auto-ubiquitination *in vitro*, and that this is sufficient to target the RING finger for degradation in the proteasome. Furthermore, mutants of the RING finger that are completely monomeric were still able to auto-ubiquitinate themselves, although perhaps less efficiently than wild type RING finger. If verified, these results would suggest that homo-dimerization of the RING finger promotes, but it not essential, for its auto-ubiquitination activity.

Auto-ubiquitination is a convenient proxy for ubiquitination, particularly in *in vitro* ubiquitination assays, since it does not require the presence of additional substrates in an already complex assay. It is assumed that many of the conclusions derived from auto-ubiquitination can be extended directly to substrate ubiquitination. If so, auto-ubiquitination should provide a convenient system for demonstrating that RBBP6 does have its own ubiquitination activity and for investigating whether homo-dimerization promotes auto-ubiquitination and, by extension, substrate ubiquitination. Hence the first objective of this thesis was to repeat the results showing the isolated RING finger can auto-ubiquitinate itself.

However, the *in vivo* auto-ubiquitination activity of the isolated RING finger is unlikely to provide a reliable representation of the *in vivo* activity of the full RBBP6 protein. All eukaryotic transcripts of RBBP6 contain the DWNN and zinc finger domains in addition to the RING domains. The corresponding fragment of full length human RBBP6 (residues 1-335), known in our laboratory as R3 and by other groups as RBBP6-N, has been hypothesized to be the minimal catalytic unit required for ubiquitination. Bio-informatics analysis suggests that the DWNN domain is separated from the zinc and RING finger domains by a flexible linker. This is supported by the fact that when all three domains of Mpe1 were crystalized in complex with the Ysh1 protein, only the DWNN domain was visible in the electron density, which suggests that the RING finger and zinc finger domains move independently of the DWNN domain (Hill *et al.*, 2019). Furthermore, when R3 is heterologously expressed in bacteria, there is a strong propensity for it to be proteolytically cleaved between the DWNN and zinc domain. The above provide reason to suspect that R2, a truncated form of R3 spanning residues 142-335, could possibly be the minimal catalytic subunit in the case of ubiquitination. If that is indeed the case, it raises the question as to whether the DWNN domain has any effect on the auto-ubiquitination potential of RBBP6. A study conducted on the E3 Parkin showed that an ubiquitin-like domain at the N-terminus of the protein was able to inhibit the ubiquitination potential of the enzyme (Chaugule *et al.*, 2011). Subsequent objectives were therefore to compare the auto-ubiquitination potentials of the R2 and R3 fragments to that of the isolated RING finger.

Unpublished results from our lab show that the R3 and R2 fragments both form homo-dimers in solution. In addition, the same mutations that monomerise the RING finger were unable to monomerise the R2 fragment, supporting the view that the surface across which the RING finger dimerises forms part of a larger surface including the zinc finger, and that therefore the R2 homo-dimer is a stronger dimer than the RING finger homo-dimer. If R2 is a stronger dimer

and if homo-dimerization promotes auto-ubiquitination, we may expect R2 to auto-ubiquitinate more efficiently than the isolated RING finger.

The aim of the investigations described in this chapter were to determine whether the conclusions arrived at using the isolated RING finger also apply in the case of R2. Particularly, whether R2 is able to auto-ubiquitinate and, if so, does it auto-ubiquitinate more efficiently than the isolated RING finger. We also set out to determine whether auto-ubiquitination of R2 is able to catalyze degradation in the proteasome, as was observed in the case of the isolated RING finger. Therefore, we decided to investigate whether bacterially expressed domains from RBBP6 were able to auto-ubiquitinate in *in vitro* assays. Before conducting experiments with R2, we began our investigation by confirming the results generated using the isolated RING finger and monomerisation mutants K313E and N312D. Previous RING auto-ubiquitination data generated in our laboratory used antibodies detecting ubiquitin specifically which would have resulted in the detection of auto-ubiquitinated proteins, as well as ubiquitin bound to other proteins within the assay sample. In our work, auto-ubiquitination was detected using antibodies targeting the HA-tag on HA-ubiquitin.

3.2 Investigation of the auto-ubiquitination potentials of RBBP6 fragments *in vitro*

3.2.1 Recombinant expression of R3, RING and monomeric mutants RING_{K313E} and RING_{N312D}

Expression constructs for the R3 and RING fragments of RBBP6, as well as the monomeric mutants RING_{K313E} and RING_{N312D}, were already available in our laboratory.

The pGEX-RBBP6-RING expression construct was transformed into *E. coli* Codon+ for expression. Induction of the *tac* promoter was carried out at 37 °C using an IPTG concentration of 0.5 mM, as described in Section 2.4.1 Since R3, RBBP6 RING, RING_{K313E} and RING_{N312D} all contain the RING finger and binds 2 zinc ions, 100 µM ZnSO₄ was added to the culture prior to induction, in order to provide sufficient zinc ions for incorporation into the over-expressed proteins. Following cell lysis, the GST-tagged proteins were separated from *E. coli* bacterial proteins using glutathione affinity chromatography, as described in Section 2.4.2.

Figure 3.1(A) indicates the successful elution of a band corresponding to GST RING in lanes 6-11, with an approximate molecular weight of 37 kDa. Fractions containing GST-RING were

pooled and concentrated, after which they were dialysed to remove free glutathione and perform cleavage of the fusion protein, as described in Section 2.4.2.3. Following dialysis and cleavage, the samples were returned to the glutathione agarose column in order to purify the RING protein away from the GST.

Figure 3.1(B) indicates the purification of cleaved RING finger. Lane 1 of Figure 3.1 (B) indicates the fusion protein before cleavage, lanes 2 and 3 indicate that the RING finger was not retained by the column and was present in the flow through and wash fractions, while lanes 5-7 indicate that the GST was retained by the column and was eluted by free glutathione. Fractions containing purified RING were pooled, concentrated and glycerol added to a final concentration of 10 %. The purified protein was stored at -20 °C for further use.

GST-R3-6His, incorporating a C-terminal 6His-tag, was expressed similarly. Figure 3.2(A) indicates elution of a band in lane 6 with an approximate molecular of 70 kDa, which is consistent with GST-R3-6His. Fractions containing GST-R3-6His were pooled and concentrated, after which they were dialysed to remove free glutathione and perform cleavage of the fusion protein, as described in Section 2.4.2.3. Following dialysis and cleavage, the samples were returned to the glutathione agarose column in order to purify the RING protein away from the GST.

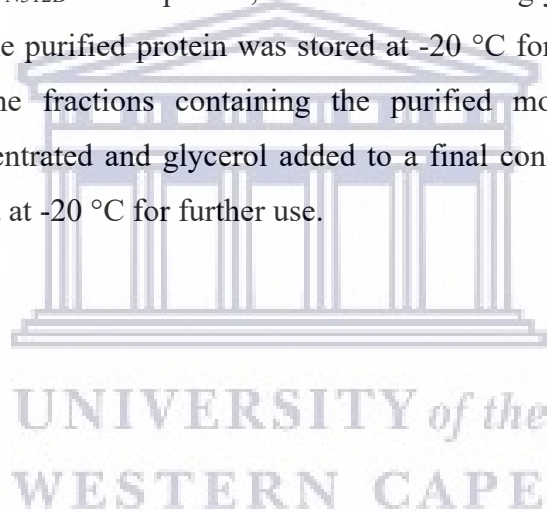
Figure 3.2(B) indicates the purification of cleaved R3-6His. Lane 1 of Figure 3.2(B) indicates the fusion protein before cleavage, lanes 2-4 indicate that the R3-6His was not retained by the column and was present in the flow through and wash fractions, while lanes 5-6 indicate that GST was retained by the column and subsequently eluted by free glutathione. Fractions containing purified R3-6His were pooled, concentrated and glycerol added to a final concentration of 10 %. The purified protein was stored at -20 °C for further use.

GST-RING_{K313E} and GST- RING_{N312D} were expressed similarly. Figures 3.3(A) indicates the elution of a band in lanes 6-9 with an approximate molecular weight of 37kDa, which is consistent with GST-RING_{K313E}. Fractions containing the fusion proteins were pooled and concentrated, after which they were dialysed to remove free glutathione and perform cleavage of the fusion protein, as described in Section 2.4.2.3.

Figure 3.3(B) indicates the purification of cleaved RING_{K313E}. Lane 1 of Figure 3.3(B) indicates the fusion protein before cleavage, lanes 2-4 indicate that the RING_{K313E} was not retained by the column and was present in the flow through and wash fractions, while lanes 5-7 indicate

that the GST was retained by the column and subsequently eluted by free glutathione. Fractions containing purified RING_{K313E} were pooled, concentrated and glycerol added to a final concentration of 10 %. The purified protein was stored at -20 °C for further use.

Figure 3.4(A) indicates the successful elution of a band corresponding to GST-RING_{N312D} in lanes 6-9 with an approximate molecular weight of 35kDa. Fractions containing the fusion proteins were pooled individually and concentrated, after which they were dialysed to remove free glutathione and perform cleavage of the fusion protein, as described in Section 2.4.2.3. Figure 3.4(B) indicates the purification of cleaved RING_{N312D}. Lane 1 of Figure 3.4(B) indicates the fusion protein before cleavage, lanes 2-5 indicate that the RING_{N312D} was not retained by the column and was present in the flow through and wash fractions, while lanes 6-8 indicate that the GST was retained by the column and subsequently eluted by free glutathione. Fractions containing purified RING_{N312D} were pooled, concentrated and glycerol added to a final concentration of 10 %. The purified protein was stored at -20 °C for further use. Following dialysis and cleavage, the fractions containing the purified monomeric mutants were individually pooled, concentrated and glycerol added to a final concentration of 10 %. The purified protein was stored at -20 °C for further use.



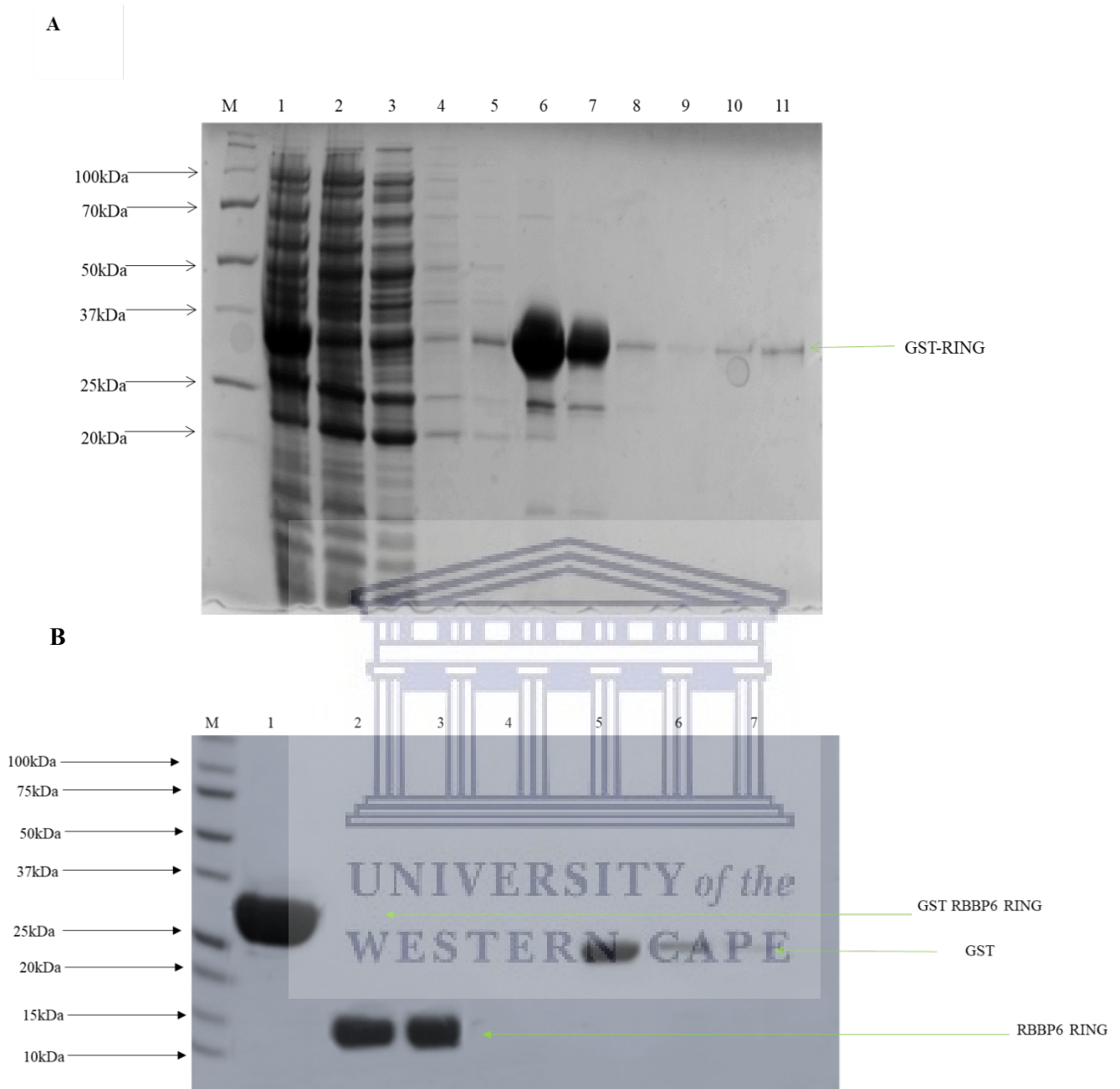


Figure 3.1: Recombinant expression and purification of GST-RING. (A) A protein of ~37 kDa, consistent with the size of GST-RING, is eluted from the glutathione-conjugated agarose column by free glutathione (lanes 6-11). Lane M indicates the molecular weight marker, lane 1 contains the pellet (insoluble protein), lane 2 indicates the lysate (soluble protein), lane 3 indicates the flow through, lanes 4 and 5 contain washes 1 and 3 respectively. (B) Purification of the isolated RING, following cleavage with 3C protease. Lane M indicates the marker, Lane 1, indicates the protein before cleavage with 3C protease, lane 2 is the flow through, lanes 3-4 are washes and lanes 5-7 are the fractions eluted from the glutathione agarose column.

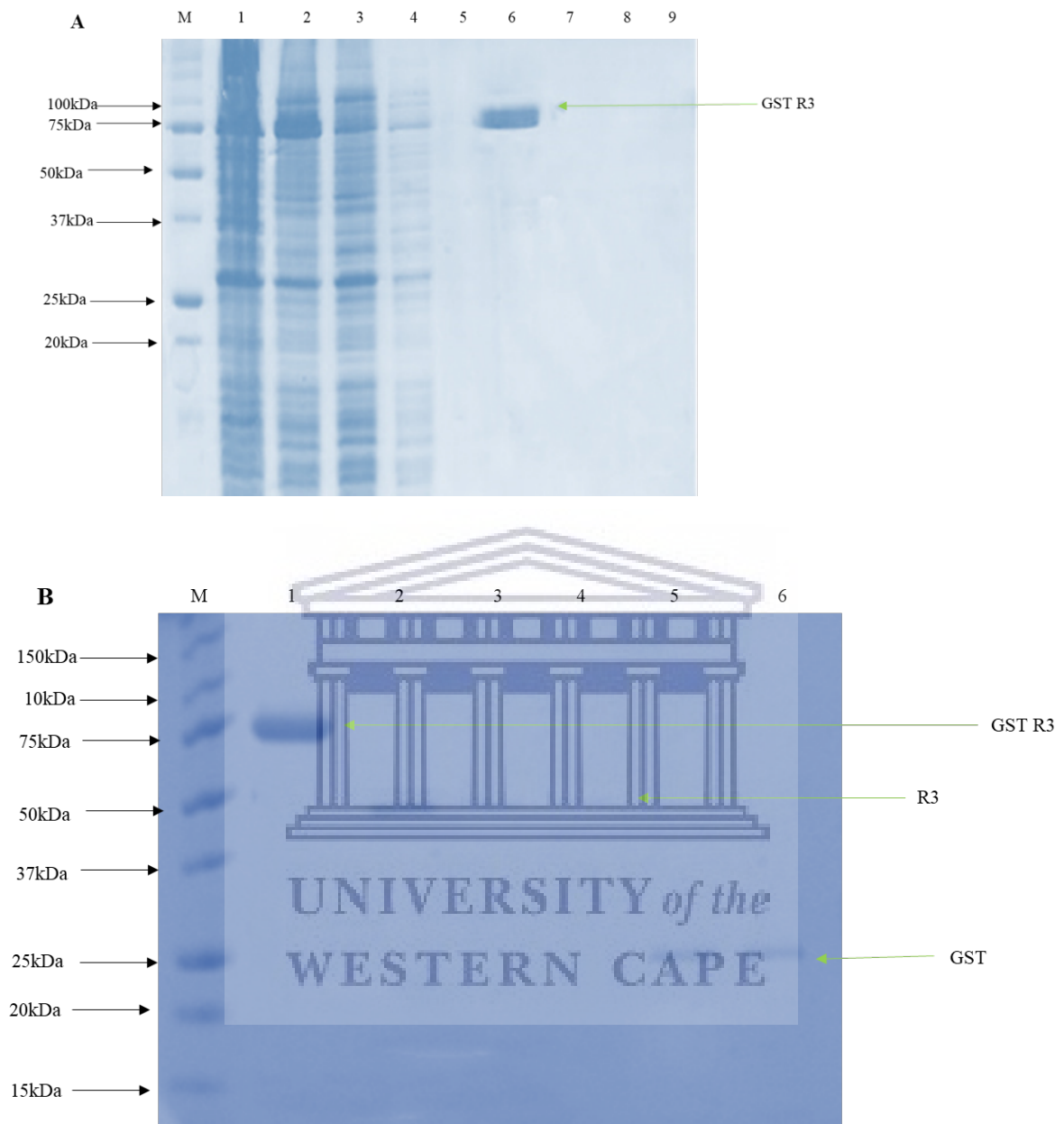


Figure 3.2: Recombinant expression and purification of GST-R3-6His. (A) A protein of ~70 kDa, consistent with the size of GST-R3, is eluted from the glutathione-affinity column by free glutathione (lanes 6-9). Lane M indicates the molecular weight marker, lane 1 contains the pellet (insoluble protein), lane 2 indicates the lysate (soluble protein), lane 3 indicates the flow through, lanes 4 and 5 contain washes 1 and 3, respectively. (B) Purification of GST-R3-6His following cleavage with 3C protease. Lane M indicates the marker, Lane 1, indicates the protein before cleavage with 3C protease, lane 2 is the flow through, lanes 3-4 are washes and lanes 5-6 are the fractions eluted from the glutathione agarose column.

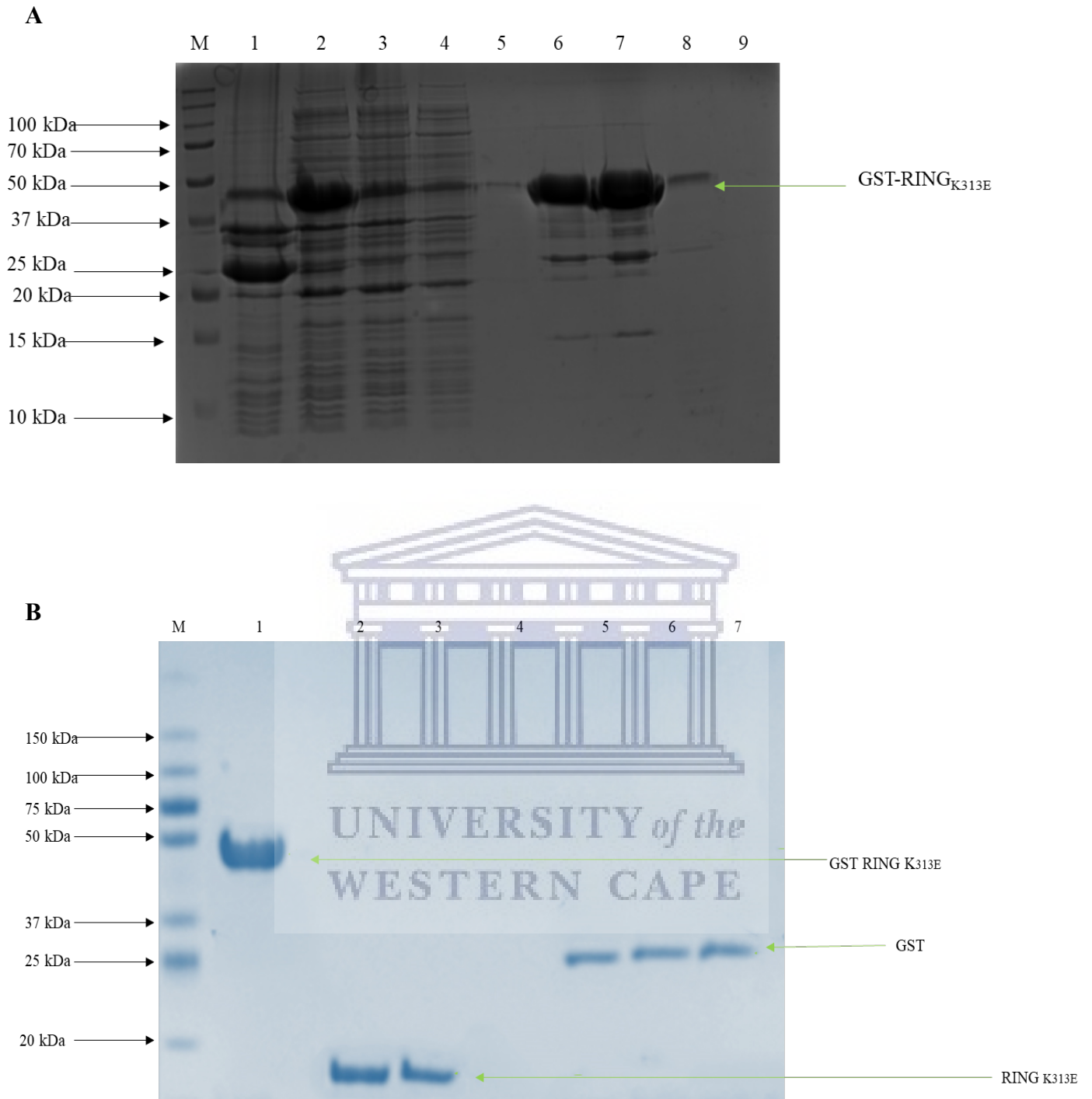


Figure 3.3: Recombinant expression and purification of GST-RING_{K313E}. (A) A protein of ~37 kDa, consistent with the size of GST-RING_{K313E}, is eluted from the glutathione-conjugated agarose column by free glutathione (lanes 6-9). Lane M indicates the molecular weight marker, lane 1 contains the pellet (insoluble protein), lane 2 indicates the lysate (soluble protein), lane 3 indicates the flow through, lanes 4 and 5 contains wash 1 and 3 respectively. (B) Purification of GST-RING_{K313E} following cleavage with 3C protease. Lane M indicates the marker, Lane 1, indicates the protein before cleavage with 3C protease, lane 2 is the flow through, lanes 3-4 are washes and lanes 5-7 are the fractions eluted from the glutathione agarose column.

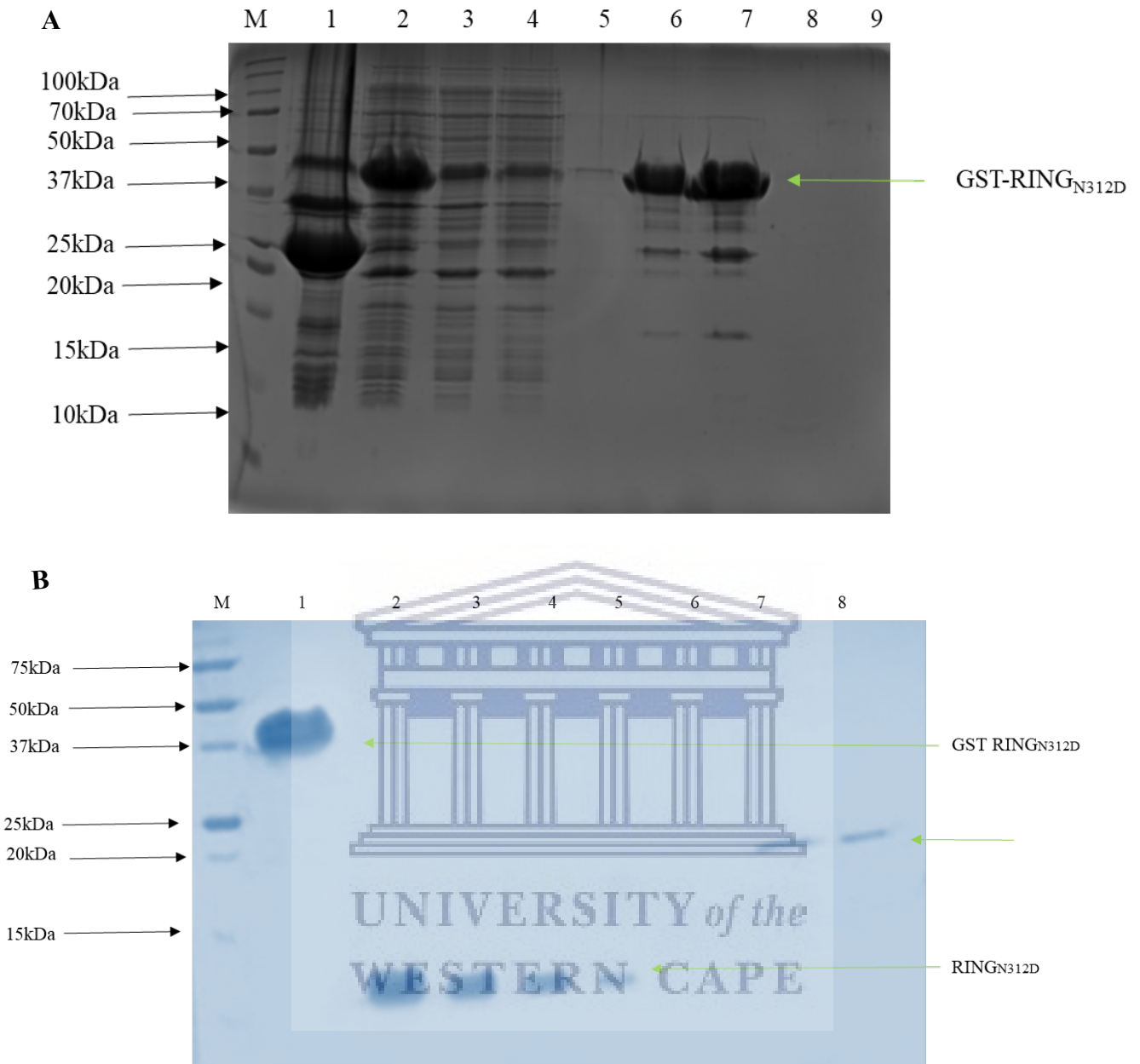


Figure 3.4: Recombinant expression and purification of GST-RING_{N312D}. (A) A protein of ~35 kDa, consistent with the size of GST-RING_{N312D}, is eluted from the glutathione-conjugated agarose column by free glutathione (lanes 6-9). Lane M indicates the molecular weight marker, lane 1 contains the pellet (insoluble protein), lane 2 indicates the lysate (soluble protein), lane 3 indicates the flow through, lanes 4 and 5 contains wash 1 and 3 respectively. (B) Purification of GST-RING_{N312D} following cleavage with 3C protease. Lane M indicates the marker, Lane 1, indicates the protein before cleavage with 3C protease, lane 2 is the flow through, lanes 3-5 are washes and lanes 6-8 are the fractions eluted from the glutathione agarose column.

3.2.2 Generation of the pGEX-R2-6His expression construct

The pGEX-R3-6His construct, codon-optimized for expression in *E. coli*, was used as a template from which to amplify pGEX-R2-6His. The primers were designed as shown in Table 3. The forward primer, incorporated a BamHI restriction site and the reverse primer an XhoI restriction site for directional cloning into pGEX-6P-2. Figure 3.5(A) shows successful amplification of R2-6His in lane 3, corresponding to the expected size of 615 bp. The PCR product was purified using a GeneJet gel purification Kit (GE Healthcare), digested with BamHI and XhoI and ligated into pGEX-6P-2, following digestion of the vector with BamHI and XhoI as described in Section 2.3.3. Subsequent ligation reactions were transformed into *E. coli* XL Gold competent cells and plated onto LB-amp agar plates. Plates were incubated at 37 °C overnight. Putative positive clones were selected from experimental plates and overnight cultures were prepared for plasmid DNA isolation. Plasmid DNA from the presumptive positive clones was isolated and subjected to restriction enzyme-mediated screening. Lanes 6-9 of Figure 3.5(B) shows successful amplification of an insert corresponding to the expected size of approximately 615 bp. Sequences were confirmed by direct sequencing (Inqaba Biotechnical Industries), and found to be 100 % in agreement with the expected sequence.

Table 3: Oligonucleotide primers for amplification of R2-6His. BamHI and XhoI restriction sites are indicated in purple and green respectively. Annealing regions are underlined.

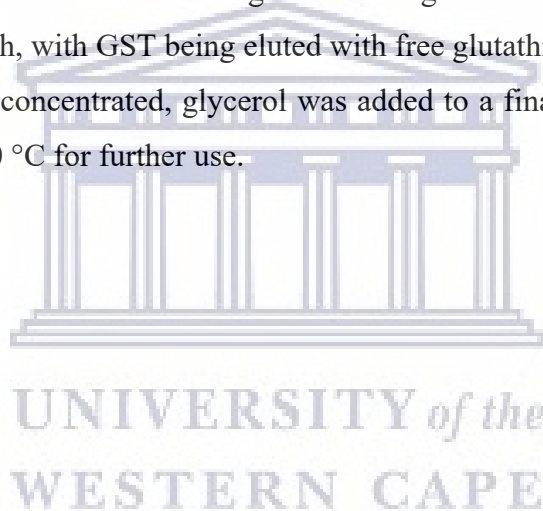
Name	DNA sequence	T _m (°C)
R2-F	5'- GAG GCG <u>GGA TCC</u> <u>GAC CCG ATC AAC</u> TAC ATG AAA AA -3'	64
R2-R	5'- GAG GCG <u>CTC GAG</u> <u>TTA TTA ATG ATG</u> ATG ATG -3'	64

3.2.3 Recombinant expression of pGEX-R2-6His

Expression of GST-R2-6His, using the pGEX-R2-6His construct, was carried out as described above. Figure 3.6(A) (lanes 5-9) indicates the successful elution of a band with an approximate molecular weight of 50 kDa, corresponding to GST-R2-6His. The band corresponding to GST-R2-6His can also be seen in the flow through (lane 3), which indicates that the capacity of the

column was insufficient to retain all of the protein. Fractions containing GST-R2-6His were pooled and concentrated, dialyzed into dialysis buffer. An aliquot was made and glycerol was added to a concentration of 10 %, after which it was stored at -20 °C for use in GST-pull-down assays.

The remaining GST-R2-6His was cleaved and dialyzed as described in Section 2.4.2.3 to remove free glutathione within the sample. Figure 3.6(B) indicates the purification of cleaved R2-6His. Lane 1 of Figure 3.6(B) indicates the fusion protein before cleavage, lanes 2-3 indicate that the R2-6His was not retained by the column and was present in the flow through while lanes 4 and 6 indicate that the GST was retained by the column and was eluted by free glutathione. Fractions containing purified R2-6His were pooled, concentrated and glycerol added to a final concentration of 10 %. The purified protein was stored at -20 °C for further use. Cleaved samples were returned to the glutathione agarose column and R2-6His was collected in the flow through, with GST being eluted with free glutathione. Fraction containing R2-6His were pooled and concentrated, glycerol was added to a final concentration of 10 % and they were stored at -20 °C for further use.



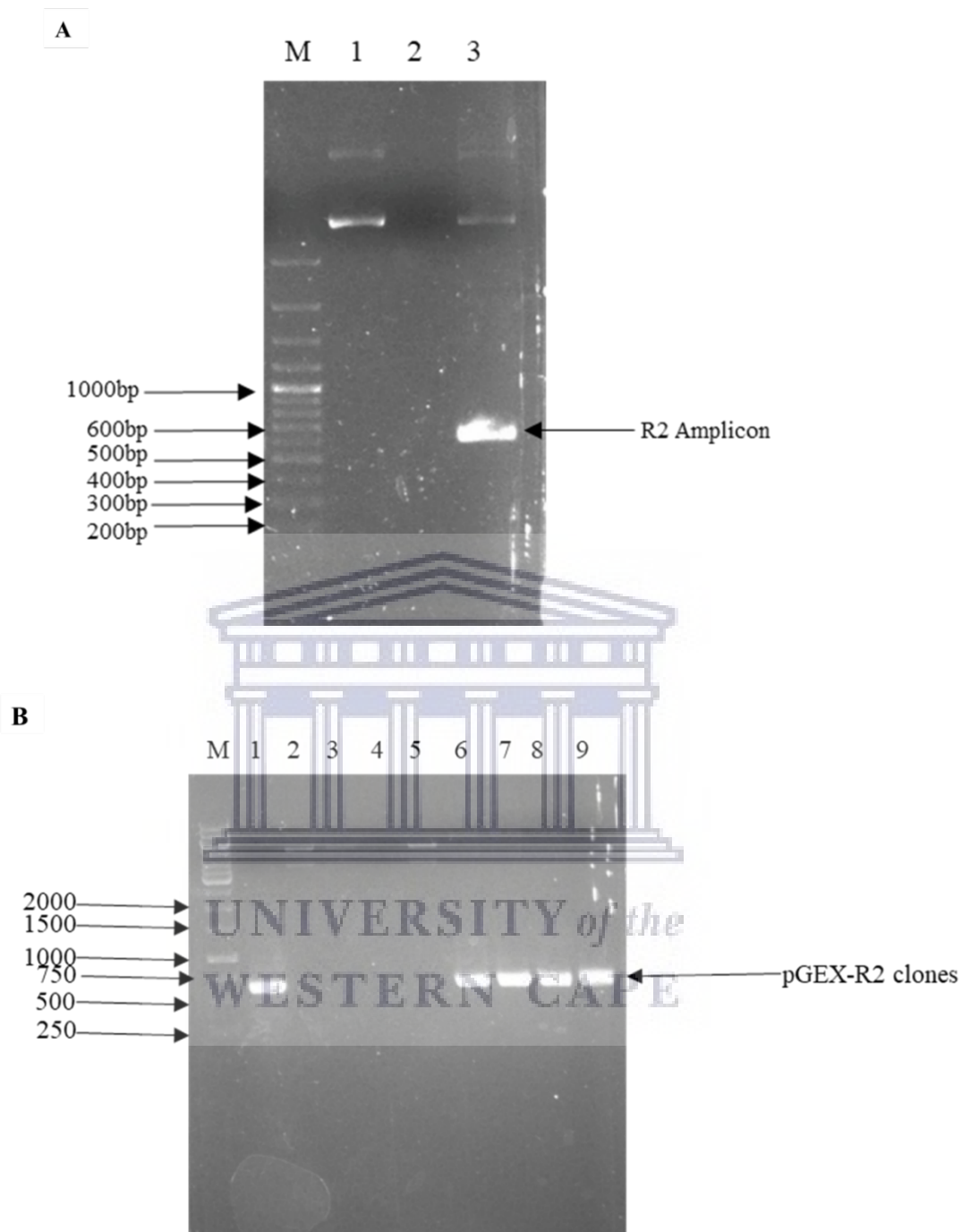


Figure 3.5: Cloning of pGEX-R2-6His. (A) The R2-6His amplicon was amplified from pGEX-R3-6xHis with a size of approximately 615 bp, as can be seen in lane 3. (B) Confirmation of putative clones using colony PCR. The bands in lanes 6-9 are consistent with the expected insert size of 615 bp.

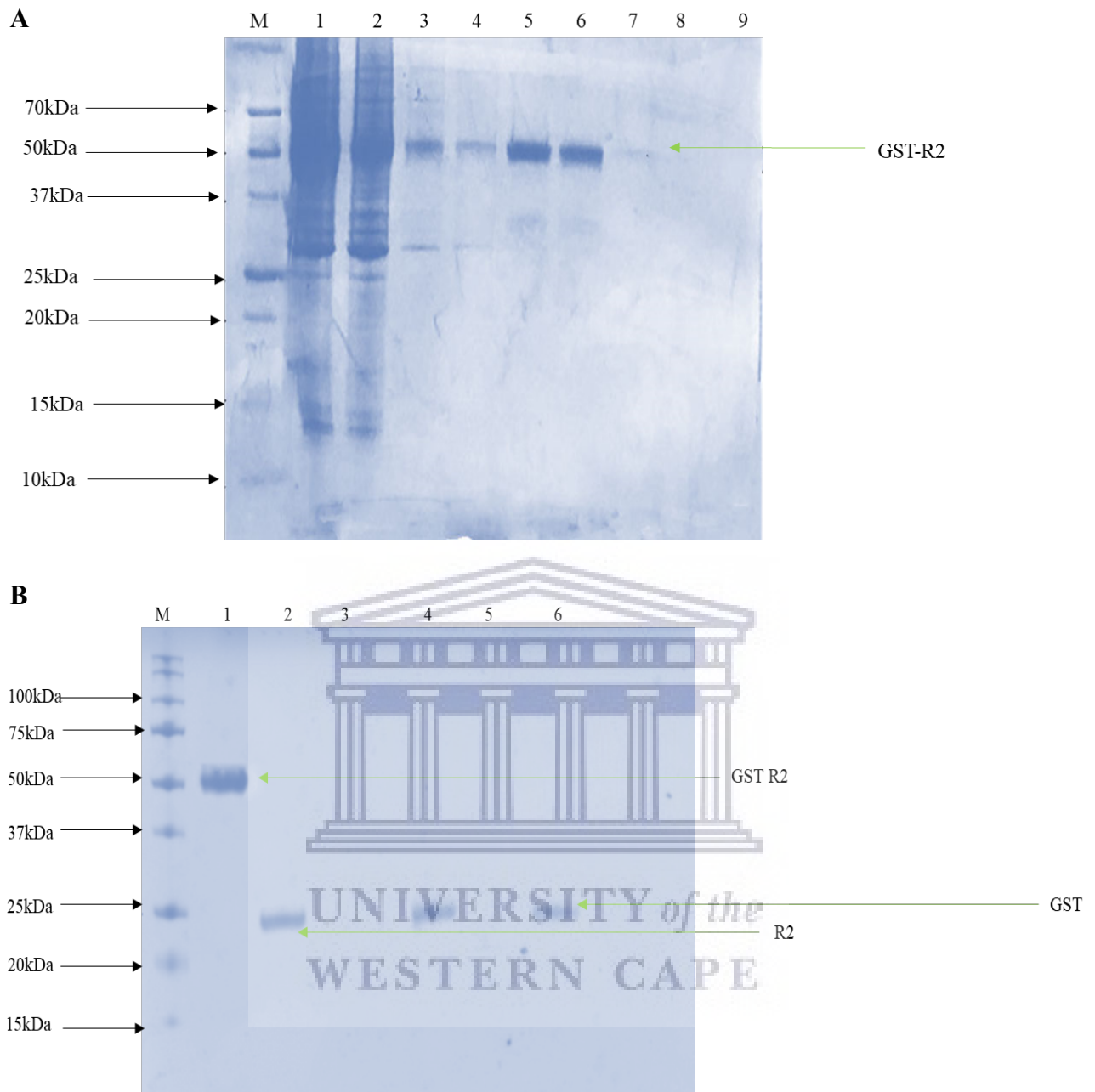


Figure 3.6: Recombinant expression and purification of GST-R2-6His. (A) A protein of ~50 kDa, consistent with the size of GST-R2, is eluted from the glutathione-conjugated agarose column by free glutathione (lanes 5 and 6). Lane M indicates the molecular weight marker, lane 1 contains the lysate (soluble protein), lane 2 indicates the flow through, lanes 3 and 4 contains wash 1 and 3 respectively. Lanes 5-9 contain the fractions eluted from the glutathione agarose column by addition of free glutathione. (B) Purification of GST-R2-6His. following cleavage with 3C protease. Lane M indicates the marker, Lane 1, indicates the protein before cleavage with 3C protease, lane 2 is the flow through, lanes 3 are washes and lanes 4 and 6 are the fractions eluted from the glutathione agarose column.

3.2.4 Bacterial expression and purification of associated ubiquitination enzymes

All of the above proteins were intended to serve as E3 ligases. A number of associated proteins were expressed in bacteria by the author, using expression plasmids available in the laboratory. These were human E1 enzyme, the E2 enzymes UbcH5b and UbcH5c, and HA-tagged ubiquitin (data not shown). Purification of the proteasome was also carried out by the author, as described in Section 2.8.

3.3 Investigation of the auto-ubiquitination potentials of fragments of RBBP6 and RING monomeric mutants

Bacterially-expressed R3, R2, wild-type RBBP6 RING and the RING_{K313E} and RING_{N312D} mutants were used as E3 enzymes in fully *in vitro* auto-ubiquitination assays. The assays were set up as described in Section 2.8. Ubiquitinated species were detected by western blotting with antibody targeting the HA-tag on the ubiquitin. A well-established characteristic of poly-ubiquitination is its ability to catalyze the degradation of the target protein in the 26S proteasome, which is closely associated with lysine48-linked poly-ubiquitin chains. To determine whether auto-ubiquitination of the RBBP6 fragments rendered it susceptible to degradation by the 26S proteasome, intact proteasome purified from mammalian cell lysates were added to the experimental reactions, as described in Section 2.8.

The screen was first conducted using a number of bacterially expressed E2s, namely UbcH6, UbcH8, UbcH1 (all expressed by a co-worker, Dr Andrew Faro) and UbcH5a-c, in order to identify one or more E2 enzymes which catalyse auto-ubiquitination in combination with the fragments of RBBP6. The screen was conducted using bacterially expressed R3 and results indicated that UbcH5b and UbcH5c were the most effective (data not shown).

3.3.1 Auto-ubiquitination of the isolated RING finger and monomerising mutants

Previous data generated in our lab by Ms Matodzi Portia Maumela showed substantial auto-ubiquitination of the wild type RING finger, corresponding to molecular weights far exceeding 200 kDa. Auto-ubiquitination of the monomeric mutants N312D and K313E was also observed, although it was possibly less efficient than in the case of wild type RING. From this data it was deduced that auto-ubiquitination can be catalyzed by monomeric RING finger, although it appears to be more efficient when the RING finger is dimeric. Addition of purified proteasome

almost totally abolished the higher molecular weight species in the case of wild type RING, and to a lesser extent in the case of the N312D and K313E mutants. This indicates that the higher molecular weight species correspond to the attachment of poly-ubiquitin chains, rather than addition of single ubiquitin molecules to multiple lysine's on the target (known as "multiple mono-ubiquitination").

The investigations in this chapter begin with repetition and confirmation of the above results.

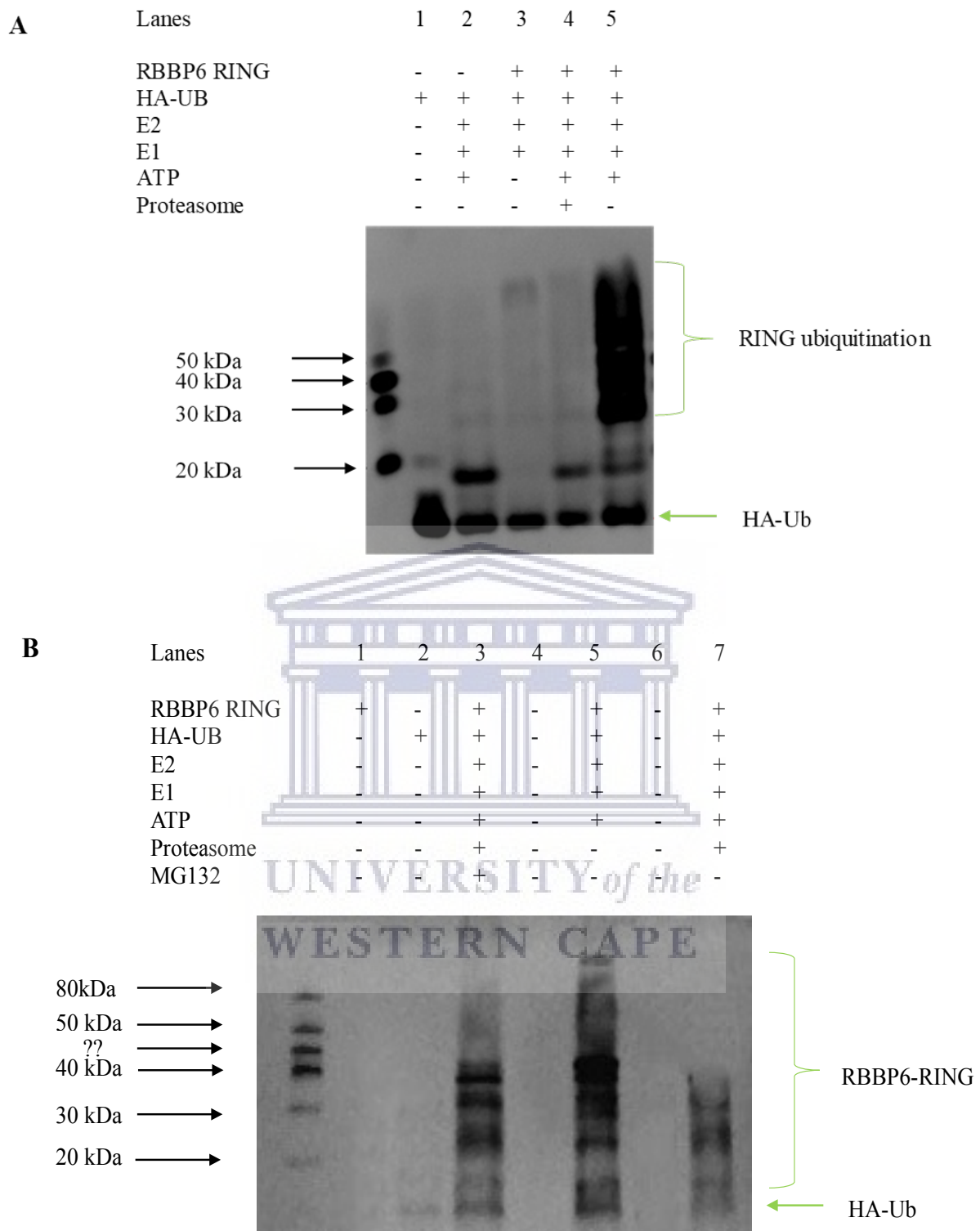
Lane 5 of Figure 3.7 (A) shows that the isolated RING finger from RBBP6 is able to auto-ubiquitinate itself very efficiently in the presence of Mg-ATP, E1, E2 and HA-ubiquitin. Significantly, minimal auto-ubiquitination is observed when Mg-ATP is omitted (lane 3), confirming that the effect is ATP-dependent, which is a requirement for a ubiquitination reaction. Based on these results, we concluded that omitting ATP from subsequent reactions (rather than E1 or E2, for example) would serve as a useful negative control in all of our auto-ubiquitination assays. When purified proteasome was added to the reaction (lane 4), the higher MW bands disappeared, indicating that the auto-ubiquitination was sufficient to target the RING finger to the proteasome. This suggests that the higher MW bands consist of lysine48-linked poly-ubiquitin chains, since these are most strongly associated with proteasomal targeting. Lane 1 of Fig 3.7 contains only HA-tagged ubiquitin, and confirms that the signals detected by the anti-HA antibody originate from the HA-tagged ubiquitin. Lane 2 demonstrates that poly-ubiquitination only takes place in the presence of the RING finger, and does not involve the assembly of free-floating poly-ubiquitin chains, as has been observed in other ubiquitination reactions.

A similar result is seen in lane 5 of panel B. The high MW species disappear following addition of purified proteasome (lane 7), leaving lower MW species consistent with multi-ubiquitination. However, if the proteasome is pre-incubated with MG132, the higher MW bands are partially rescued (lane 3). This result is significant because it shows that removal of the ubiquitination is due to the proteasome, which is specifically inhibited by MG132, and not due to de-ubiquitination activity co-purified with the proteasome, which is not inhibited by MG132.

RING_{K313E} is a mutant form of the isolated RING which was previously reported to be entirely monomeric in solution (Kappo *et al.*, 2012). Figure 3.8 shows that RBBP6 RING_{K313E} is able to auto-ubiquitinate itself in the presence of Mg-ATP, E1, E2 and ubiquitin (lane 5), but not in the absence of ATP (lane 4). The addition of purified proteasome to the sample in lane 5 leads to complete abolition of the higher molecular weight species (lane 6), indicating that RING_{K313E}

was targeted for degradation by the 26S proteasome. Pre-incubation of the proteasome with MG132 leads to rescue of the higher MW bands (lane 8), confirming that the proteasome is responsible for the degradation in lane 6 and not de-ubiquitination activity co-purifying with the proteasome. It should be noted that lanes 5, 6 and 8 are derived from the same auto-ubiquitination reaction; following completion of the reaction, the sample was divided into three aliquots, and proteasome was added to one (lane 6), proteasome pre-incubated with MG132 was added to another (lane 8) and nothing was added to the last (lane 5). Hence the absence of higher molecular weight bands in lane 6 is not due to failure of the auto-ubiquitination reaction, and so can only be due to the presence of proteasome. Again, the fact that the auto-ubiquitination is rescued by MG132 indicates that the effect is due to degradation in the proteasome, which is specifically inhibited by MG132, rather than de-ubiquitination by proteases co-purifying with the proteasome, which are not inhibited by MG132.





3.7: Auto-ubiquitination and proteasomal degradation of the isolated RING finger from RBBP6. (A) Wild type RING is ubiquitinated in the presence of ubiquitin, E1 and E2 and ATP (lane 5), but not in the absence of ATP (lane 3). When purified proteasome was added to the sample in lane 5, the higher MW bands disappeared, indicating that the auto-ubiquitination was sufficient to target the RING finger to the proteasome (lane 4). (B) Higher MW species consistent with poly-ubiquitination (lane 5), disappear following addition of purified proteasome, leaving lower MW species consistent with multi-ubiquitination (lane 7). However, if the proteasome is pre-incubated with MG132 the higher MW bands are partially rescued (lane 3).

Since the RING_{K313E} is known to be monomeric, it is clear from Figure 3.8 that homo-dimerisation is not required for auto-ubiquitination of the isolated RING finger. Nevertheless, the amount of auto-ubiquitination in Figure 3.8 (lane 5) does appear to be less than that in Figure 3.8A (lane 4); since the same amount of RING was used in both assays, it may suggest that the auto-ubiquitination potential of the partial homo-dimer may be somewhat greater than that of the monomer. However, since the mutant and the wild type were not used in the same assay, comparison is difficult and therefore the assays should be repeated under identical conditions. Furthermore, measurements performed using nuclear magnetic resonance spectroscopy estimated that the dissociation constant of the RING homo-dimer is in the region of 100 μ M. Since the effective concentration of RING used in these assays is 10 μ M, we conclude that the wild type is primarily monomeric in these assays. The strong auto-ubiquitination observed in Figures 3.6 and 3.7 therefore suggests that, even in its monomeric form, the wild type RING is nevertheless strongly auto-ubiquitinated.

The same result is seen for the N312D mutant of the isolated RING, which is also entirely monomeric, as shown in Figure 3.9A. RING_{N312D} auto-ubiquitinates itself in the presence of Mg-ATP, E1, E2 and ubiquitin (lane 5) but not in the absence of ATP (lane 4). The addition of purified proteasome to the sample in lane 5 leads to the complete abolition of the higher molecular weight species (lane 6), indicating that RING_{N312D} was targeted for degradation in the 26S proteasome. The same result is seen in panel B; RING_{N312D} is auto-ubiquitinated (lane 4), but addition of the proteasome to the sample in lane 4 leads to disappearance of the higher MW species (lane 2). The higher molecular weight bands are rescued when the proteasome is pre-incubated with MG132 (lane 3). Although the same amount of RING_{N312D} was used here as wild type RING in Figure 3.7 and RING_{K313E} in Figure 3.8, the intensity of the higher molecular weight bands appears to be less intense, which perhaps provides evidence for the conclusion that the monomeric mutant is auto-ubiquitinated less efficiently than wild type (partially dimeric) RING. However, these assays should be repeated under identical conditions.

Previous data of RBBP6-RING auto-ubiquitination generated in our laboratory used anti-ubiquitin antibodies to detect auto-ubiquitinated species, whereas the data generated in this chapter used anti-HA antibodies to target the HA tag on the ubiquitin. The fact that the results obtained are essentially identical confirms that the previous data was reliable and did not depend on the antibody used.

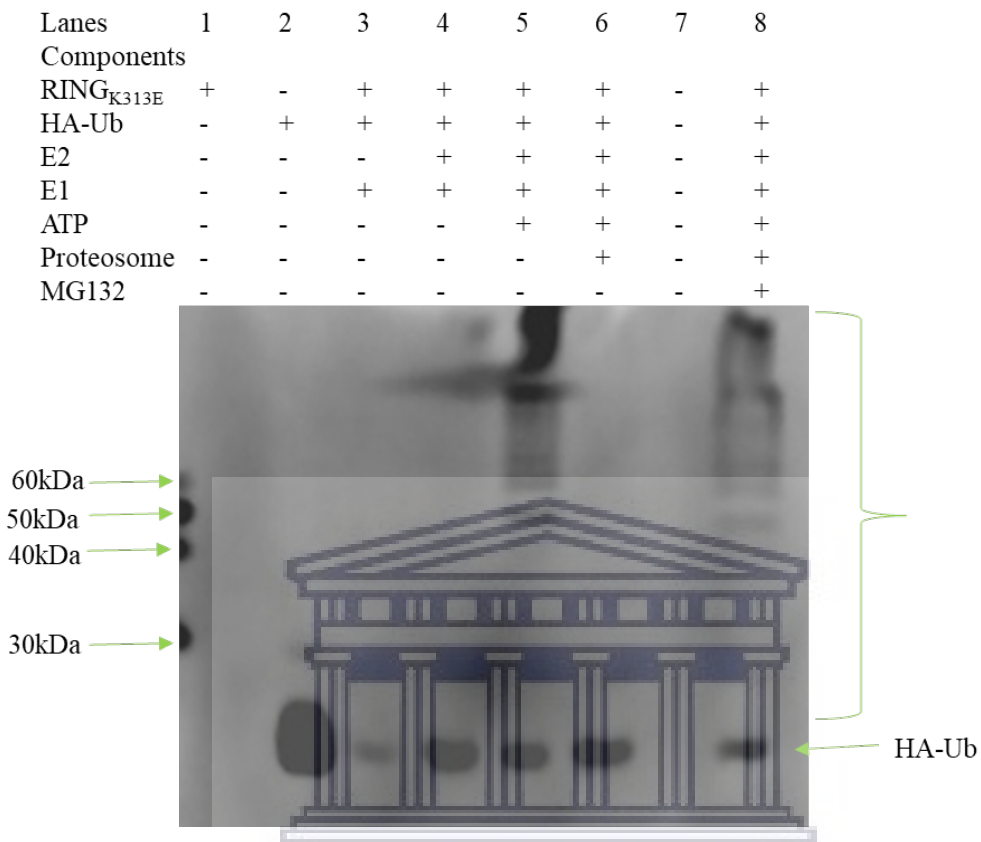
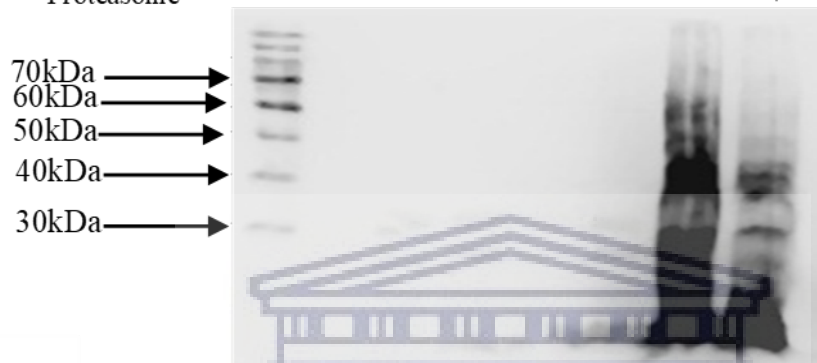


Figure 3.8: Auto-ubiquitination and proteasomal degradation of the RING_{K313E} monomeric mutant. (A) RING_{K313E} is ubiquitinated in the presence of ubiquitin, E1 and E2 and ATP (lane 5), but not in the absence of ATP (lane 4) and not in the presence of purified proteasome (lane 6). RING_{K313E} auto-ubiquitination is rescued by the addition of MG132 which is indicated by the presence of the higher molecular weight bands in the presence of proteasome and MG132 (lane 8).

A

Lanes	1	2	3	4	5	6
RBBP6 RING _{N312D}	-	+	+	+	+	+
HA-UB	+	-	+	+	+	+
E2	-	-	-	+	+	+
E1	-	-	+	+	+	+
ATP	-	-	-	-	+	+
Proteasome	-	-	-	-	-	+

**B**

Lanes	1	2	3	4
RING _{N312D}	-	+	+	+
HA-UB	+	+	+	+
E2	-	+	+	+
E1	-	+	+	+
ATP	-	+	+	+
Proteasome	-	+	+	+
MG132	-	-	+	-

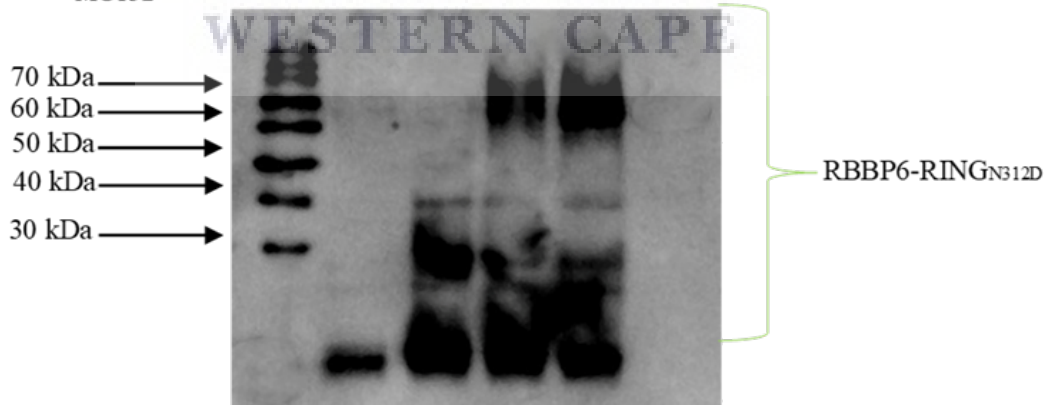


Figure 3.9: Auto-ubiquitination and proteasomal degradation of the RING_{N312D} monomeric mutant(A) RING_{N312D} is ubiquitinated in the presence of ubiquitin, E1 and E2 and ATP (lane 5), but not in the absence of ATP (lane 4) and not in the presence of purified proteasome (lane 6). (B) Higher MW species consistent with auto- ubiquitination (lane 3) However, if the proteasome is pre-incubated with MG132 the higher MW bands are partially rescued (lane 4).

3.3.2 Auto-ubiquitination of the R3 fragment of RBBP6

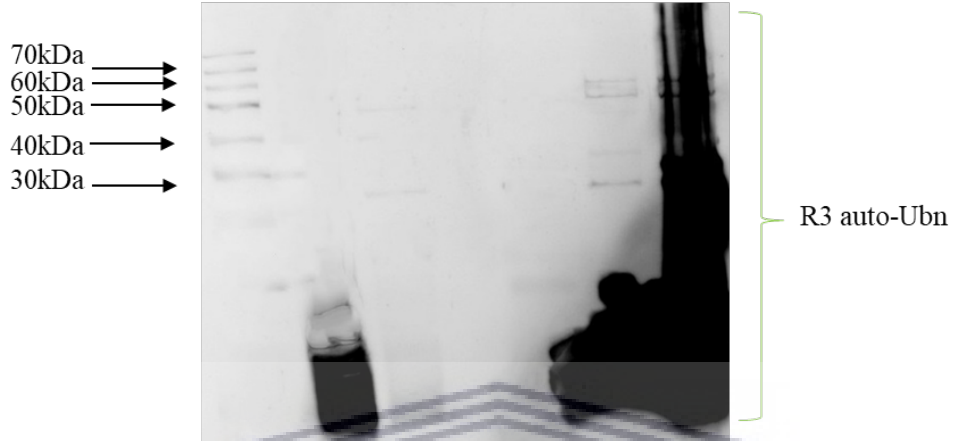
Panel A of Figure 3.10 shows that R3 is able to auto-ubiquitinate itself in the presence of Mg-ATP, E1, E2 and ubiquitin (lane 6), but not in the absence of ATP (lane 4). No auto-ubiquitination was observed when the sample in lane 6 was pre-incubated with purified proteasome (lane 5), which indicates that the ubiquitination was sufficient to target R3 to the 26S proteasome.

The ladder in lane 6 extends right up to the top of the western blot, and well past the 100 kDa marker, suggesting that the bands correspond to poly-ubiquitination. However, the marker no longer provides a reliable estimate of the molecular weight of the bands; in addition, at this molecular weight the PAGE gel may no longer follow the expected behavior. However, R3 itself has a molecular weight of 30 kDa, and each ubiquitin moiety has a molecular weight of 8 kDa. There are 32 lysine residues in R3 and therefore 32 possible attachment sites for ubiquitin's. It is therefore not impossible that the data correspond to multiple mono-ubiquitination, where a single ubiquitin is attached to a number of different lysine's, rather than poly-ubiquitination, where multiple ubiquitin's are attached to a single lysine. However, the fact that the high-MW species can be removed by addition of purified proteasome is strong evidence that the bands correspond to lysine48-linked poly-ubiquitination at one or more sites.

Panel B shows even more efficient auto-ubiquitination of R3 (lane 5), stretching right up to the top of the lane, which is almost totally removed by subsequent addition of purified proteasome (lane 3). As seen previously, the bands are rescued by addition of MG132, confirming that degradation in the proteasome is responsible for the loss of high molecular weight bands, which is selectively inhibited by MG132, rather than by de-ubiquitinating enzymes co-purifying with the proteasome, which are not inhibited by MG132.

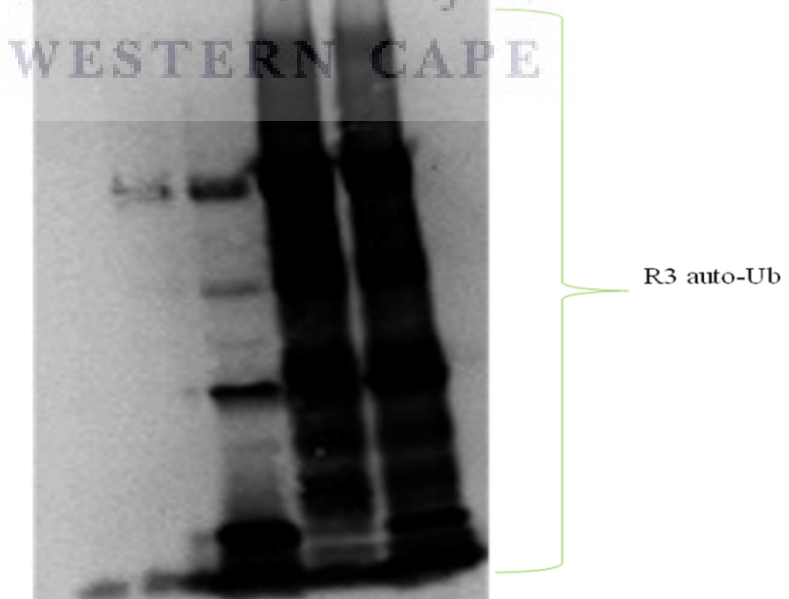
A

Lanes	1	2	3	4	5	6
R3	-	+	+	+	+	+
HA-Ub	+	+	-	+	+	+
E2	-	-	-	+	+	+
E1	-	+	-	+	+	+
ATP	-	-	-	-	+	+
Proteasome	-	-	-	-	+	-



B

Lanes	1	2	3	4	5
R3	-	+	+	+	+
HA-Ub	+	+	+	+	+
E2	-	+	+	+	+
E1	-	-	+	+	+
ATP	-	-	+	+	+
Proteasome	-	+	+	+	+
MG132	-	-	-	+	-



C

Lanes	1	2	3	4	5
R3	+	+	+	+	+
HA-UB	+	+	+	+	+
E2	+	+	+	+	+
E1	+	+	+	+	+
ATP	+	+	+	+	+
Proteasome	+	+	+	+	+
MG132	+	+	+	+	+

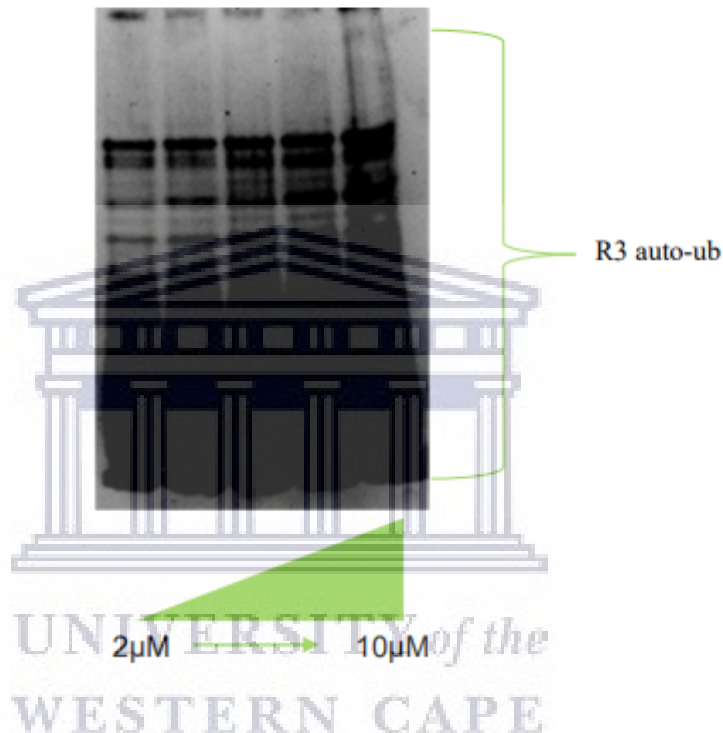


Figure 3.10: Auto-ubiquitination and proteasomal degradation of the R3 fragment of RBBP6. (A) R3 is able to auto-ubiquitinate itself in the presence of Mg-ATP, E1, E2 and ubiquitin (lane 6), but not in the absence of ATP (lane 4). No auto-ubiquitination was observed when the sample in lane 6 was incubated with purified proteasome prior to loading on the gel (lane 5), which indicates that the ubiquitination was sufficient to target R3 to the 26S proteasome. (B) Auto-ubiquitinated species in lane 5 are efficiently removed by addition of proteasome (lane 3), but are rescued from proteasomal degradation when the proteasome is pre-incubated with 15 μ M MG132 (lane 4). (C) The auto-ubiquitinated species shown in lane 6 of panel A are partially rescued from proteasomal degradation by pre-incubation with increasing concentrations of MG132 (lanes 1-5). The maximum concentration of MG132, 10 μ M, is less than the 15 μ M used in panel B, which may therefore account for the incomplete rescue.

The results in Figure 3.10(B) show that R3 is able to auto-ubiquitinate itself in the presence of Mg-ATP, E1, E2 and ubiquitin (lane 5), but not in the absence of ATP (lane 2). No auto-ubiquitination was observed when the sample in lane 5 was pre-incubated with purified proteasome (lane 3), which indicates that the ubiquitination was sufficient to target R3 to the

26S proteasome The ladder in lane 5 extends right up to the top of the western blot, and well past the 100 kDa marker, suggesting that the bands correspond to poly-ubiquitination. Ladder in lane 4 shows that with the addition of MG132 pre-incubated proteasome, higher molecular weight species were recovered. Panel C confirms that MG132 inhibits the proteasome in a dose-dependent manner. At the lowest MG132 concentration the bands are almost completely removed, consistent with what is seen in lane 3 of Fig 3.10B. However, the highest concentrations of MG132 are insufficient to rescue all of the poly-ubiquitinated species. Had more MG132 been added, it is likely that complete recover of the poly-ubiquitinated species would have been observed.

MG132 is made up in DMSO (the vehicle). To confirm that MG132 was responsible for inhibition of the proteasome and not the DMSO, DMSO was used as a vehicle control in a set of experiments (data not shown). The results showed that DMSO alone was not able to rescue the high-MW bands, whereas 15 μ M MG132 dissolved in the same amount of DMSO was able to rescue the high-MW bands. Hence, we conclude that MG132 was responsible for blocking degradation of the high-MW bands by the proteasome, and not the DMSO.

3.3.3 Auto-ubiquitination of R2

Figure 3.11 shows that the above results apply also to the R2 fragment. In panel (A), R2 is able to auto-ubiquitinate itself in the presence of Mg-ATP, E1, E2 and ubiquitin (lane 5), but not in the absence of ATP (lane 3). Significantly less auto-ubiquitination is observed when the sample in lane 5 was subsequently incubated with purified proteasome, which indicates that the R2 was targeted for degradation by the 26S proteasome. As in the case of R3, the molecular weight marker is not clear enough to allow an accurate estimate of the MWs of the highest bands, and therefore does not rule out the possibility that the bands may correspond to multiple mono-ubiquitination, rather than pol-ubiquitination. However, the sensitivity of the high-MW bands to degradation in the proteasome strongly suggests that at least some of the bands correspond to lysine48-linked poly-ubiquitination.

Note that there is a striking similarity between Figure 3.7(A), which involves RING, and Figure 3.11(A), which involves R2. Despite the similarity, they are in fact different blots, as can be seen from the differences in the MW markers. Also note the band at just less than 20 kDa in lanes 2, 4 and 5. Since it is present in lane 2 it cannot involve R2. And since it is not present in

lane 3, it is ATP-dependent, but its size is too small for either Ub-conjugated E1 or E2. It is possible that it corresponds to isopeptide-bonded di-ubiquitin.

To confirm that the disappearance of high-MW bands in lane 5 is due to the proteasome, and not de-ubiquitination activity accompanying the purified proteasome, the proteasome was pre-incubated with MG132 prior to addition to the sample in lane 5. The results are shown in panel B. Pre-incubation of the proteasome with MG132 (lane 4) restored much of the auto-ubiquitination present when the proteasome was not added at all (lane 3). The result would have been even more persuasive had the effect of the un-inhibited proteasome (lane 4 of panel A) also been demonstrated in panel B. Nevertheless, the conclusion is clear: auto-ubiquitination of R2 is sufficient to catalyze degradation in the 26S proteasome, and the effect can be inhibited by MG132.

The above results confirm that the R3 fragment is sufficient to catalyze auto-ubiquitination of RBBP6 and target it for degradation in the 26S proteasome. Hence it suggests a mechanism whereby RBBP6 can keep its own levels low when not required, and may account for the low levels of RBBP6 in most human tissues.

One of the aims of this work was to investigate whether R2, which is known to be more strongly homo-dimeric than the isolated RING, auto-ubiquitinates itself more efficiently than the isolated RING. Answering that question conclusively was hampered by the lack of fully monomeric forms of R2; the mutants which are known to monomerise the RING were not able to monomerise R2. It was originally intended to search for second mutants (possibly in the zinc finger domain) which would be sufficient to monomerise R2, but time did not allow for this to be pursued.

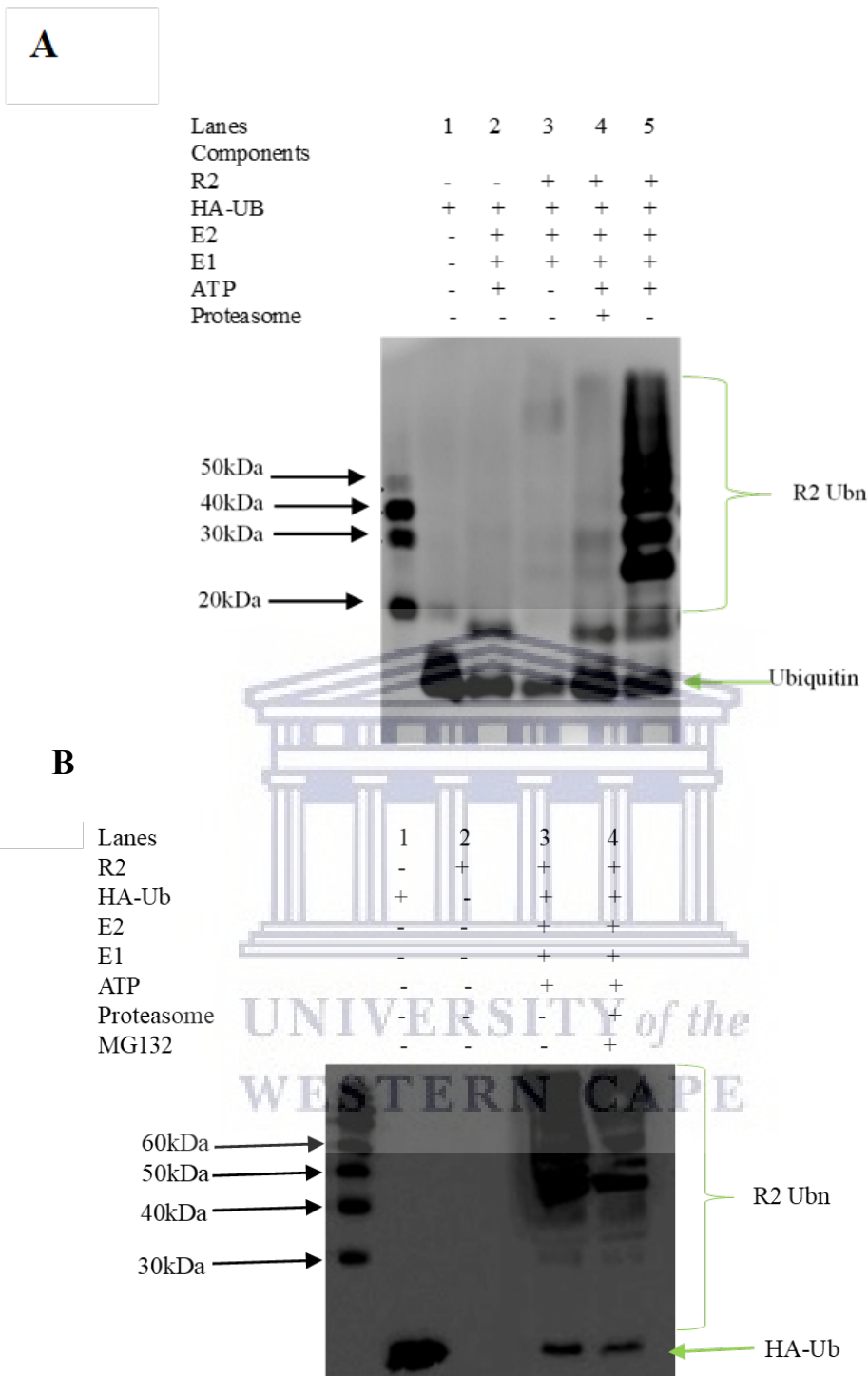


Figure 3.11: Auto-ubiquitination and proteasomal degradation of the R2 fragment of RBBP6. (A) R2 is able to auto-ubiquitinate itself in the presence of Mg-ATP, E1, E2 and ubiquitin (lane 5), but not in the absence of Mg-ATP (lane 3). Auto-ubiquitination is significantly reduced in the presence of the purified proteasome (lane 4). (B) The same poly-ubiquitination of R2 is seen in lane 3. Pre-incubation of the proteasome with MG132 prior to addition (lane 4) leads to reduction in the amount of high-MW species, which is consistent with partial rescue of the poly-ubiquitinated species. This result could have been made more convincing by including the reaction shown in lane 4 of panel A, in order to demonstrate that the un-inhibited proteasome is able to remove the poly-ubiquitinated species completely under the conditions used in this assay.

3.4 Ubiquitination of p53QM by a combination of GST-RBBP6-RING and GST-MDM2-RING

Li and co-workers previously concluded that RBBP6 cooperates with MDM2 in ubiquitinating p53, but is not itself active in the ubiquitination reaction (Li *et al.*, 2006). However, previous unpublished results from our laboratory suggest that R3 is able to catalyze ubiquitination of p53 with the assistance of MDM2, although there is a possibility that the ubiquitination is significantly more efficient in the presence of both RBBP6 and MDM2.

The previous results have shown that RBBP6 is able to efficiently catalyze ubiquitination of itself, and the ubiquitination is sufficient to catalyze degradation in the 26S proteasome. This lends support to our previous results suggesting that RBBP6 is able to catalyze ubiquitination of p53 on its own. Since we had already expressed FLAG-tagged p53 in *E. coli* as part of the interaction study described in Chapter 4, we decided to test directly whether the RING finger of RBBP6 is able to catalyze ubiquitination of p53 *in vitro*. The same reagents were used as for the auto-ubiquitination reactions, including UbcH5b and UbcH5c as the E2; however, the substrate was now FLAG-p53QM, and detection was carried out by Western Blotting using anti-FLAG antibodies. Production of FLAG-p53QM is described in detail in Section 4.2. The role of the E3 was played by the RING finger of RBBP6 or the RING finger of MDM2. A sample of the RING finger of MDM2 was a kind gift of a co-worker, Mr Po-An Chen.

Figure 3.12 shows that GST-RBBP6-RING is able to act as E3 ligase to catalyze ubiquitination of p53QM (lane 3). It was a surprise to us that an isolated RING finger is able to catalyze ubiquitination, but the evidence is clear, in the form of a smear extending up to above 90 kDa. It should be remembered that what is being detected here, by the anti-FLAG antibody, is FLAG-p53QM itself, rather than HA-Ub in the previous assays. The large number of ubiquitin moieties attached to a single substrate means that the intensity of the signal detected using antibodies targeting ubiquitin is likely to be much stronger than when detecting the substrate directly, even when the extent of ubiquitination is similar. Hence, although it is much fainter, the smear in Figure 3.12 is likely to be as significant as the more intense smears in previous assays. The strong band immediately above the band corresponding to FLAG-p53 is likely to correspond to mono-ubiquitination.

In order to be absolutely confident that the smear present in lane 3 is due to ubiquitination catalysed by GST-RBBP6-RING, and not due to E3-independent ubiquitination of FLAG-

p53QM due to the combined efforts of the E1 and E2 enzymes, in the presence of ATP, a negative control containing the same components as lane 3, but excluding both GST-RBBP6-RING and GST-MDM2-RING, would have been useful and should be included in future repeats of this result.

Lane 4 shows that GST-RING-MDM2 produces very much the same effect as GST-RBBP6-RING. Again, the biological significance of ubiquitination catalyzed by an isolated RING finger is not clear, but ubiquitination is nevertheless taking place. The same band, possibly corresponding to mono-ubiquitination, is present just above the band corresponding to p53. Interestingly, when both RBBP6-RING and MDM2-RING are used together, the ubiquitination is unmistakably more extensive. The high MW ladder stretches right up to the top of the gel, suggesting that it may represent poly-ubiquitination. However, the higher MW bands disappear completely when Mg-ATP is omitted from the reaction (lane 2), confirming that it is a ubiquitination-mediated effect. Lane 1, which contains only FLAG-p53QM, confirms that p53 is being detected by the Western Blot, and that the higher MW bands in lanes 3-5 represent modifications of p53.

Lane 5 of Figure 3.12 raises the question of whether the increased ubiquitination produced by both RINGs acting together represents a cooperative effect, or whether it is simply the additive effect of both RINGs acting independently. Judging by eye, the intensity of the ladder in lane 5 would appear to be stronger than the sum of the ladders in lanes 3 and 4, which would support the hypothesis that the RINGs act cooperatively. However, in the absence of quantitative densitometric analysis, it is not possible to reach a firm conclusion on this question.

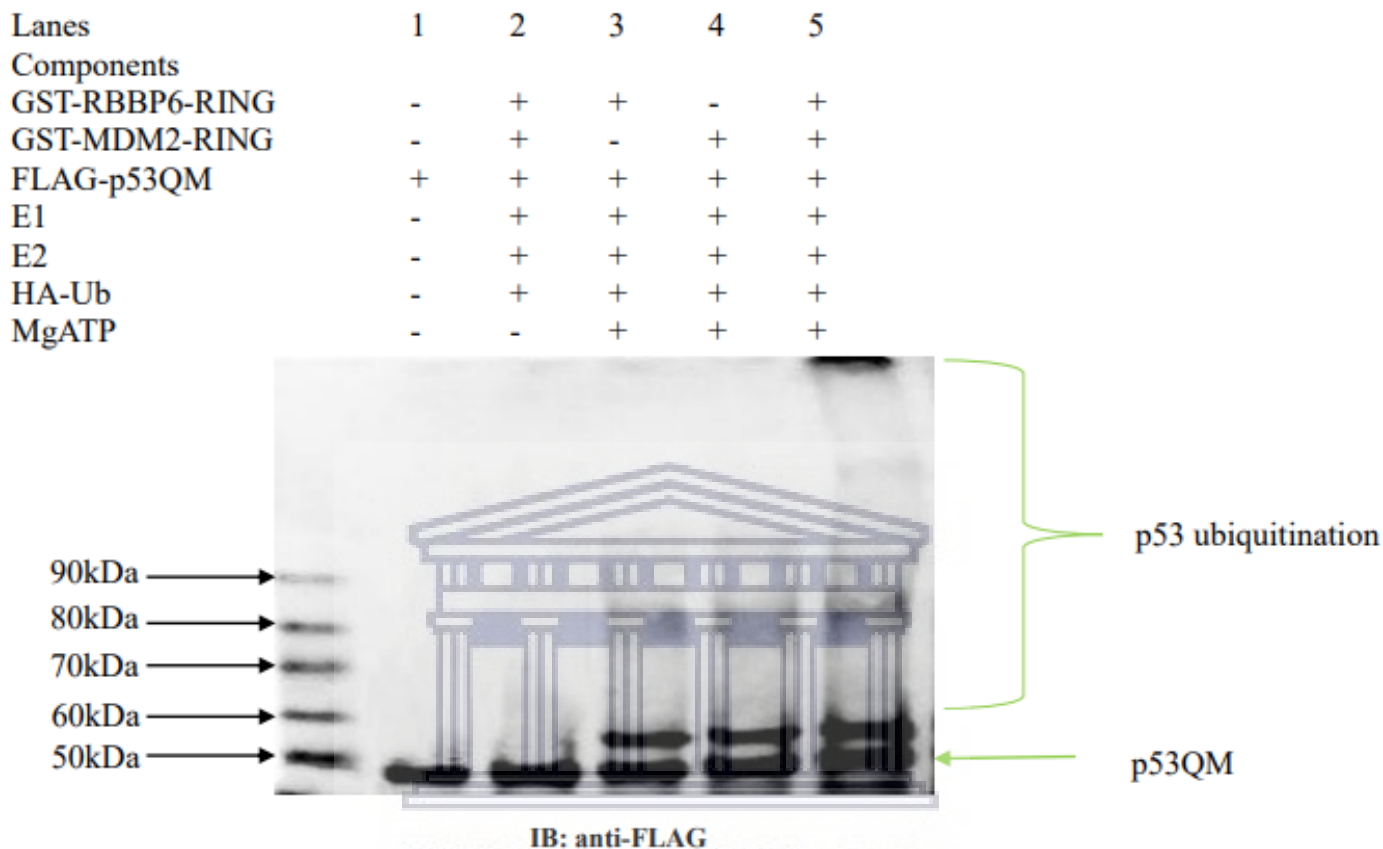
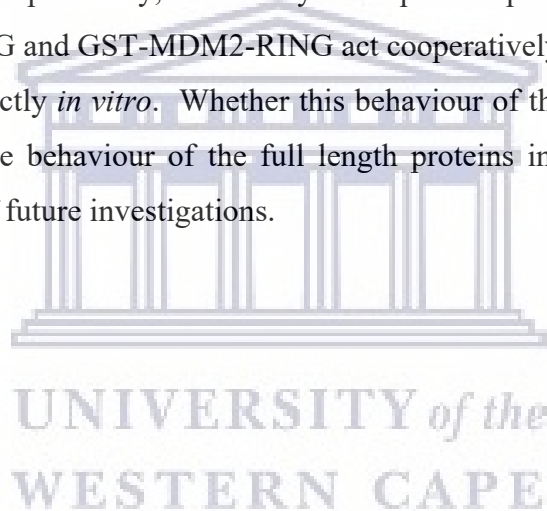


Figure 3.12: *In vitro* p53 ubiquitination by a combination of GST-RBBP6 RING and GST-MDM2 RING. In the absence of Mg-ATP no p53 ubiquitination is observed (lane 2). Lane 3 indicates mono-ubiquitination in the presence of FLAG-p53QM and GST-RBBP6 RING but the absence of GST-MDM2 RING. Lane 4 indicates mono-ubiquitination of p53 in the absence of GST-RBBP6 RING but in the presence of GST-MDM2 RING. The higher molecular weight smear extends further up the western blot in lane 5 (contains both GST RBBP6 RING and GST MDM2 RING) as compared to lanes 3 and 4. A similar banding pattern can be seen in lanes 3 and 4 however, when the GST MDM2 RING is added jointly with GST RBBP6 RING, the density of the ubiquitination increases (lane 5).

In conclusion, RBBP6-RING as well as monomeric mutants K313E and N312D were successfully expressed and used in *in vitro* auto-ubiquitination assays using UbcH5b-c as the E2 enzymes. Our results confirmed previous results showing that the isolated RING finger is capable of auto-ubiquitinating itself efficiently, leading to its degradation in the proteasome. The monomeric mutants were able to auto-ubiquitinate and catalyse their own degradation, although, consistent with previous results, this was less efficient than that of the wild type RING. As expected, no auto-ubiquitination was observed in the absence of ATP. Our results confirm that R2 and R3 are both able to efficiently auto-ubiquitinate and catalyse their own

degradation in the proteasome, suggesting that this may represent a mechanism for self-regulation of full length RBBP6 *in vivo*. No clear difference was observed between the ubiquitination potentials of R2 and R3, which suggests that the DWNN domain may not play an important role in the ubiquitination potential of RBBP6.

Finally, we investigated whether the isolated RING finger from RBBP6 is able to ubiquitinate p53. The results indicate that it is, resulting in a smear of higher molecular weight isoforms of FLAG-p53QM stretching to above 90 kDa. The higher molecular weight bands could correspond to poly-ubiquitination or multiple mono-ubiquitination, and the strong band immediately above p53 is likely to correspond to mono-ubiquitination at one or more lysines. Similar results were achieved when GST-MDM2-RING was used as an E3. However, GST-RBBP6-RING and GST-MDM2-RING, acting together, produced a qualitatively different result from when acting independently, which may correspond to poly-ubiquitination. If so, it suggests that RBBP6-RING and GST-MDM2-RING act cooperatively, which in turn suggests that they may interact directly *in vitro*. Whether this behaviour of the isolated RING fingers tells us anything about the behaviour of the full length proteins *in vivo*, or even *in vitro*, deserves to be the focus of future investigations.



CHAPTER 4: Identification of a novel interaction between p53 and the N-terminus of RBBP6, *in vitro*

4.1 Introduction

It was previously reported that p53 interacts with a region near the C-terminus of RBBP6, as shown schematically in Figure 1.1 (Simons *et al.*, 1997). Li and co-workers reported that RBBP6 interacts with MDM2 *in vivo*, and promotes ubiquitination of p53 by MDM2, but without being actively involved in the ubiquitination reaction, leading them to conclude that RBBP6 plays the role of a scaffolding protein, positioning p53 and MDM2 to facilitate ubiquitination (Li *et al.*, 2007). On the other hand, unpublished data from our laboratory suggests that the R3 fragment of RBBP6, which comprises the DWNN domain, zinc knuckle and RING finger domain, but not the existing p53-interaction site, is able to ubiquitinate p53 *in vitro* without the assistance of MDM2. This led us to suspect that there must be a second interaction site for p53 within the R3 fragment. To test this hypothesis, we set out to express fragments of p53 and RBBP6 in bacteria and investigate whether they interacted *in vitro*.

4.2 Recombinant expression of FLAG-p53QM

Samples of the RING and R2 fragments of RBBP6 were expressed *in E. coli* as GST fusion proteins, from which the GST was subsequently removed, as described in Section 2.4.2.3. The zinc finger of RBBP6 was expressed in a similar manner by a co-worker, Mr Po-An Chen.

The p53 protein is well known to be unstable when expressed in bacteria; hence we decided to express the stabilized form of the protein reported by Nikolova and co-workers (Nikolova *et al.*, 1998). This contains four amino acid substitutions—M133L, V203A, N239Y and N268D—all within the core DNA binding domain. A pET28a bacterial expression plasmid coding for the stabilized p53, which we named p53QM (for “p53 quadruple mutant”), and incorporating an N-terminal 6His tag, had been generated previously in our laboratory by an MSc student, Ms Lauren Jooste (L. Jooste, MSc thesis, UWC 2015). A FLAG immunotag was subsequently inserted between the 6His-tag and the start of p53QM by another MSc student, Mr Mihlali Mlaza (M. Mlaza, MSc thesis, UWC 2017). pET28a-FLAG-p53QM was transformed into *E. coli* Codon⁺ cells and expression of 6His-FLAG-p53QM carried out at 25

°C using an IPTG concentration of 1 mM, based on conditions previously established in our laboratory. Following cell lysis, the 6His-tagged protein was purified away from *E. coli* bacterial proteins using nickel ion affinity chromatography, as described in Section 2.4.2.4.

Lane 8 of Figure 4.1 shows elution of a protein with an approximate molecular weight of 50 kDa, which is consistent with the size of FLAG-p53QM. FLAG-p53QM was dialyzed, as described in Section 2.4.2.3, followed by the addition of 10 % glycerol and stored at -20 °C for further use.



Figure 4.1: Expression and purification of FLAG-p53QM using nickel ion affinity. The 50 kDa protein eluting at 300 mM imidazole in lane 8 corresponds to p53. Lane 1 contains the pellet, lane 2 contains the soluble lysate and lane 3 the flow through. Lanes 4 and 5 contains washes 1 and 3 respectively. Lanes 6-9 contains the elutions at a range of 100-400mM imidazole.

4.3 Far Western analysis

A Far Western blot differs from a pull-down or an immunoprecipitation assay in that it detects the prey as it binds to bait proteins immobilized on a PVDF membrane. It has the advantage that more than one bait protein can be immobilised on the membrane simultaneously, and their relative interactions with a single prey protein determined in a single assay. However, it should be noted that the position of each band on a Far Western blot corresponds to the MW of the bait protein immobilized on the membrane, rather than of the prey protein which is being detected by the antibody.

Far Western analysis was carried out as described in Section 2.12. Bacterially-expressed samples of DWNN, zinc, RING and R2 (following removal of the GST affinity tag), as well as free GST and p53QM were separated on a 16 % SDS-PAGE gel and then transferred to a PVDF membrane in the same manner as for a Western Blot. The PVDF membrane was blocked using 1 % casein to minimize non-specific interactions, and then incubated in a buffer containing 100 mM FLAG-p53QM for 1 hour, after which it was processed as for a normal Western Blot. A mouse anti-FLAG antibody was used to detect FLAG-p53 bound to proteins immobilized on the membrane, in combination with a goat anti-mouse secondary conjugated to HRP.

Lane 4 of panel A contains a strong band corresponding to the size of R2, which is what was loaded in that lane. Since FLAG is being detected, this indicates that FLAG-p53QM is bound to the R2 immobilized on the membrane. Lane 1 provides some evidence, albeit not totally convincing, that p53QM also binds to the zinc finger. The complete absence of bands in lane 2 and 3 indicate that p53QM does not bind to the DWNN domain nor to GST. The absence of binding to GST represents an important negative control, since it rules out the possibility that p53QM binds to any protein immobilized on the membrane. The band in lane 5, at the MW of p53QM, is consistent with p53QM binding to itself. While this is expected, the band may also correspond to direct detection of the FLAG-p53QM immobilized on the membrane by the anti-FLAG antibody, in the same manner as a conventional Western Blot.

The blot in panel B was carried out in the same manner, but with R2 and the zinc finger replaced by the RING finger domain. Consistent with the results of panel A, it shows that p53QM does not bind to the DWNN domain (lane 1), nor to GST (lane 2), and that it binds to itself (lane 3, although, as before, it is also possible that this represents a direct interaction between the antibody and the p53QM on the membrane. Lane 4 shows that p53QM also binds to the RING finger. Taken together, panels A and B suggest that p53QM binds strongly to the R2 fragment of RBBP6, as well as to the zinc and RING finger domains making up the R2 fragment.

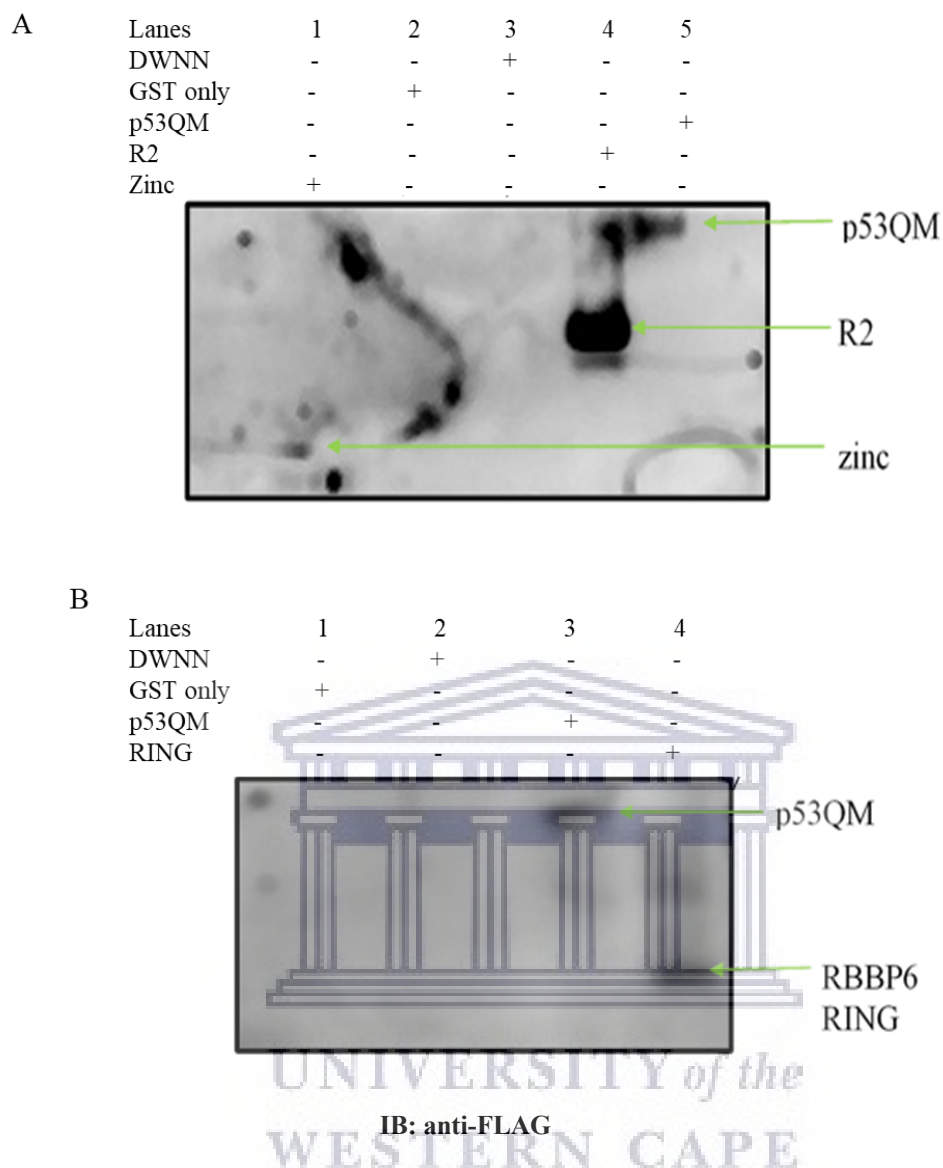


Figure 4.2: Far Western analysis of FLAG-p53QM with N-terminal fragments of RBBP6. (A) Detection of native p53QM binding to the membrane suggests that p53QM interacts strongly with the R2 fragment of RBBP6, and weakly with the zinc finger domain, but not with the DWNN domain or with GST. The band in the lane labeled “p53QM” is more likely to correspond to direct detection of p53QM immobilized on the membrane, rather than the native p53QM detected in other lanes. The blobs of signal detected near the GST and zinc finger lanes are likely to represent noise. (B) Consistent with panel A, no interaction is observed between p53QM and the DWNN or GST, but an interaction is observed between p53QM and the RING finger. As in panel A, the band in the “p53QM” lane is likely to correspond to direct detection of immobilized p53QM by the anti-FLAG antibody.

4.4 GST pull-down assays

The results obtained using Far Western were replicated using the more commonly used method of co-precipitation, coupled with Western Blot analysis. FLAG-p53QM was first incubated with R2 (GST tag removed) and precipitated using anti-FLAG antibodies. Western Blotting

with anti-RING antibodies was then used to detect co-precipitated R2, which contains the RING finger. However, this approach was abandoned when cross-reactivity was found between the anti-RING antibody and FLAG-p53QM (data not shown). Strictly speaking, since the anti-FLAG antibody was used for precipitation, cross reactivity of the anti-RING antibody should have affected only the detection phase and have no effect on the precipitation. Since FLAG-p53QM is easily distinguished from R2 on the basis of MW, the cross-reactivity could have been ignored. Nevertheless, it was decided to precipitate GST-R2 instead, using glutathione agarose, and detect co-precipitated FLAG-p53QM with anti-FLAG.

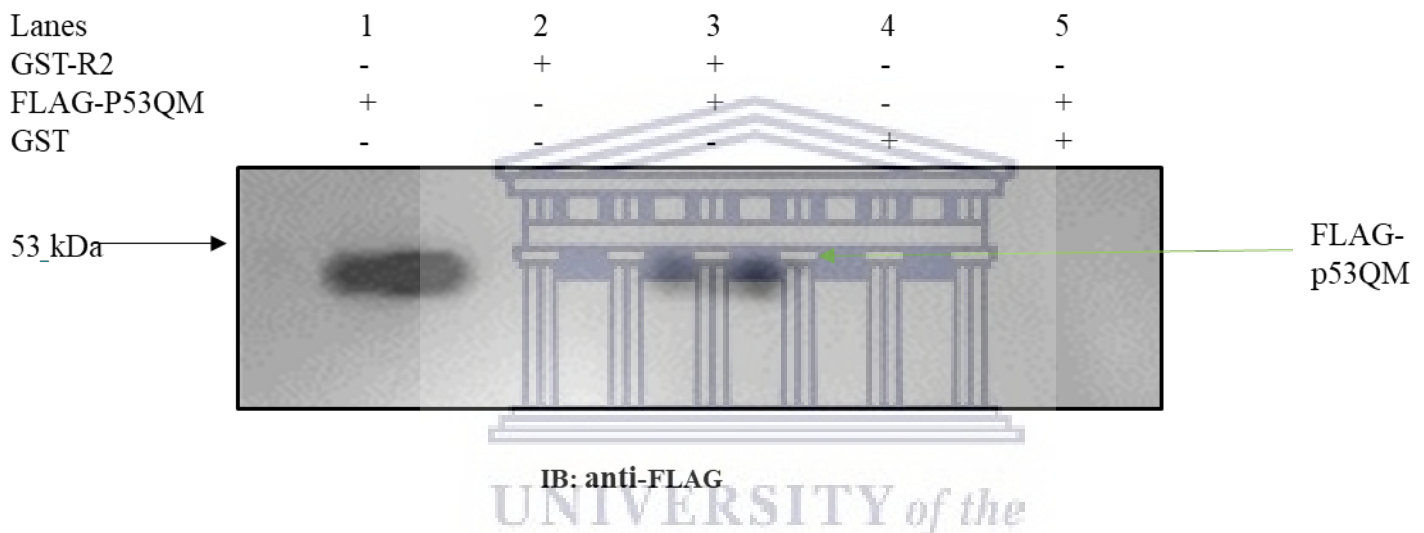


Figure 4.3: Co-precipitation of FLAG-p53QM with GST-R2. GST-R2 is able to co-precipitate FLAG-p53QM (lane 3), but GST alone is not (lane 5). Lanes 1, 2, and 4 contain FLAG-p53QM, GST-R2 and GST, respectively loaded directly onto the gel without being subjected to precipitation; together they confirm that the band seen in lane 3 corresponds to FLAG-p53QM and not to GST-R2, nor to GST.

The results can be seen in Figure 4.3. FLAG-p53QM is co-precipitated by GST-R2 (lane 3), but not by GST alone (lane 5). This confirms the result of Far Western that it is R2, and not GST, that is responsible for co-precipitation of p53QM. Hence we have identified a new interaction site for p53 on RBBP6. Lane 1, which contains p53QM loaded directly onto the gel, without being subjected to precipitation or washing, confirms that the band seen in lane 3 does in fact correspond to p53QM. Lane 2, which contains GST-R2 loaded directly onto the gel, without being subjected to precipitation or washing, confirms that the bands seen in lane 3 does not correspond to GST-R2. Lane 4 contains GST loaded directly onto the gel without being subjected to precipitation or washing. A FLAG-only negative control (with GST-R2 as bait) could arguably have been added to this experiment, to rule out the possibility that the interaction

between FLAG-p53QM and R2 is due to an interaction between the FLAG tag and R2. However, the small size of the FLAG tag (8 amino acids) makes it highly unlikely that it would interact directly with R2. Expressing the FLAG tag on its own in bacteria is also likely to be difficult, due to its small size. A better alternative would have been to express a FLAG-tagged version of protein that is known not to interact with R2, or expected not to interact with R2 (a so-called “dummy” protein). As will be seen below, the fact that the FLAG-tagged N-terminus of p53QM does not interact with R2 rules out the possibility that FLAG-tag interacts with R2.

In conclusion, the results of the GST pull-down assay confirm the result of Far Western analysis, that p53QM binds to the R2 fragment of RBBP6, as well as to both the zinc finger and the RING finger domains.

4.5 Cloning of p53N for interaction studies

Next, we attempted to further localize the interaction site of RBBP6 within p53QM.

Human p53 is a 393-residue protein that can be roughly divided into an N-terminal region (residues 1-94), a DNA Binding Domain (residues 95-292) and a C-terminal region (residues 293-393) (Joerger and Fersht., 2010). We hypothesized that the N-terminal region was the region most likely to interact with RBBP6, because it is known to interact with another E3 ligase, MDM2. We therefore set out to generate an expression construct which would express residues 1-101 of human p53. In the existing pET28a-FLAG-p53QM expression construct, p53QM is cloned between the NdeI and BamHI sites of the pET28a vector; in addition, a sequence coding for the FLAG tag had been inserted between the 6His tag and the NdeI site by a co-worker in the laboratory, Mr Mihlali Mlaza. Oligonucleotide primers were therefore designed to amplify a cDNA stretching from the BglII site, which is upstream of the MCC and therefore includes the FLAG tag, to residue 101 of p53; primers p53N-F and p53N-R are shown in Table 4.1 below. An XhoI site was incorporated into the 3'-end primer to allow cloning into the BglII/XhoI sites of pET28a, following excision of the BglII/XhoI fragment containing FLAG-p53QM.

Panel A of Figure 4.4(A) shows amplification of a 518 bp insert in lanes 3 and 4, which is consistent with the size of FLAG-p53N. The amplicon was digested with BglII and XhoI and cloned into the same restriction sites in pET28b. The colony PCR screen in panel B shows successful amplification an insert of the same size. Sequences were confirmed by direct sequencing (Inqaba Biotechnical Industries).

Table 4.1 Oligonucleotide primers for restriction endonuclease-mediated cloning of p53 constructs. Oligonucleotide primers for restriction endonuclease-mediated cloning of p53 constructs. The XhoI restriction site is indicated in purple, stop codon indicated in red and the Bgl II restriction site is indicated in green.

Name	DNA sequence	T _m (°C)
FLAG-p53N-F	5'-GAGGATCGAGATCTCGATCCCGC	62
FLAG-p53N-R	5'-GAGGCGCTCGAGTCAATTCTGGCTCGGCACACTAGAGC	62
FLAG-p53DBD-R	5'-GAGGCGCTCGAGTCAATTCTTCTTCGGTGCACGG	59

pET28a-FLAG-p53N was transformed into *E. coli* Codon⁺ cells and expression of FLAG-p53N was carried out at 25 °C, using an IPTG concentration of 1 mM, as described in Section 2.4.1. Following cell lysis, the 6His-tagged protein was purified from the *E. coli* bacterial proteins using nickel ion affinity chromatography, as described in Section 2.4.2.4. The FLAG-p53N protein was dialyzed into dialysis buffer as described in Section 2.4.2.3, followed by the addition of glycerol to a concentration of 10 % and stored at -20 °C for further use.

GST pull-down assays were performed using the GST-R2 as the “bait” and the FLAG-p53N as the “prey”, as described in Section 2.8. Detection was carried out by Western Blot, using an antibody targeting the FLAG tag incorporated into p53N.

The results are shown in Figure 4.5. The absence of a band in lane 5 shows that, contrary to expectations, FLAG-p53N was not co-precipitated by R2. Lane 1 contains FLAG-p53N loaded directly onto the gel and not subjected to precipitation or washes; the presence of a band corresponding to FLAG-p53N confirms that, had FLAG-p53 been present in lane 5, it would have been detected by the anti-FLAG antibody at the same position as in lane 1. The assay was repeated three times in triplicate, but each time the conclusion was the same: p53N does not interact with R2. We conclude that the site of interaction of R2 with p53 must be in the remainder of p53, which we named p53ΔN.

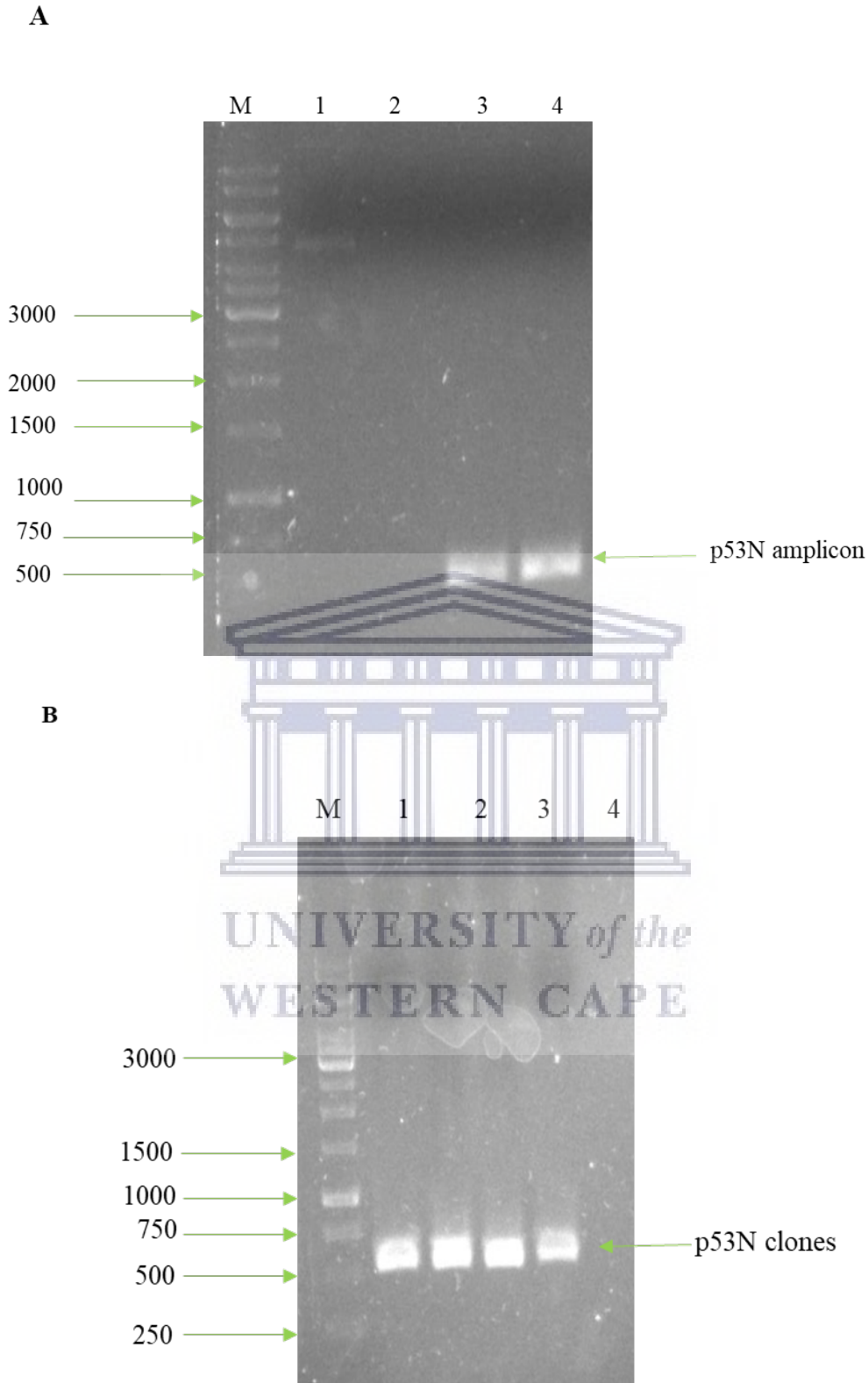
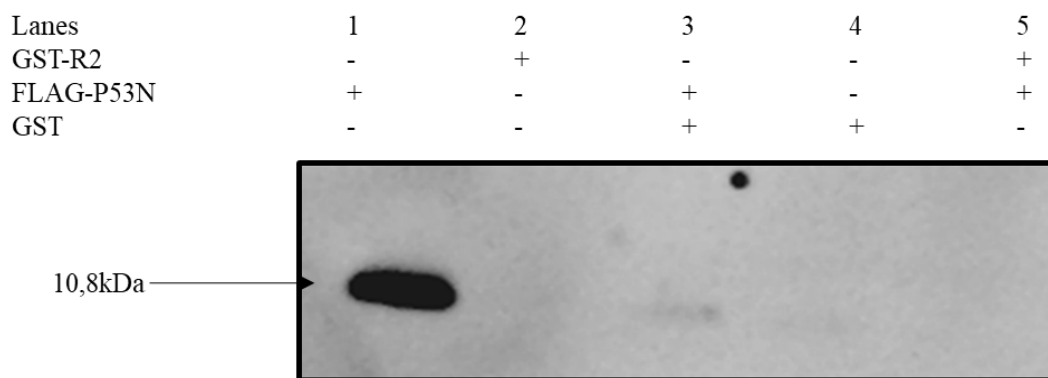


Figure 4.4: Molecular cloning of pet28b-FLAG-p53N.(A) PCR amplification of the p53N amplicon. The 518 bp fragments in lanes 3 and 4 were amplified from pET28-FLAG-p53-QM. Lanes 1 and 2 contain the template DNA and negative control respectively. (B) Confirmation of putative clones using colony PCR. The bands in lanes 1-4 are consistent with the expected insert size of 518 bp.



IB: anti FLAG

Figure 4.5. FLAG-p53N is not co-precipitated by GST-R2. Co-precipitated FLAG-p53N is not present in lane 5, despite the presence of GST-R2. FLAG-p53N in lane 1 was loaded directly onto the gel without being subjected to washes. This shows where FLAG-p53N is expected to appear on the Western blot and confirms that FLAG-p53N would be detected if it were present.

4.5.1 Generation of an expression construct for FLAG-p53 Δ N using deletion mutagenesis

Initial attempts to clone p53 Δ N using PCR amplification and restriction enzyme-mediated cloning were unsuccessful, so we attempted to use deletion mutagenesis instead. Deletion of residues 1-94 of p53^{QM} was carried out using the method of non-overlapping primers, as described in Section 2.3. The sequences of the oligonucleotide primers Delta-p53N-F (in green) and Delta-p53N-R (in blue) can be found in Table 4.2 below. The whole of the forward primer is homologous to the 3'-flank of the deletion, as shown in Fig 4.6(B), beginning at codon 95 of p53. The 3'-end of the reverse primer is exactly homologous to the 5'-flank of the deletion; the 5'-end of the reverse primer overlaps with the 5'-end of the forward primer. Since the NdeI site had proved problematic in our earlier attempt to clone the deletion using restriction enzymes, the NdeI site was replaced with an AvrII site (CCTAGG – shown in yellow) in the reverse primer; AvrII was chosen because it is an uncommon 6-base cutter that is not present in p53 and was currently in use in our lab for the cloning of RBBP6 constructs. The complete reverse primer therefore represents the desired sequence spanning the deletion, which is indicated by the “|” symbol in Table 4.2.

Exponential amplification of the linearized FLAG-p53 Δ N construct was successful in 2 out of 2 reactions as can be seen in lanes 6 and 10 of Figure 4.7(A). The band is consistent with the

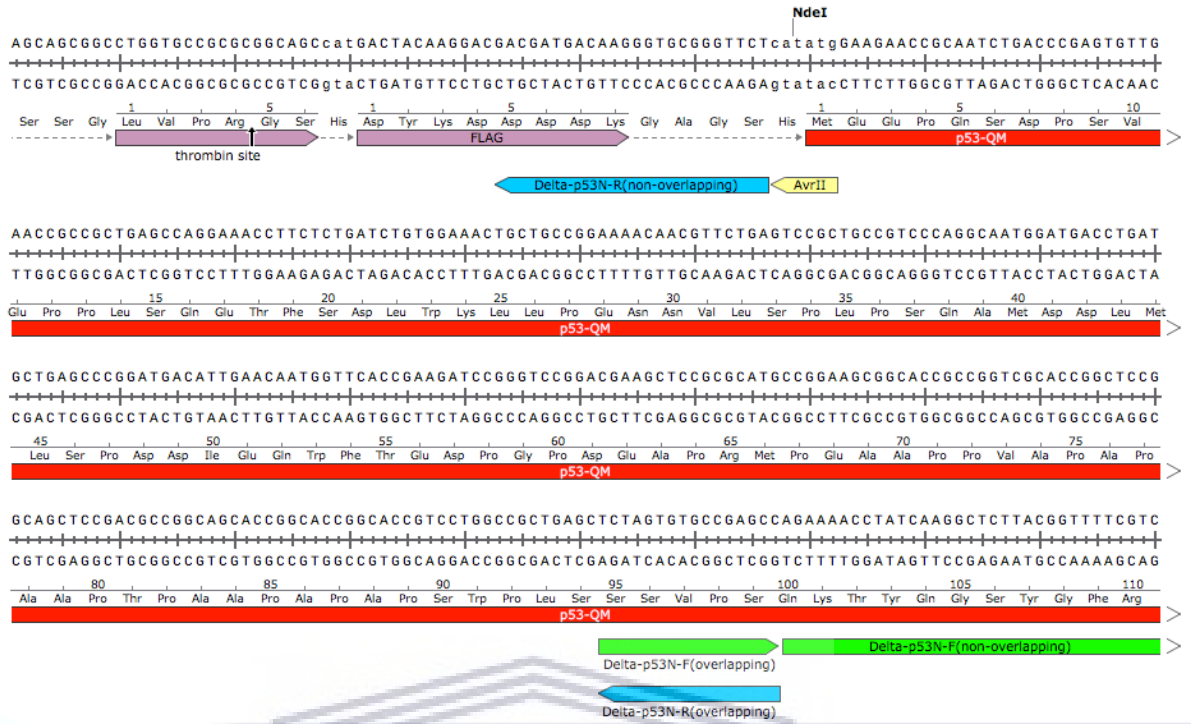
expected size of 6291 bp. This should be compared to the template (p53QM) DNA in lane 1, which migrates at a significantly higher MW than the expected 6554 bp, due to the fact that it is closed circular. Even though the concentration of amplicon is significantly greater than that of the template, the fact that the template (also called the parental) is already circular means that it will transform more efficiently than the linear amplicon with the result that parental colonies will greatly outnumber colonies resulting from homologous recombination of the amplicon. To suppress this background, the reaction was digested with DpnI prior to transformation into *E. coli* cells; DpnI should digest only the parental DNA, since it is methylated, and leave the amplicons untouched, since they are un-methylated. To serve as a background control, the same reaction was carried out, omitting only the primers (lane 4); hence any transformants resulting from this reaction could only arise from parental DNA which had escaped digestion by DpnI.

The contents of lane 6 (+primers) and lane 4 (-primers) were transformed into the recombination-competent XL gold strain of *E. coli*, producing 4 and 12 colonies respectively. This was unexpected, since the +primers plate was expected to contain mutant transformants as well as parental transformants, whereas the -primers plate was expected to contain only parental transformants; hence the + primer plate should have contained more colonies than the primer plate. Nevertheless, plasmid DNA was extracted and digested with AvrII and XhoI, to release the expected fragment of ~900 bp corresponding to p53ΔN; since parentals contains an NdeI site instead of the AvrII site, they are not expected to produce this fragment. Bands of this size are clearly visible in lanes 5, 9 and 11 of Fig 4.7(B). Putative clones were verified by direct sequencing and found to be exactly as expected.

Table 4.2 Sequence-specific oligonucleotides for the generation of p53 deletion mutagenesis constructs. Overlapping regions are underlined with straight lines and non-overlapping regions with wavy lines. The reverse primer contains an AvrII site, indicated in yellow. The annealing temperature for the overlapping region (T_{mo}) is chosen to be around 10 °C less than the overlapping regions (T_{mno}), to suppress primer-dimers.

Name	Primer sequence	T_{mo} (°C)	T_{mno} (°C)
Delta-p53N-F	5'- <u>TCTAGTGTGCCGAGCCAGAAAACCTATCAAGGCTC</u> <u>TTACGGTTTTTCGTCT</u>	54	64
Delta-p53N-R	5'- <u>GGCTCGGCACACTAGA</u> <u>CCTAGG</u> <u>AGAACCCGCACC</u> <u>CTTGTCATCGTC</u>	54	64
p53C-F	5'- <u>AACCTGCGTAAGAAAGGCGAACCCGCATCACC</u>	48	60
p53C-R	5'- <u>CTTCTTACGCAGGTTCCCTAGGAGAACCCGCACCC</u>	48	60

A



B

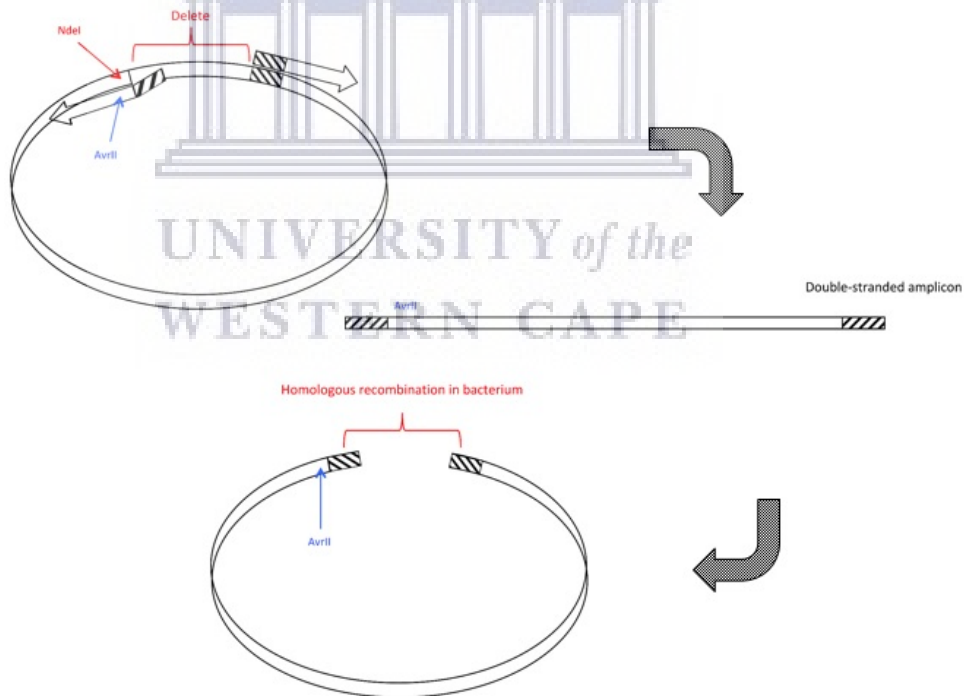
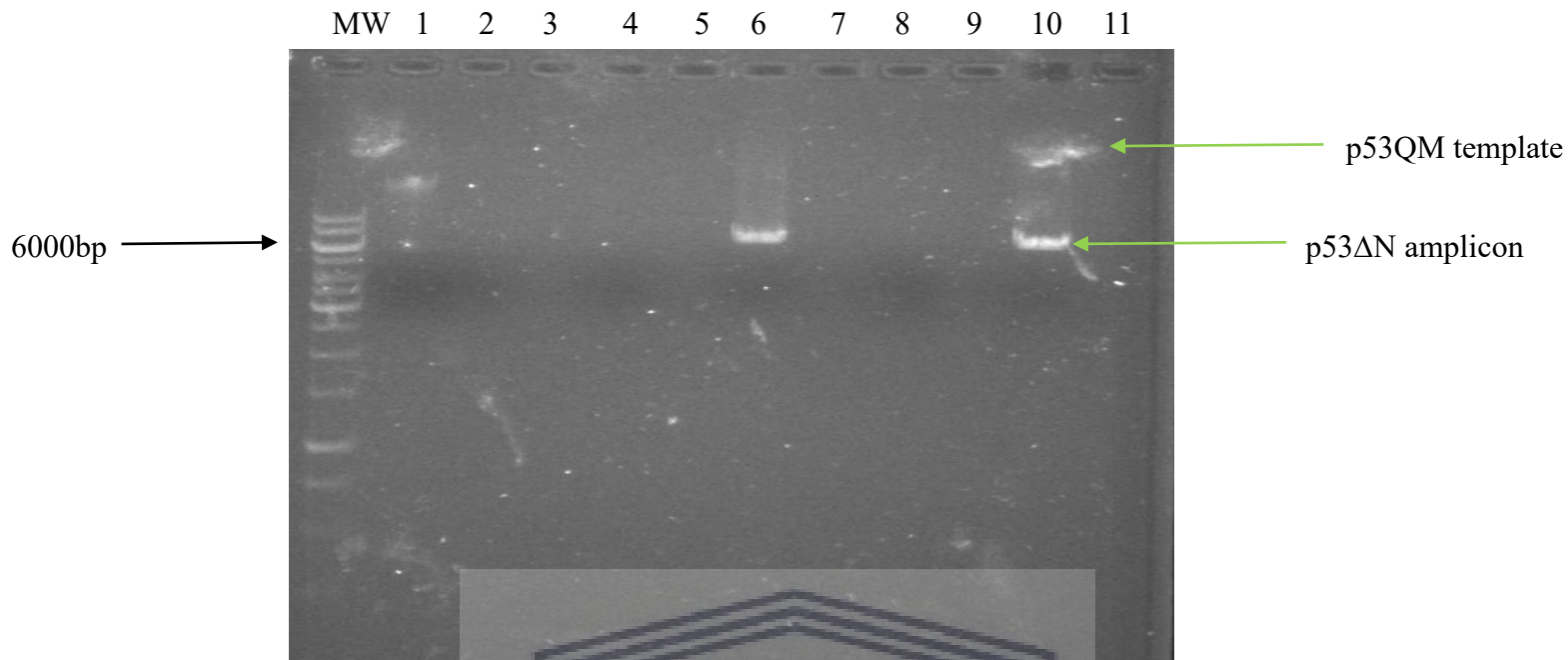


Figure 4.6 Schematic representation of the deletion mutagenesis strategy. (A) Sequence of pET28a-FLAG-p53QM showing where the forward primer (in green) and the reverse primer (in blue) anneal. The annealing temperature is chosen so that the 3'-end of the reverse primer (non-overlapping) is able to anneal, whereas the 5'-end is not, and nor are the overlapping regions able to anneal to themselves. The substituted AvrII site is shown in yellow. (B) Extension away from the overlapping region (hashed) leads to linear amplicons with an identical copy of the overlapping region on each end. In addition, an AvrII site in the reverse primer replaces the NdeI site in the template with the AvrII site. Homologous recombination of the linear amplicon into a circular plasmid removes one of the overlapping copies.

A



B

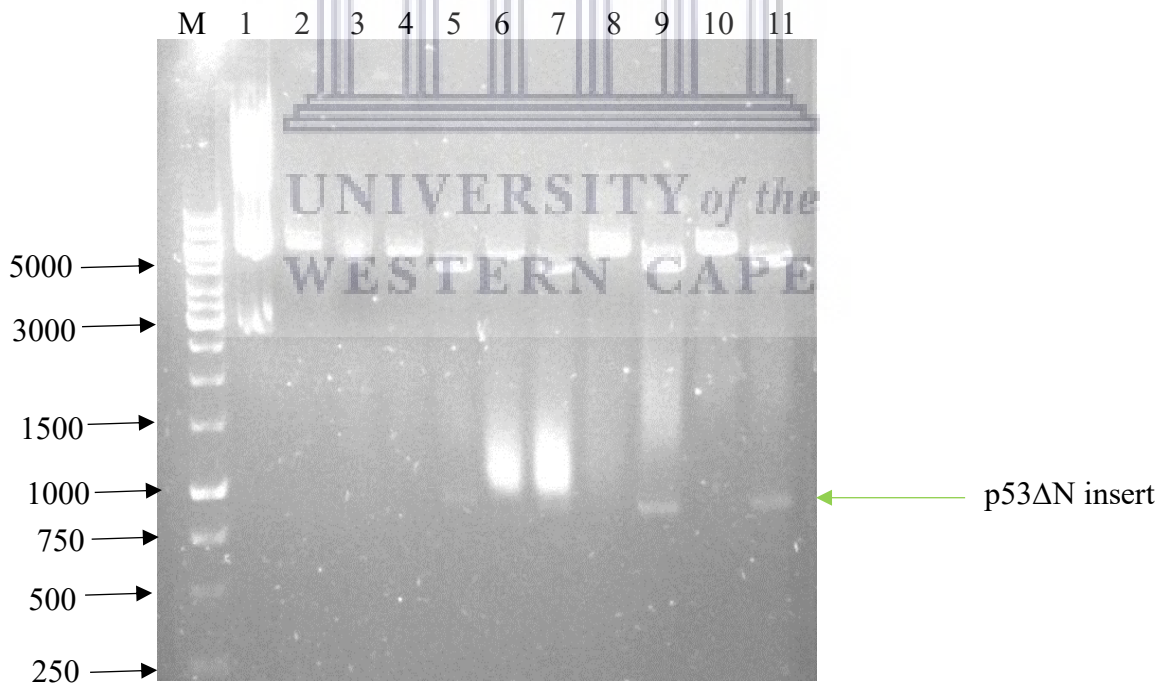


Figure 4.7 Deletion mutagenesis of *pet28a*-FLAG-*p53ΔN*. (A) PCR amplification of the *p53ΔN* amplicon (6291 bp) can be seen in lanes 6 and 10. Lane 1 contains only the template DNA (*p53QM*) which is running higher than the expected 6554 bp because it is closed circular. Lane 4 contains the no-primer control which serves as a background control for the transformations. (B) Putative *p53ΔN* clones were screened by digesting with *AvrII* and *XhoI*. Presumptive positive clones can be identified by the release of an insert at approximately 1000 bp in lanes 5, 9 and 11. Lanes 6-8 are screened colonies from the “-” primer plate.

pET28a-FLAG-p53 Δ N was transformed into *E. Coli* Codon⁺ cells and expression of FLAG-p53 Δ N carried out at 25 °C. Following cell lysis, the 6His-tagged protein was purified away from *E. coli* bacterial proteins using nickel ion affinity chromatography, as described in Section 2.4.2.4. Figure 4.8. indicates the successful elution of a protein of approximately 33 kDa, which is consistent with the expected size of FLAG-p53 Δ N (lanes 6-9). The FLAG-p53 Δ N was dialyzed as described in Section 2.4.2.3 followed by the addition of glycerol to a 10 % concentration and stored at -20 °C for further use.

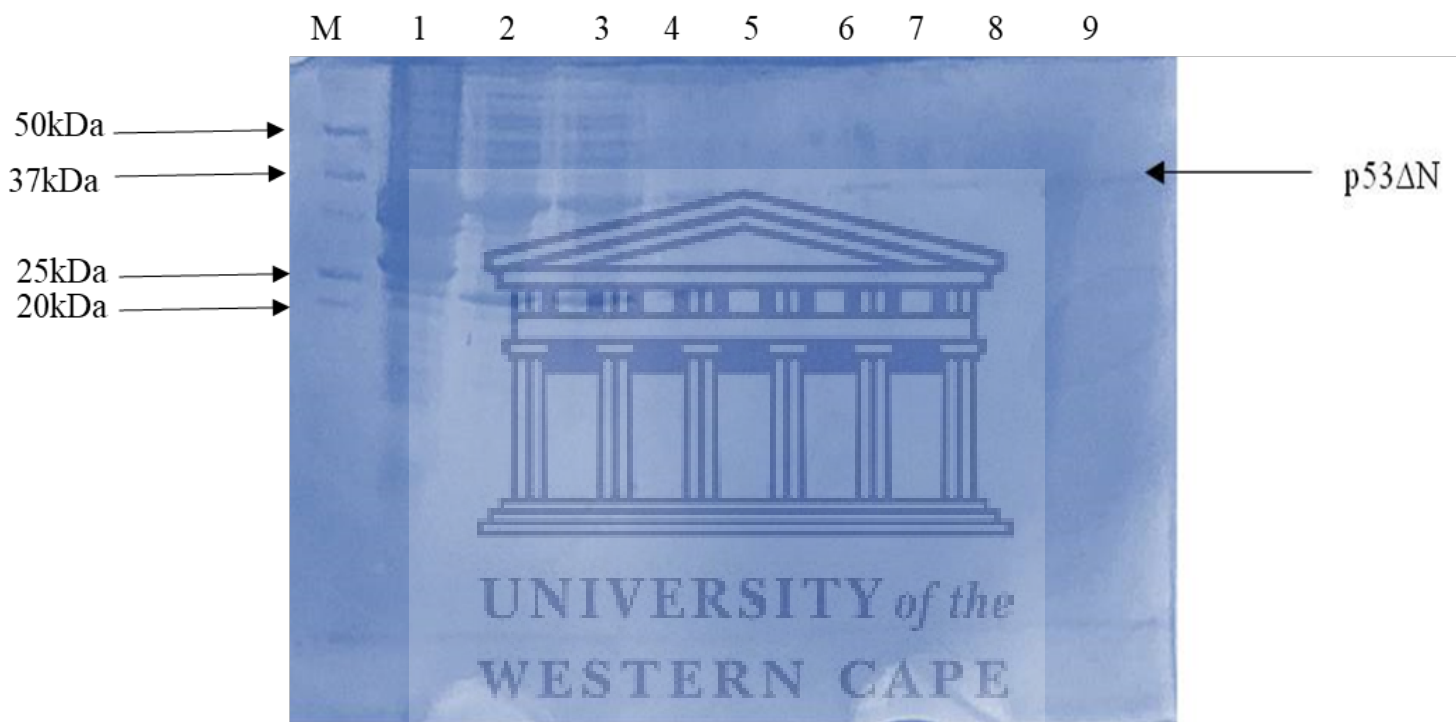


Figure 4.8 Expression and purification of FLAG-p53 Δ N using nickel ion affinity chromatography. A protein of ~37 kDa, consistent with the size of p53 Δ N, is eluted from the nickel ion column (lanes 6-9). Lane M indicates the molecular weight marker, Lane 1 contains the pellet, lane 2 contains the lysate and lane 3 contains the flow through. Lanes 4 and 5 contains washes 1 and 3 respectively. Lanes 6-9 contain the elutions at a range of 100-400mM imidazole.

GST pull-down assays were carried out using GST-R2 as “bait” and p53 Δ N as the “prey”, as described in Section 2.8. Detection was carried out by western blot using antibodies targeting the FLAG tag on p53, as described in Section 2.12. Figure 4.9 shows that GST-R2 was able to co-precipitate FLAG-p53 Δ N, producing a clear band at the same molecular weight as FLAG-p53 Δ N in lane 2, which was loaded directly onto the gel and not subjected to a GST pull-down.

GST alone was not able to co-precipitate FLAG-p53 Δ N (lane 3), and neither was the glutathione agarose on its own (lane 6).

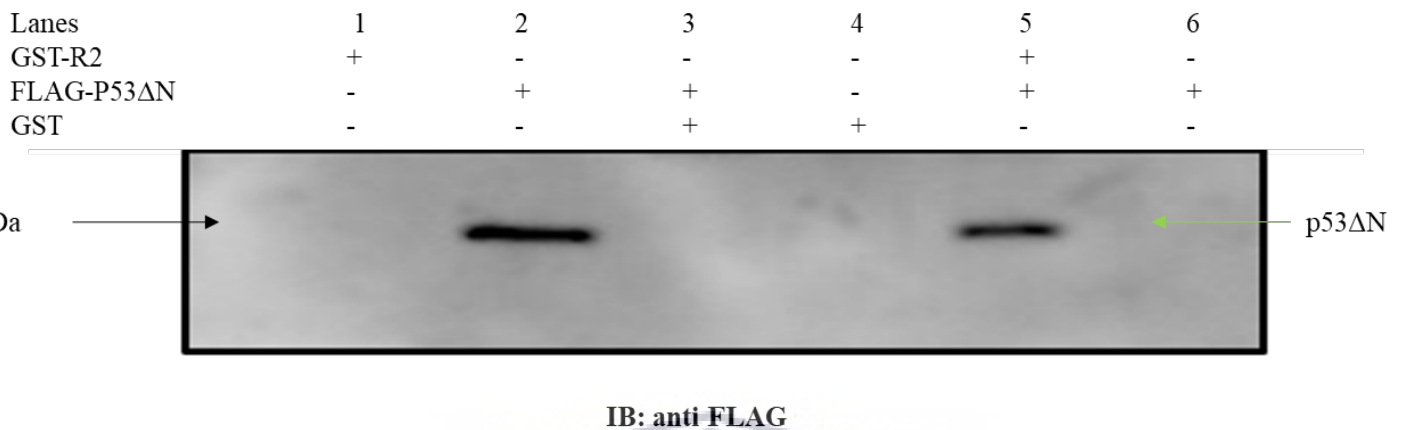


Figure 4.9 FLAG-p53 Δ N is co-precipitated by GST-R2. (A) FLAG-p53 Δ N is co-precipitated by GST-R2 (lane 5), but not by GST alone (lane 4), nor by glutathione agarose on its own (lane 6).-FLAG-p53 Δ N in lane 2 was loaded directly onto the gel without being subjected to washes; it confirms that the band in lane 5 is FLAG-p53 Δ N. The absence of a band in lane 1, which contains GST-R2 loaded directly onto the gel without being subject to washes, shows that the band in lane 5 is not GST-R2

4.5.2 Generation of expression constructs for FLAG-p53DBD and FLAG-p53C

We attempted to further localize the site of interaction in p53 Δ N by dividing it into 2 separate fragments: residues 95-287, containing principally the DNA Binding domain (DBD), and residues 288-393, containing the tetramerization domain and the C-terminal regulatory domain. These fragments were named “p53DBD” and “p53C” respectively.

p53DBD was PCR-amplified out of pET28a-FLAG-p53 Δ N using the forward primer used to amplify p53N and a new reverse primer to truncate p53 Δ N immediately after the DBD. The sequences of primers p53N-F and p53DBD-R can be found in Table 4.2. p53N-F could be used because it anneals upstream of the FLAG tag and the MCC, where pET28a-FLAG-p53QM and pET28a-FLAG-p53 Δ N are identical; nevertheless, the amplicon includes the N-terminal 6His tag, FLAG tag and AvrII site present in pET28a-FLAG-p53 Δ N, followed by codon 95 of p53. p53DBD-R incorporated a TAG stop codon into the amplicon immediately following codon 287 of p53, followed in turn by an XhoI restriction site.

Panel A of Figure 4.10 shows successful amplification of a fragment of around 1000bp, which is consistent with the expected size of 811 bp. The amplicon was digested with BglII and XhoI and inserted into the pET28a-FLAG-p53 Δ N vector following excision of the BglII-XhoI fragment. Putative transformants were screened by restriction digest with BglII and XhoI, which released an insert (lanes 5-10) of approximately 800bp (lane 1). Sequences were confirmed by direct sequencing (Inqaba Biotechnical Industries).

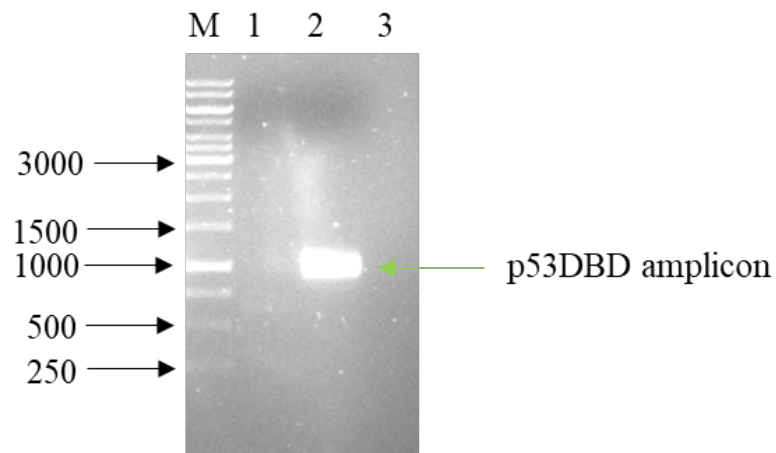
The pET28a-FLAG-p53C construct was generated from pET28a-FLAG-p53 Δ N using the same deletion mutagenesis strategy used for generating pET28a-FLAG-p53 Δ N. The nucleotide sequences of primers p53C-F and p53C-R can be found in Table 4.2; the positions where they anneal on the template is shown in Figure 4.11. As before, the whole of the forward primer is homologous to the 3'-flank of the deletion, beginning at codon 288 of p53. The 3'-end of the is exactly homologous to the 5'-flank of the deletion; the 5'-end of the reverse primer overlaps with the 5'-end of the forward primer. Lane 7 in figure 4.12 indicate successful amplification of pet28-FLAG-P53C at approximately 6000 bp. pet28-FLAG-p53C amplicon was subjected to restriction enzyme digest with DpnI which targets the methylated template DNA. Following digestion with DpnI, the DNA was transformed into *E. coli* XL gold as described in section 2.2.2 and plated onto LB kanamycin plates.

As previously mentioned, the fact that the template in lane 1 of Figure 4.12 is already circular means that it will transform more efficiently than the linear amplicon and therefore outnumber the colonies which result from homologous recombination of the amplicon. Therefore, to suppress this background, the reaction was digested with DpnI prior to transformation into *E. coli* cells, digesting only the parental DNA and subsequently leaving the amplicons untouched.

To serve as a background control, the same reaction was carried out, omitting only the primers (lane 3). The contents of lane 4 (-primers) and lane 7 (+primers) were transformed into the recombination competent XL gold strain of *E. coli*, producing 2 and 20 colonies respectively. This was expected, since the +primers plate was expected to contain mutant transformants as well as parental transformants, whereas the -primers plate was expected to contain only parental transformants, therefore the +primer plate should contain more colonies than the -primer plate.

Nevertheless, plasmid DNA was extracted and digested with AvrII and XhoI, to release the expected fragment of ~318 bp corresponding to p53C, as shown in Fig 4.12(B). Putative clones were verified by direct sequencing and found to be exactly as expected.

A



B

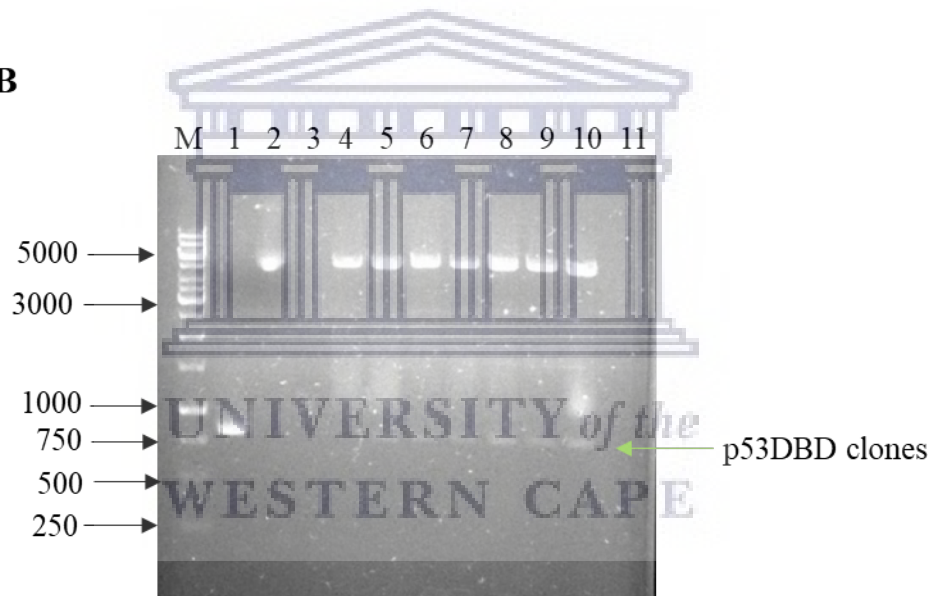


Figure 4.10 Generation of pET28a-FLAG-p53DBD. (A) PCR amplification of p53DBD at ~1000 bp (lane 2). (B) Restriction digest of putative p53DBD transformants with BglII and XhoI (lanes 5-10) released a fragment of the approximately 800 bp (lanes 5-10). Lane 2 contains the p53 Δ N template DNA and lane 3 the negative control.

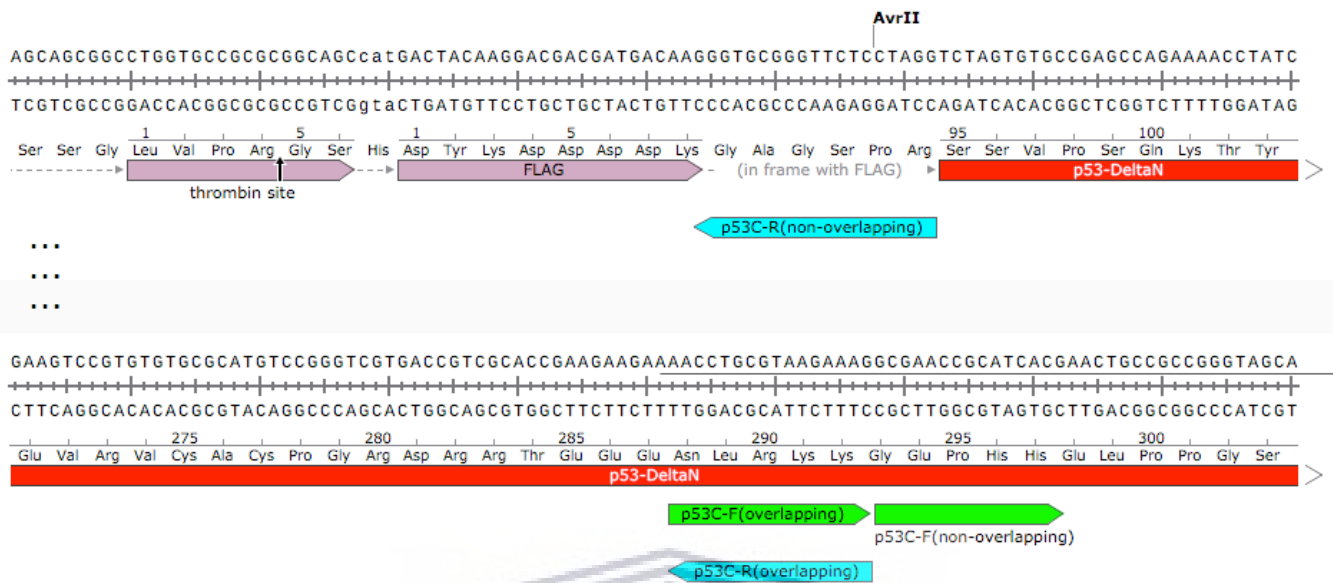
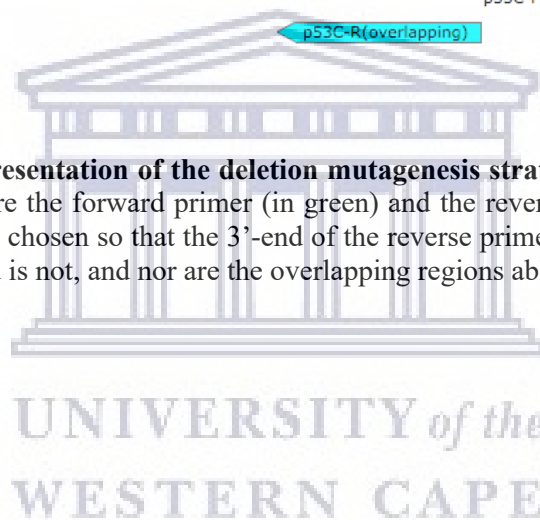


Figure 4.11 Schematic representation of the deletion mutagenesis strategy. Sequence of pET28a-FLAG-p53ΔN showing where the forward primer (in green) and the reverse primer (in blue) anneal. The annealing temperature is chosen so that the 3'-end of the reverse primer (non-overlapping) is able to anneal, whereas the 5'-end is not, and nor are the overlapping regions able to anneal to themselves.



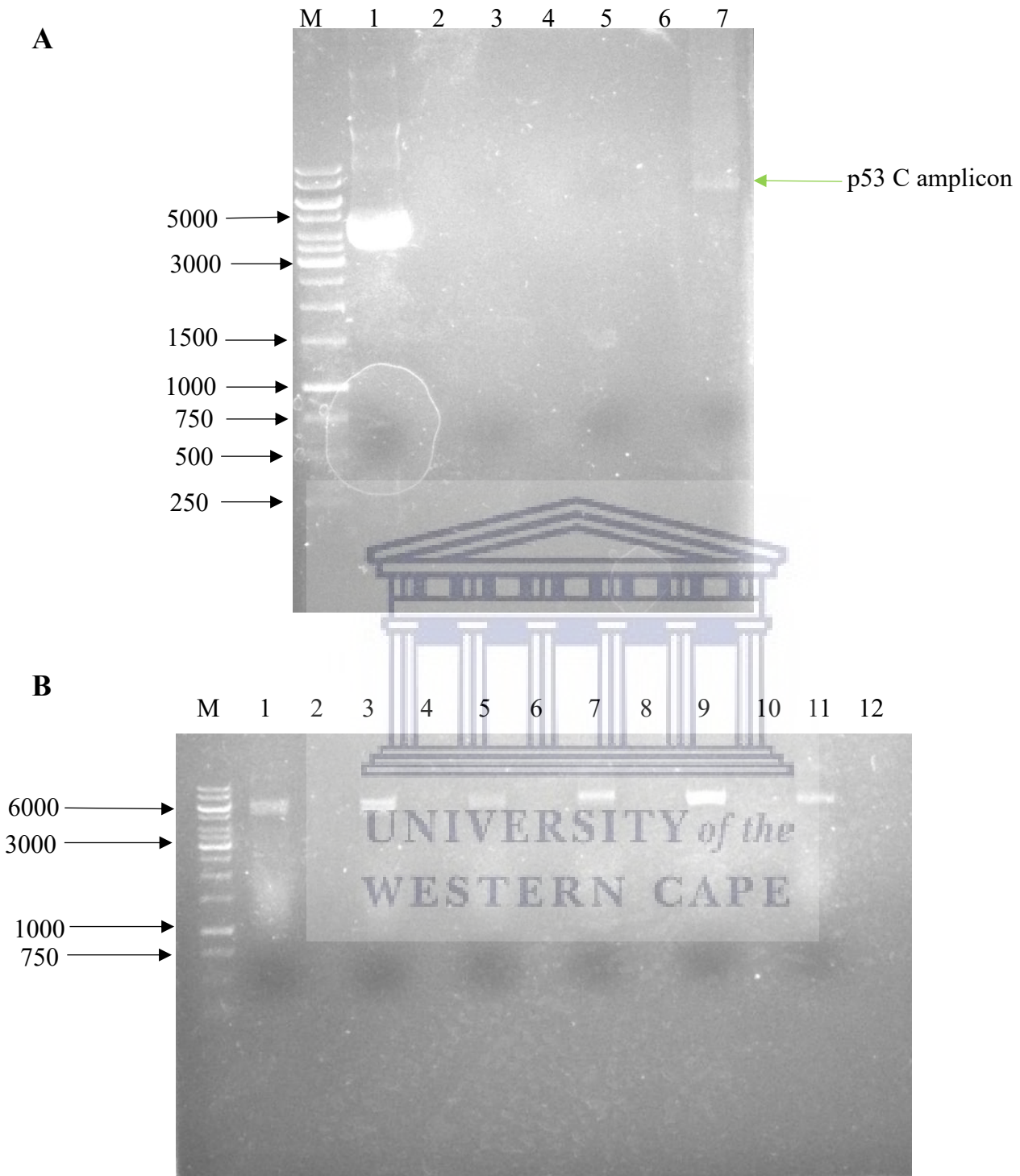


Figure 4.12 Deletion mutagenesis of *pet28-FLAG-p53C*. (A) PCR amplification of the p53C amplicon. Lane 7 confirms amplification of p53C at approximately 6000 bp. Lane 1 contains the p53 Δ N template DNA, lane 4 contains the $-$ primers control. (B) Putative p53C clones were screened by digesting with AvrII and XhoI.

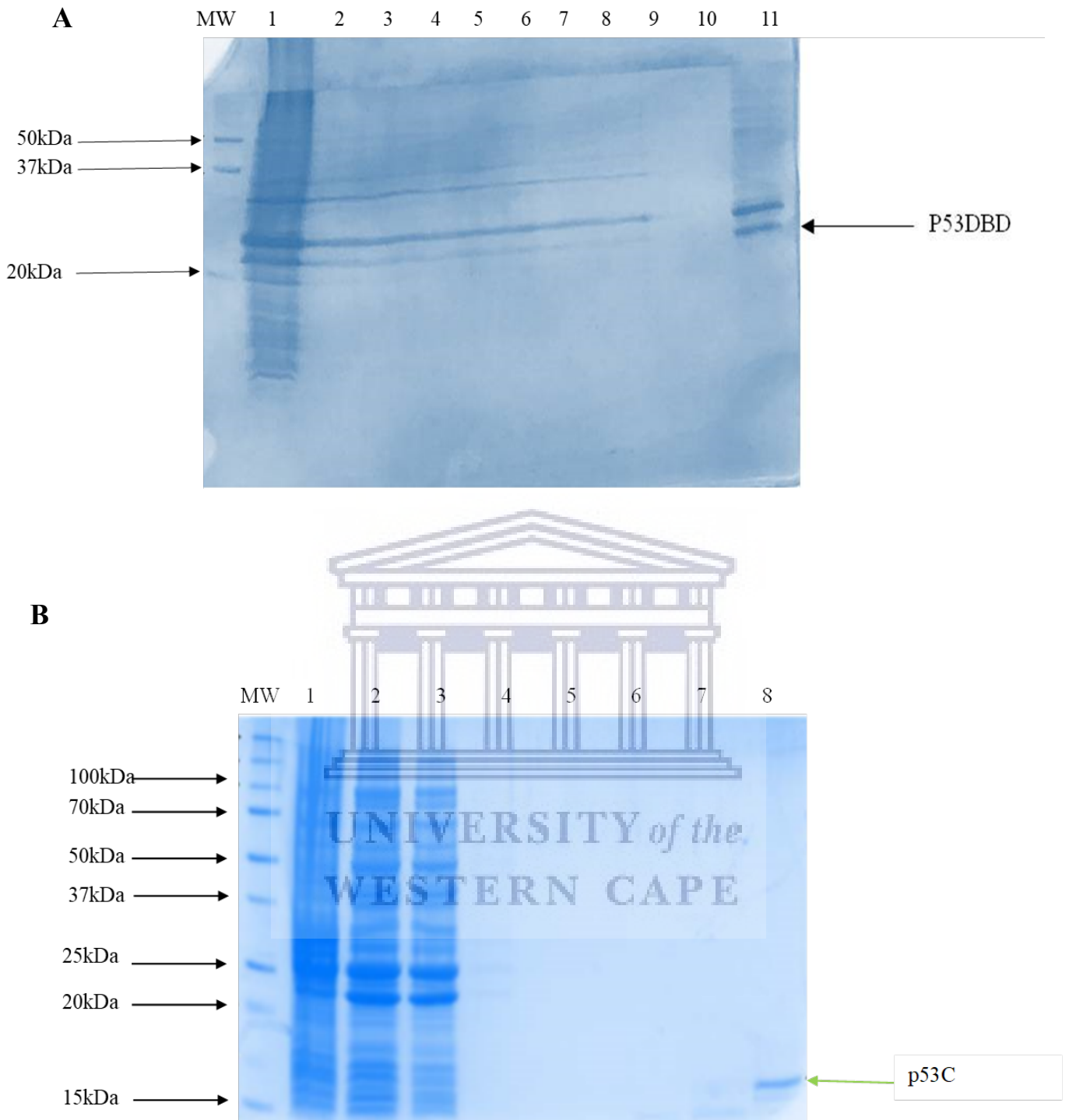


Figure 4.13 Expression and purification of FLAG-p53DBD and FLAG-p53C using nickel ion affinity. (A) A protein of ~22 kDa, consistent with the size of p53DBD, is eluted from the nickel ion column (lanes 6-11). Lane M indicates the molecular weight marker. Lane 1 contains the pellet, lane 2 contains the lysate and lane 3 contains the flow through. Lanes 4 and 5 contains washes 1 and 3 respectively. Lanes 6-11 contains the elutions at a range of 100-400 mM imidazole (B) A protein of approximately 15 kDa, consistent with the size of p53C is eluted from the nickel ion column (lane 8). Lane M indicates the molecular weight marker. Lane 1 contains the pellet, lane 2 contains the lysate and lane 3 contains the flow through. Lanes 4 and 5 contains washes 1 and 3 respectively. Lanes 6-8 contains the elutions at a range of 100-400 mM imidazole.

FLAG-p53DBD and FLAG-p53C were expressed in *E. coli* and purified using nickel ion affinity chromatography, as described previously. Bands corresponding to the expected sizes of FLAG-p53DBD (22 kDa, lane 11) and FLAG-p53C (15 kDa, lane 8) can be seen in panels A and B of Figure 4.13 respectively. FLAG-p53DBD and FLAG-p53C was concentrated and dialyzed described in Section 2.4.2.3, followed by the addition of 10 % glycerol and stored at -20 °C for further use.

4.6 **GST-pull-down assays to localise interaction of N-terminus of RBBP6 within p53**

GST pull-down assays were carried out using GST-R2 as “bait” and p53 domains as the “prey”, as described in Section 2.8. Detection was carried out by western blot using antibody raised against the FLAG tag on p53, as described in Section 2.11.

Figure 4.14, shows FLAG-p53DBD is co-precipitated by and GST-R2 (lane 5), but not by GST alone (lane 3) and neither were the glutathione agarose beads on their own (lane 4). The band in lane 1, which contains only FLAG-p53DBD, loaded directly onto the gel without washing, confirms that the band co-precipitated in lane 5 is in fact FLAG-p53DBD. The absence of a band in lane 2, which contains only GST-R2, loaded directly onto the gel without washing, confirms that the band co-precipitated in lane 5 is not GST-R2. We conclude that GST-R2 on its own is responsible for the co-precipitation of FLAG-p53. Nevertheless, the feintness of the band in lane 5 suggests that the interaction between GST-R2 and the p53DBD is not strong.

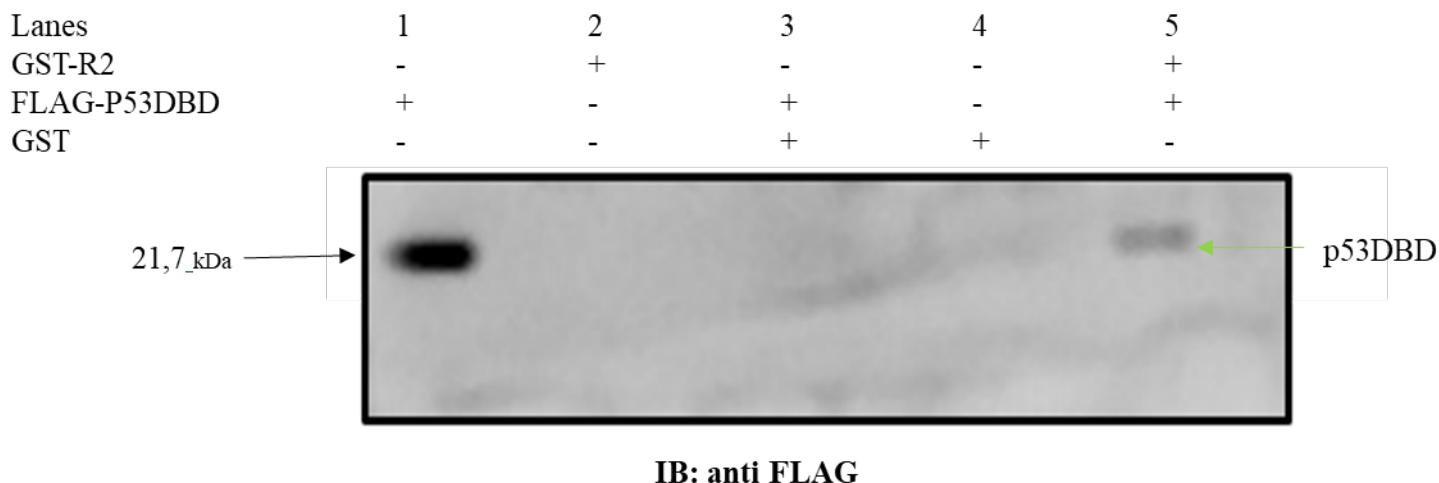


Figure 4.14 GST-R2 is able to co-precipitate FLAG-p53DBD. Co-precipitated FLAG-p53DBD is present in lane 5, in the presence of GST-R2. FLAG-p53DBD in lane 1 was loaded directly onto the gel without being subjected to washes; this shows where FLAG-p53DBD is expected to appear on the western blot and confirms that FLAG-p53DBD should be detected if present. GST alone was not able to co-precipitate the FLAG-p53DBD (lane 3) and neither were the glutathione agarose beads on their own (lane 4).

The fact that GST-R2 interacts with both FLAG-p53DBD and FLAG-p53 Δ N, as well as the fact that the interaction with FLAG-p53DBD (Figure 4.14) is weaker than that of p53 Δ N (comprised of the DBD and the C-terminus), suggests that there is a possible binding interface on the C-terminus of p53. In order to further determine where within p53 the interaction site lies, we cloned the C-terminus of p53 excluding the DNA binding domain (named “p53C”).

Figure 4.15 shows that GST-R2 was able to co-precipitate FLAG-p53C (lane 5), producing a clear band at the same molecular weight as FLAG-p53C (lane 1), which was not subjected to a pull-down. GST alone was unable to co-precipitate the FLAG-p53C (lane 3) and neither were the glutathione agarose beads on their own (lane 2). We conclude that R2 interacts with p53C, as well as the DBD domain of p53.

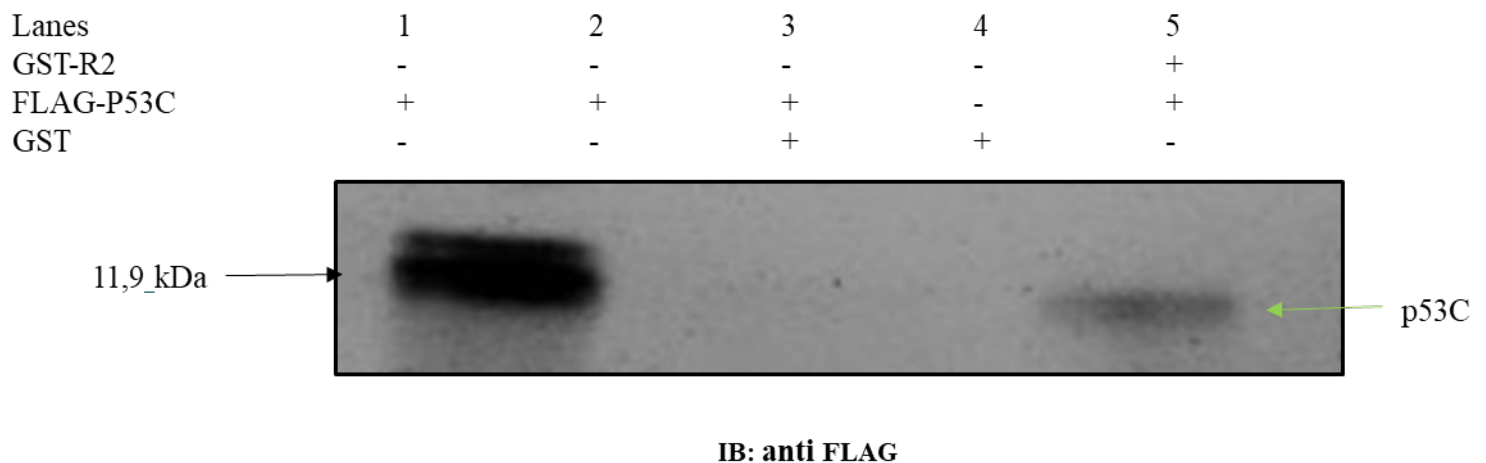


Figure 4.15 Co-precipitated FLAG-p53C in presence of GST-R2. Co-precipitated FLAG-p53C is present in lane 5, despite the presence of GST-R2. FLAG-p53C in lane 1 was loaded directly onto the gel without being subjected to washes. This shows where FLAG-p53C is expected to appear on the western blot and confirms that FLAG-p53C should be detected, if present. GST alone was not able to co-precipitate the FLAG-p53C (lane 3).

Based on the results presented in the previous chapter, we expected fragments of RBBP6 RING capable of catalyzing the ubiquitination of p53 to be able to interact directly with p53 *in vitro*. Initial Far Western analysis suggested that p53QM bound to R2, to the RING finger domain the zinc domain, and not at all to the DWNN domain or to GST. GST pull-down assays confirmed that FLAG-p53QM is co-precipitated by GST-R2. Based on these results, we attempted to further localize the interaction within p53. We cloned and expressed both the N-terminal domain of p53, FLAG-p53N, and the remainder of the protein, FLAG-p53ΔN; GST pull down assays showed that FLAG-p53N did not interact with R2, whereas FLAG-p53ΔN did interact.

We further attempted to localize the interaction by separating p53ΔN into p53DBD and p53C. GST pulldown suggested that both FLAG-p53DBD and FLAG-p53C interacted with R2.

Chapter 5: Conclusions and outlook

5.1 RBBP6 auto-ubiquitinates itself efficiently *in vitro*

Many E3 ubiquitin ligases are able to catalyse their own ubiquitination, known as auto-ubiquitination, in addition to substrate ubiquitination. Auto-ubiquitination serves as a useful proxy for substrate ubiquitination, allowing aspects of the catalytic mechanism to be uncovered without the need for a (possibly) unstable substrate. It is also interesting for more biological reasons, as a potential mechanism for self-suppression of the E3 ligase, such as has been reported for MDM2.

RBBP6 is too large and unstable for heterologous expression in bacteria, and therefore smaller fragments were used in this study. These include the R3 domain, spanning the first 335 residues of the protein, and including the DWNN domain, zinc knuckle and RING finger domains, which has been hypothesised to perform the core ubiquitination function of the protein. The R2 domain spans residues 142-335 and contains only the zinc knuckle and the RING finger domain. The RING finger domain is reported to be partially homo-dimeric (Kappo et al 2012), although the N312D and K312E mutants are totally monomeric. Unpublished data from our laboratory has shown that the R2 and R3 domains are homo-dimers in solution.

Results previously generated in our laboratory suggested that the isolated RING finger was able to auto-ubiquitinate itself, and that the resulting poly-ubiquitination was sufficient to target it to the 26S proteasome. The proteasome was purified from mammalian cell lysates; to our knowledge this is the first report of proteasomal degradation of ubiquitinated substrate *in vitro*. The results also suggested that the monomeric mutants of the RING finger were nevertheless able to catalyse ubiquitination and degradation in the proteasome, although evidence suggested it was less efficient than that of wild type RING.

The first aim of this thesis was to repeat the above results using an antibody targeting the HA-tag on HA-ubiquitin, rather than the anti-ubiquitin antibody used in the previous study. The isolated wild type RING finger and monomeric mutants K313E and N312D were successfully expressed. *In vitro* auto-ubiquitination assays conducted using UbcH5b and UbcH5c as E2 enzymes, and the isolated RING finger as E3, confirmed our previous results, showing that the isolated RING finger is able to auto-ubiquitinate very efficiently and catalyse its degradation

in the proteasome. As before, the monomeric mutants were able to auto-ubiquitinate and catalyse its degradation in the process, although it appeared to be less efficient than that of the wild type RBBP6 RING. Significantly, no auto-ubiquitination was observed in the absence of ATP, confirming that the ubiquitination effect is ATP dependent as is expected. Based on this last result, a no-ATP control was routinely included in all of our ubiquitination assays from that point on.

We would have liked to extend our investigation of the effect of monomerisation to R2 and R3 fragments. However, the N312D and K313E mutants that has monomerised the RING finger had been shown to be insufficient to monomerise either R2 or R3. Future investigations should attempt to identify additional or alternative mutations that would monomerise R2 and R3.

Nevertheless, our results confirmed that both R2 and R3, like the isolated RING finger, are able to catalyse efficient poly-ubiquitination, targeting them for degradation in the proteasome. Our data shows no clear difference between the auto-ubiquitination potentials of R2 and R3. This would appear to suggest that the DWNN domain, which makes up the N-terminus of R3 but is absent from R2, plays no role in auto-ubiquitination. In particular, it would appear to rule out an inhibitory role, similar to that found in the case of Parkin (Chaugule *et al.*,2011). However, it has been observed that R3 is more sensitive to proteolysis than R2 in solution, and it appears to be the DWNN domain which is being lost. This is consistent with what appears to be an area of low complexity on the C-terminal side of the DWNN domain, which may correspond to flexible linker between the DWNN domain and the rest of R3. It is therefore possible that the R3 samples used in this thesis are not much different to the R2 samples, in which case no conclusions regarding the role of the DWNN domain could be drawn.

Whereas auto-ubiquitination of the isolated RING finger could be dismissed as biologically insignificant, R3 is highly similar to the forms of RBBP6 found in lower eukaryotes. Our results therefore suggest that auto-ubiquitination may play a significant role *in vivo*, as a mechanism whereby RBBP6 can self-regulate its own expression levels.

While the previous auto-ubiquitination data generated in our laboratory used anti-ubiquitin antibodies, this study used antibodies targeting the HA-tag on ubiquitin. Hence, we have shown that the effects reported here are not antibody-specific.

5.2 The RING finger of RBBP6 ubiquitinates p53

The availability of all the necessary reagents for *in vitro* ubiquitination assays allowed us to investigate whether the isolated RBBP6-RING finger of RBBP6 was able to ubiquitinate p53. To our surprise, GST-RBBP6-RING was able to ubiquitinate FLAG-p53QM, as detected in a western blot using antibodies targeting the FLAG-tag incorporated into FLAG-p53QM. Although much fainter than the auto-ubiquitination assays reported earlier in this thesis, the extent of ubiquitination may be comparable, considering that what is being detected by anti-FLAG is the single FLAG-p53QM molecule, rather than the multitude of HA-Ub molecules detected by anti-HA. The bands extend up to around 10 kDa, which may correspond to poly-ubiquitination or multiple mono-ubiquitination. In addition, there is a strong band just above p53QM which is likely to correspond to mono-ubiquitination. A very similar pattern is observed when GST-MDM2-RING is used as an E3. But when both GST-RBBP6-RING and GST-MDM2-RING were used together, the pattern of ubiquitination was very different, with clear evidence of very high molecular weight species which can only correspond to poly-ubiquitination. Since the effect of both E3s appears to be different from the sum of their individual activities, we conclude that our data provides evidence that the RBBP6-RING and MDM2-RING may act cooperatively.

5.3 p53 interacts directly with the N-terminus of RBBP6

The evidence presented in this thesis, that the RING finger domain of RBBP6 is able to catalyse ubiquitination of p53, supports results generated previously in our laboratory, that the RING, R2 and R3 fragments of RBBP6 are all able to catalyse ubiquitination of p53, without any assistance from MDM2. If this is true, then we would expect these same fragments to interact directly with p53 *in vitro*. In an initial exploratory screen, Far Western analysis suggested that p53QM bound strongly to the R2 fragment of RBBP6, and to the RING finger domain, less strongly to the zinc finger domains and not at all to the DWNN domains or to GST, as a negative control. GST pull-down assays confirmed that FLAG-p53QM is co-precipitated by GST-R2.

Next, attempts were made to localize the interaction within p53. The N-terminal domain of p53, residues 1-95, was expressed in bacteria as FLAG-p53N. Contrary to our expectations, GST-R2 was not able to co-precipitate FLAG-p53N in GST pull-down assays. Therefore, FLAG-p53ΔN, spanning residues 95 – 339 of p53, was cloned using deletion mutagenesis and

expressed in bacteria. We subsequently concluded, that the interaction site must be in the remaining fragment of p53, which we cloned using deletion mutagenesis and denoted p53 Δ N. GST pull-down assays of using p53 Δ N shows that GST-R2 was able to co-precipitate p53 Δ N, producing a clear band at the same molecular weight as FLAG-p53 Δ interaction.

Further attempts were made to localize the site of the interaction by dividing FLAG-p53 Δ N into the DNA binding domain and C-terminal domain. The FLAG-p53DBD and FLAG-p53C were cloned and successfully expressed in bacteria. However, GST pulldown assays using these constructs did not produce clear cut results, as both FLAG_p53DBD and FLAG-p53C co-precipitated with R2.

The original focus of this thesis, investigating the possibility of DWNNylation, is reported in Appendix I. pGEX expression constructs coding for GST-FLAG-DWNN-GG and GST-FAG-DWNN-PI were cloned and the proteins expressing in bacteria. DWNN-GG represents the DWNN domain, terminating immediately following the di-glycine motif and DWNN-PI the DWNN terminating immediately before the di-glycine motif. Following removal of the GST tags, both proteins were incubated with mammalian cell lysates and then probed by western blot with antibodies targeting the FLAG-tagged proteins. If the DWNN domain becomes covalently attached to cellular proteins, then we should expect to see a ladder of proteins in the lane containing FLAG-DWNN-GG but not in the lane containing FLAG-DWNN-PI. However, no clear evidence for DWNNylation was found and so the investigation was not pursued.

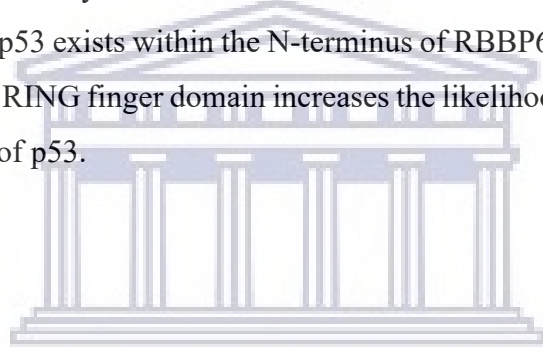
5.4 Future investigations

Future work will focus on further localization of the interaction reported here between the R2 fragment of RBBP6 and p53 Δ N. In addition to repeating the investigation aimed at localizing the interaction within p53 Δ N, existing expression constructs coding for the isolated zinc finger and RING finger domains will be used to further localize the interaction within R2. Additional controls should be included in the experimental design when repeating the investigation in order to rule out the possibility of non-specific interactions between the FLAG moiety and GST R2. While this is unlikely and the possibility can be excluded due to the 8 amino acid length of the FLAG tag, the possibility exists and should be effectively controlled for in future studies. The results obtained are a preliminary study and therefore the identities of the p53 fragments should be further validated in future studies. The final aim is to localize the interaction

sufficiently that it can be taken forward into structural studies, using both Nuclear Magnetic Resonance (NMR) spectroscopy and X-ray crystallography. In addition to determining the structure of the bound complex, we will aim to generate mutants which abolish the interaction, which can then be taken into functional studies in cultured cells, to investigate the importance of the interaction for the regulation of p53.

5.5 Summary

In summary, this thesis provides evidence that RBBP6 is able to efficiently auto-ubiquitinate itself. It also provides evidence that RBBP6 is able to ubiquitinate p53 without the assistance of MDM2, possibly acting cooperatively with MDM2. In support of this conclusion, we show that, in addition to the previously-identified interaction site near the C-terminus of RBBP6, another interaction site for p53 exists within the N-terminus of RBBP6 (residues 142-335). The proximity of this site to the RING finger domain increases the likelihood that RBBP6 is directly involved in ubiquitination of p53.



UNIVERSITY *of the*
WESTERN CAPE

BIBLIOGRAPHY

ADAMS, P.D. 2001. Regulation of the retinoblastoma tumor suppressor protein by cyclin/cdks. *Biochem Biophys Acta*, 1471, 123-33.

ANDERSEN, P., KRAGELUND, B.B., OLSEN, A.N., LARSEN, F.H., CHUA, N.H., POULSEN, F.M., AND SKRIVER, K. 2004. Structure and biochemical function of a prototypical Arabidopsis U-box domain. *J Biol Chem*, 279, 40053-40061.

ANTUNES, R.J. 2008. *Characterization of the DWNN domain and RING finger-like motif within the DCM of the Drosophila melanogaster SNAMA protein*. Master of Science Dissertation, University of the Witwatersrand.

AMEMIYA, Y., AZMI, P. & SETH, A. 2008. Autoubiquitination of BCA2 RING E3 ligase regulates its own stability and affects cell migration. *Molecular Cancer Research*, 6, 1385-1396.

ARAVIND L, KOONIN EV. 2000. The U box is a modified RING finger - a common domain in ubiquitination. *Current Biology*, 10, 132-134.

ASAKUNO, K., KOHNO, K., UCHIUMI, T., KUBO, T., SATO, S., ISONO, M. & KUWANO, M. 1994. Involvement of a DNA binding protein, MDR-NF1/YB-1, in human MDR1 gene expression by actinomycin D. *Biochemical and biophysical research communications*, 199, 1428-1435.

ARAI, R., YOSHIKAWA, S., MURAYAMA, K., IMAI, Y. 2006. Structure of human ubiquitin-conjugating enzyme E2 G2 (UBE2G2/UBC7). *Acta Crystallogr. Sect. F. Struct. Biol. Cryst. Commun*, 62, 330-334.

BABOSHINA, O.V., CRINELLI, R., SIEPMANN, T.J., HAAS, A.L. 2001. N-end rule specificity within the ubiquitin/proteasome pathway is not an affinity effect. *J. Biol. Chem*, 276, 39428-39437.

BAE, K.H., KWON, Y.D., SHIN, H.C., HWANG, M.S., RYU, E.H., PARK, K.S., YANG, H.Y., LEE, D.K., LEE, Y., PARK, J., KWON, H.S., KIM, H.W., YEH, B.I., LEE, H.W., SOHN, S.H., YOON, J., SEOL, W., KIM, J.S. 2003. Human zinc fingers as building blocks in the construction of artificial transcription factors. *Nat Biotechnol*, 21, 275-80.

BATRA, J., HULTQUIST, J.T., LIU, D., SHTANKO, O., VAN DOLLEN, J., SATKAMP, L., JANG, G.M., LUTHRA, P., SCHWARZ, T.M., SMALL, G.I., ARNETT, E., ANANTPADMA, M., REYES, A., LEUNG, D.W., KAAKE, R., HAAS, P., SCHMIDT, C.B., SCHLESINGER, L.S., LACOUNT, D.J., DAVEY, R.A., AMARASINGHE, G.K., BASLER, C.F., KROGAN, N.J. 2018. Protein Interaction Mapping Identifies RBBP6 as a Negative Regulator of Ebola Virus Replication. *Cell*, 175, 1917-1930.

BAI, L. & ZHU, W. 2006. p53 : Structure , Function and Therapeutic Applications. *Journal of Cancer Molecules*, 2, 141–153.

BELZILE, J.P., RICHARD, J., ROUGEAU, N., XIAO, Y., COHEN, E.A. 2010. HIV-1 Vpr Induces the K48-Linked Polyubiquitination and Proteasomal Degradation of Target Cellular Proteins To Activate ATR and Promote G2 Arrest. *Journal of virology*, 84, 3320–3330.

BROOKS, C.L., LI, M., GU, W. 2004. Monoubiquitination: The Signal for p53 Nuclear Export? *Cell Cycle*, 3, 436–438.

BROWN, C.J., LAIN, S., VERMA, C.S., FERSHT, A.R. & LANE, D.P. 2009. Awakening guardian angels: drugging the p53 pathway. *Nature reviews, Cancer*, 9, 862–73.

BROOKS, C. L., GU, W. 2006. p53 ubiquitination: MDM2 and beyond. *Mol Cell*, 21, 307–315.

BURROUGHS, A. M., JAFFEE, M., IYER, L. M. & ARAVIND, L. 2008. Anatomy of the E2 ligase fold: implications for enzymology and evolution of ubiquitin/Ub-like protein conjugation. *Journal of structural biology*, 162, 205-218.

CAPILI, A.D., EDGHILL, E.L., WU, K., BORDEN, K.L. 2004. Structure of the C-terminal RING finger from a RING-IBR-RING/TRIAD motif reveals a novel Zn²⁺ -binding domain distinct from a RING. *J Mol Biol*, 340, 1117-1129.

CHAUGULE, V. K., BURCHELL, L., BARBER, K. R., SIDHU, A., LESLIE, S. J., SHAW, G. S. & WALDEN, H. 2011. Autoregulation of Parkin activity through its ubiquitin-like domain. *The EMBO journal*, 30, 2853-2867.

CHANG, C., SIMMONS, D.T., MARTIN, M.A., MORA, P.T. 1979. Identification and partial characterization of new antigens from simian virus 40-transformed mouse cells. *J Virol*, 31, 463-471.

CHEN, J., TANG, H., WU, Z., ZHOU, C., JIANG, T., XUE, Y., HUANG, G., YAN, D. & PENG, Z. 2013. Overexpression of RBBP6, alone or combined with mutant tp53, is predictive of poor prognosis in colon cancer. *The Journal of cell biology*, 8, 1-9.

CHEN, Z.J., 2005. Ubiquitin signalling in the NF-kappaB pathway. *Nature Cell Biology*, 7(8), 758–65.

CHIBI, M., MEYER, M., SKEPU, A., REES, D. J., MOOLMAN-SMOOK, J. C. & PUGH, D. J. R. 2008. RBBP6 interacts with multifunctional protein YB-1 through its RING finger domain, leading to ubiquitination and proteosomal degradation of YB-1. *J Mol Biol*, 384, 908-916.

CHUNG, K. K. K., DAWSON, V. L. & DAWSON, T. M. 2001. The role of the ubiquitin-proteasomal pathway in Parkinson's disease and other neurodegenerative disorders. *Trends in neurosciences*, 24, 7-14.

CIECHANOVER, A. & STANHILL, A. 2014. The complexity of recognition of ubiquitinated substrates by the 26S proteasome. *Biochimica et biophysica acta*, 1843, 86–96.

CORDIER, F., GRUBISHA, O., TRAINCARD, F., VÉRON, M., DELEPIERRE, M. & AGOU, F. 2009. The zinc finger of NEMO is a functional ubiquitin-binding domain. *Journal of Biological Chemistry*, 284, 2902-2907.

CYR, D. M., HÖHFELD, J. & PATTERSON, C. 2002. Protein quality control: U-box containing E3 ubiquitin ligases join the fold. *Trends in biochemical sciences*, 27, 368-375.

DAVIES, A.H., BARRET, M.R., PAMBID, K., HU, A.L., STRATFORD, S., FREEMAN, I.M., BERQUIN, S., PELECH, R., HIETER, C., MAXWELL., DUNN, S.E. 2011. YB-1 evokes susceptibility to cancer through cytokinesis failure, mitotic dysfunction and HER2 amplification. *Oncogene*, 30, 3649-6.

DE BIE, P. & CIECHANOVER, A. 2011. Ubiquitination of E3 ligases: self-regulation of the ubiquitin system via proteolytic and non-proteolytic mechanisms. *Cell Death and Differentiation*, 18 1393–1402.

DELEO, A.B., JAY, G., APPELLA, E., DUBOIS, G.C., LAW, L.W., OLD, L.J. 1979. Detection of a transformation-related antigen in chemically induced sarcomas and other transformed cells of the mouse. *Proc Natl Acad Sci U S A*, 76, 2420-2424.

DENSHAM, R.M., GARVIN, A.J., STONE, H.R., STRACHAN, J., BALDOCK, R.A., MARTIN, M.D., FLETCHER, A., BLAIR-REID, S., BEESLEY, J., JOHAL, B., PEARL, L.H., NEELY, R., KEEP, N.H., WATTS, F.Z., MORRIS, J.R. 2006. Human BRCA1-BARD1 ubiquitin ligase activity counteracts chromatin barriers to DNA resection. *Nature structural and molecular biology*, 23, 647-655

DESHAIES, R. J. & JOAZEIRO, C. A. 2009. RING domain E3 ubiquitin ligases. *annu rev biochem*, 78, 399-434.

DI GIAMMARTINO, D. C., LI, W., OGAMI, K., YASHINSKIE, J. J., HOQUE, M., TIAN, B. & MANLEY, J. L. 2014. RBBP6 isoforms regulate the human polyadenylation machinery and modulate expression of mRNAs with AU-rich 3' UTRs. *Genes Dev*, 28, 2248-2260.

EFEYAN, A. & SERRANO, M. 2007. The Guardian of the Genome and Policeman of the Oncogenes. *Cell Cycle*, 6, 1006–1010.

GROSSMAN, S.R., DEATO, M.E., BRIGNONE, C., CHAN, H.M. 2003. Polyubiquitination of p53 by a ubiquitin ligase activity of p300. *Science*, 300, 342-344.

HANZAWA, H., DE RUWE, M.J., ALBERT, T.K., VAN DER VLIET, P.C., TIMMERS, H.T., AND BOELENS, R. 2001. The structure of the C4C4 ring finger of human NOT4 reveals features distinct from those of C3HC4 RING fingers. *J Biol Chem*, 276, 10185-10190.

HASHIZUME, R., FUKUDA, M., MAEDA, I., NISHIKAWA, H., OYAKE, D., YABUKI, Y., OGATA, H., OHTA, T. 2001. The RING hetero-dimer BRCA1-BARD1 is a ubiquitin ligase inactivated by a breast cancer derived mutation. *J Biol Chem.*, 276, 14537-14540.

HARMS, K. L. & CHEN, X. 2006. The functional domains in p53 family proteins exhibit both common and distinct properties. *Cell Death and Differentiation*, 13, 890-897.

HATAKEYAMA, S., YADA, M., MATSUMOTO, M., ISHIDA, N., NAKAYAMA, K.I. 2001. U box proteins as a new family of ubiquitin-protein ligases. *J. Biol. Chem*, 276, 33111-33120.

HAUPT, Y., MAYA, R., KAZAZ, A., OREN, M. 1997. Mdm2 promotes the rapid degradation of p53. *Nature*, 387, 296-299.

HERSHKO, A. & CIECHANOVER, A. 1998. The ubiquitin system. *Annual review of biochemistry*, 67, 425-79.

HILL, C.H., BOREIKAITE, V., KUMAR, A., CASANAL, A., KUBIK, P., DEGLIESPOST, G., MASLEN, S., MARIANI, A., VON LOEFFELHOLZ, O., GIRBIG, M., SKEHEL, M., PASSMORE, L.A. 2019. Activation of the Endonuclease that Defines mRNA 3' Ends Requires Incorporation into an 8-Subunit Core Cleavage and Polyadenylation Factor Complex. *Molecular Cell*, 73, 1-15

HO, W.C., LUO, C., ZHAO, K., CHAI, X., FITZGERALD, M.X., MARMOSTEIN, R. 2006. High-resolution structure of the p53 core domain: implications for binding small-molecule stabilizing compounds. *Acta crystallographica. Section D, Biological crystallography*, 62, 1484-93

HOCK, A.K. & VOUSDEN, K.H. 2014. The role of ubiquitin modification in the regulation of p53. *Biochimica et biophysica acta*, 1843, 137-49.

HOE, K.K., VERMA, C.S. & LANE, D.P. 2014. Drugging the p53 pathway: understanding the route to clinical efficacy. *Nature reviews. Drug discovery*, 13, 217-36.

HONDA, R., TANAKA, H. & YASUDA, H. 1997. Oncoprotein MDM2 is a ubiquitin ligase E3 for tumor suppressor p53. *FEBS letters*, 420, 25-7.

HUANG, K., JOHNSON, K.D., PETCHERSKI, A.G., VANDERGON, T., MOSSER, E.A., COPELAND, N.G., JENKINS, N.A., KIMBLE, J., BRESNICK, E.H. 2000. A HECT domain ubiquitin ligase closely related to the mammalian protein WWP1 is essential for *Caenorhabditis elegans* embryogenesis. *Gene* 252, 137-145.

HUNZIKER A, JENSEN MH, KRISHNA S. 2010. Stress-specific response of the p53-Mdm2 feedback loop. *BMC Systems Biology*, 4, 94.

JENTSCH, S. & PYROWOLAKIS, G. 2000. Ubiquitin and its kin: how close are the family ties?. *Trends in Cell Biology*, 10, 335-342.

JOERGER, A.C., ALLEN, M.D. & FERSHT, A.R. 2004. Crystal structure of a superstable mutant of human p53 core domain. Insights into the mechanism of rescuing oncogenic mutations. *The Journal of biological chemistry*, 279, 2, 1291-6.

JOAZEIRO, C. & WEISSMAN, A. 2000. RING finger proteins: mediators of ubiquitin ligase activity. *Cell*, 102, 549-552.

JOOSTE, L.S. 2015. *In vitro investigation of the ubiquitination and degradation of p53 by Murine Double Minute 2 (MDM2) and Retinoblastoma Binding Protein 6 (RBBP6)*. Msc Biotechnology, University of the Western Cape.

JIN, J., LI, X., GYGI, S. P. & HARPER, J. W. 2007. Dual E1 activation systems for ubiquitin differentially regulate E2 enzyme charging. *Nature*, 447, 1135-1138.

KAO, A., RANDALL, A., YANG, Y., PATEL, V.R., KANDUR, W., GUAN, S., RYCHNOVSKY, S.D., BALDI, P. & HUANG, L. 2012. Mapping the structural topology of the yeast 19S proteasomal regulatory particle using chemical cross-linking and probabilistic modeling. *Molecular & cellular proteomics*, MCP, 11, 1566–77.

KAPPO, M. A., AB, E., HASSEM, F., ATKINSON, R. A., FARO, A., MULEYA, V., MULAUDZI, T., POOLE, J. O., MCKENZIE, J. M., CHIBI, M., MOOLMAN-SMOOK, J. C., REES, D. J. & PUGH, D. J. 2012. Solution structure of RING finger-like domain of retinoblastoma-binding protein-6 (RBBP6) suggests it functions as a U-box. *J Biol Chem*, 287, 7146-7158.

KELLENBERGER, E., DOMINGUEZ, C., FRIBOURG, S., WASIELEWSKI, E., MORAS, D., POTERSZMAN, A., BOELEN, R., KIEFFER, B. 2005. Solution structure of the C-terminal domain of TFIIH P44 subunit reveals a novel type of C4C4 ring domain involved in protein-protein interactions. *J Biol Chem*, 280, 20785-20792.

KERSCHER, O., FELBERBAUM, R. & HOCHSTRASSER, M. 2006. Modification of proteins by ubiquitin and ubiquitin-like proteins. *Annu. Rev. Cell Dev. Biol.*, 22, 159-180.

KIM, H., KIM, K., LLEDIAS, F., KISSELEV, A., SCAGLIONE, K., SKOWYRA, GYGI, D. AND GOLDBERG, A. 2007. Certain pairs of ubiquitin-conjugating Enzymes (E2s) and ubiquitin-protein ligases (E3s) synthesize non degradable forked ubiquitin chains containing all possible isopeptide linkages. *The journal of biological chemistry*. 282,17375–17386.

KUMARI, R., SEN, N., DAS, S. 2014. Tumour suppressor p53: understanding the molecular mechanisms inherent to cancer. *Current science.*, 107(5).

LEE, S. D. & MOORE, C. L. 2014. Efficient mRNA polyadenylation requires a ubiquitin-like domain, a zinc knuckle, and a RING finger domain, all contained in the Mpe1 protein. *Mol Cell Biol*, 34, 3955-3967.

- LI, L., DENG, B., XING, G., TENG, Y., TIAN, C., CHENG, X., YIN, X., YANG, J., GAO, X., ZHU, Y., SUN, Q., ZHANG, L., YANG, X. & HE, F. 2007. PACT is a negative regulator of p53 and essential for cell growth and embryonic development. *Proc Natl Acad Sci USA*, 104, 7951-7956.
- LIU, D.P., SONG, H. & XU, Y. 2010. A common gain of function of p53 cancer mutants in inducing genetic instability. *Oncogene*, 29, 949–56.
- LIU, H. & NAISMITH, J.H. 2008. An efficient one step site directed deletion, insertion, single and multiple-site plasmid mutagenesis protocol. *BMC Biotechnology*, 8, 91.
- LI, M., BROOKS, L., WU-BAER, F., CHEN, D., BAER, R., GU, W. 2003. Mono- Versus Polyubiquitination: Differential Control of p53 Fate by Mdm2. *Science*, 302, 1972-197
- LIEW CW., SUN, H., HUNTER, T., DAY, C.L. 2010. RING domain dimerization is essential for RNF4 function. *Biochemistry Journal*, 431, 23–29.
- LUTZ, M., WEMPE, F., BAHR, I., ZOPF, D., VON MELCHNER, H. 2006. Proteasomal degradation of the multifunctional regulator YB-1 is mediated by an F-Box protein induced during programmed cell death. *FEBS letters*, 580, 3921-30.
- MATTHEWS, J.M., SUNDE, M. 2002. Zinc fingers--folds for many occasions. *IUBMB Life*, 54, 351-355
- MATTHEWS, J. M., KOWALSKI, K., LIEW, C. K., SHARPE, B. K., FOX, A. H., CROSSLEY, M. & MACKAY, J. P. 2000. A class of zinc fingers involved in protein–protein interactions. *The FEBS Journal*, 267, 1030-1038.
- MAUMELA, M.P. 2016. *Characterisation of N-terminal fragments of Retinoblastoma Binding Protein 6 for structural analysis*. Msc Biotechnology, University of the Western Cape.
- METZGER, M.B., PRUNEDA, J.N., KLEVIT, R.E. & WEISSMAN, A.M. 2014. RING-type E3 ligases: master manipulators of E2 ubiquitin-conjugating enzymes and ubiquitination. *Biochimica et biophysica acta*, 1843, 47–60.
- MBITA, Z., MEYER, M., SKEPU, A., HOSIE, M., REES, J. & DLAMINI, Z. 2012. De-regulation of the RBBP6 isoform 3/DWNN in human cancers. *Mol Cell Biochem*, 362, 249-262.

MICHAEL, D. & OREN, M. 2003. The p53-Mdm2 module and the ubiquitin system. *Semin Cancer Biol*, 13, 49-58.

MIOTTO, B., CHIBI, M., XIE, P., KOUNDRIOUKOFF, S., MOOLMAN-SMOOK, H., PUGH, D., DEBATISSE, M., HE, F., ZHANG, L. & DEFOSSEZ, P. A. 2014. The RBBP6/ZBTB38/MCM10 axis regulates DNA replication and common fragile site stability. *Cell Rep*, 7, 575-587.

MOLL, U. & PETRENKO, O. 2003. The MDM2-p53 Interaction The MDM2-p53 Interaction. *Molecular Cancer Research*, 1, 1001–1008.

MOGK, A., SCHMIDT, R. & BUKAU, B. 2007. The N-end rule pathway for regulated proteolysis: prokaryotic and eukaryotic strategies. *Trends Cell Biol*, 17, 165-172.

MOTADI, L. R., BHOOLAB, K. D., & DLAMINI, Z. 2011. Expression and function of retinoblastoma binding protein 6 (RBBP6) in human lung cancer. *ELSEVIER, Immunobiology*, 216, 1065–1073

MORISAKI, T., YASHIRO, M., KAKEHASHI, A., INAGAKI, A., KINOSHITA, H., FUKUOKA, T., KASASHIMA, H., MASUDA, G., SAKURAI, K., KUBO, N., MUGURUMA, K., OHIRA, M., WANIBUCHI, H. & HIRAKAWA, K. 2014. Comparative proteomics analysis of gastric cancer stem cells. *PLoS One*, 9, e110736.

MULLER, S., BERGER, M., LEHEMBRE, F., SEELER, J. S., HAUPT, Y., DEJEAN, A. 2000. c-Jun and p53 activity is modulated by SUMO-1 modification. *Journal of Biological Chemistry*, 275, 13321-13329.

NANDI, D., TAHILIANI, P., KUMAR, A., CHANDU, D. 2006. The ubiquitin-proteasome system. *J. Biosci*, 31, 137-55

NATHAN, J. A., KIM, H. T., TING, L., GYGI, S. P., GOLDBERG, A. L. 2013. Why do cellular proteins linked to K63-polyubiquitin chains not associate with proteasomes? *The EMBO Journal*, 32, 552-565.

NIKOLAY, R., WIEDERKEHR, T., RIST, W., KRAMER, G., MAYER, M. P., BUKAU, B. 2004. Dimerization of the Human E3 Ligase CHIP via a Coiled-coil Domain Is Essential for Its Activity. *Journal of Biological Chemistry*, 279, 2673-2678.

NIKLOVA, P., HENCKEL, J., LANE, D. & FERSHT, A. 1998. Semirational design of active tumor suppressor p53 DNA binding. *Proceedings of the National Academy of Sciences*, 95, 14675–14680.

NARISAWA-SAITO, M. & KIYONO, T. 2007. Basic mechanisms of high-risk human papillomavirus- induced carcinogenesis: Roles of E6 and E7 proteins. *Cancer Science*, 98, 1505– 1511.

OHGA, T., UCHIUMI, T., MAKINO, Y., KOIKE, K., WADA, M., KUWANO, M. & KOHNO, K. 1998. Direct involvement of the Y-box binding protein YB-1 in genotoxic stress-induced activation of the human multidrug resistance 1 gene. *Journal of Biological Chemistry*, 273, 5997-6000.

PANT, V. & LOZANO, G. 2014. Limiting the power of p53 through the ubiquitin proteasome pathway. *Genes & development*, 28, 1739–1751.

PICKART, C. M. 2001. Mechanisms underlying ubiquitination. *Annual review of biochemistry*, 70, 503-533.

PRINGA, E., MARTINEZ-NOEL, G., MULLER, U., HARBERS, K. 2001. Interaction of the ring finger-related U-box motif of a nuclear dot protein with ubiquitin-conjugating enzymes. *J Biol Chem*, 276, 19617-19623.

PUGH, D. J., AB, E., FARO, A., LUTYA, P. T., HOFFMANN, E. & REES, D. J. 2006. DWN, a novel ubiquitin-like domain, implicates RBBP6 in mRNA processing and ubiquitin-like pathways. *BMC Struct Biol*, 6, 1-8.

RABUT, G. & PETER, M. 2008. Function and regulation of protein neddylation. “Protein modifications: beyond the usual suspects” review series. *EMBO Rep*, 9, 969–76.

RODRIGUEZ, M.S., DESTERRO, J.M.P., LAIN, S. & LANE, D.P. 2000. Multiple CTerminal Lysine Residues Target p53 for Ubiquitin-Proteasome-Mediated Degradation. *Molecular and Cellular Biology*, 20(22), 8458–8467.

SAKAI, Y., SAIJO, M., COELHO, K., KISHINO, T., NIIKAWA, N. & TAYA, Y. 1995. cDNA sequence and chromosomal localization of a novel human protein, RBQ-1 (RBBP6), that binds to the Retinoblastoma gene product. *Genomics*, 30, 98-101.

- SEMPLE, C.A., RIKEN GER GROUP.& GSL MEMBERS. 2003. The comparative proteomics of ubiquitination in mouse. *Genome Res*, 13, 1389–1394.
- SHADFAN, M., LOPEZ-PAJARES, V., YUAN, Z.M. 2012. MDM2 and MDMX: Alone and together in regulation of p53. *Translational cancer research*, 1, 88–89.
- SHI, D ., POP, M.S., KULIKOV, R., LOVE, I.M., KUNG, A.L., GROSSMAN, S.R. 2009. CBP and p300 are cytoplasmic E4 polyubiquitin ligases for p53. *Proceedings of the National Academy of Sciences*, 106(38), 16275–16280.
- SIMONS, A., MELAMED-BESSUDO, C., WOLKOWICZ, R., SPERLING, J., SPERLING, R., EISENBACH, L. & ROTTER, V. 1997. PACT: cloning and characterization of a cellular p53 binding protein that interacts with Rb. *Oncogene*, 14, 145-155.
- SRI KRISHNA, S., MAJUMDAR, I. & GRISHIN, N. V. 2003. Structural classification of zinc fingers. *Nucleic acids research*, 31, 532-550.
- SOROKIN, A. V., KIM, E.R., OVCHINNIKOV, L.P. 2009. Proteasome system of protein degradation and processing. *Biochemistry (Moscow)*, 74, 1411– 1442
- STOMMEL, J.M. & WAHL, G.M. 2005. A new twist in the feedback loop: stress activated MDM2 destabilization is required for p53 activation. *Cell cycle*, 4, 411-7.
- STOMMEL, J., & WAHL, G.M. 2004. Accelerated MDM2 auto-degradation induced by DNA-damage kinases is required for p53 activation. *The EMBO journal* **23**, 1547-1556
- SU, H.L.& LI, S.S.L.2002. Molecular features of human ubiquitin-like SUMO genes and their encoded proteins. *Genes*, 296, 65-73.
- TREMPE, J.F., SAUVE, V., GRENIER, K., SEIRAFI, M., TANG, M.Y., MENADE, M., AL-ABDUL-WAHID, S., KRETT, J., WONG, K., KOZLOV, G., NAGAR, B., FON, E.A., GEHRING, K. 2013. Structure of Parkin reveals mechanisms for ubiquitin ligase activation. *Science*, 340, 1451.
- VALENTE, E. M., ABOU-SLEIMAN, P. M., CAPUTO, V., MUQIT, M. M. K., HARVEY, K., GISPERS, S., ALI, Z., DEL TURCO, D., BENTIVOGLIO, A. R. & HEALY, D. G. 2004. Hereditary early-onset Parkinson's disease caused by mutations in PINK1. *Science*, 304, 1158-1160.

VAN WIJK, S.J.L. & TIMMERS, H.T.M. 2010. The family of ubiquitin-conjugating enzymes (E2s): deciding between life and death of proteins. *FASEB journal : official publication of the Federation of American Societies for Experimental Biology*, 24(4), 981–93.

VO, L., MINET, M., LACROUTE, F. & WYERS, F. 2001. Mpe1, a Zinc Knuckle protein, is an essential component of yeast cleavage and polyadenylation factor required for the cleavage and polyadenylation of mRNA. *Molecular and Cellular Biology*, 21, 8346–8356.

WANG, X., WANG, J. & JIANG, X. 2011. MdmX protein is essential for Mdm2 protein-mediated p53 polyubiquitination. *The Journal of biological chemistry*, 286(27), 23725–34.

WADE, M., CHENG LI, Y., WAHL, G.M. 2013. MDM2, MDMX and p53 in oncogenesis and cancer therapy. *Nat Rev Cancer*, 13(2), 83-96

WEINBERG, R. 2007. *The Biology of Cancer. 7th Edition*. New York: Garland Sciences.

WOELK, T., SIGISMUND, S., PENENGO, L., POLO S. 2007. The ubiquitination code: a signalling problem. *Cell Division*, 2,1-1

WINDHEIM, M., PEGGIE, M. & COHEN, P. 2008. Two different classes of E2 ubiquitin-conjugating enzymes are required for the mono-ubiquitination of proteins and elongation by polyubiquitin chains with a specific topology. *The Biochemical journal*, 409, 723–729.

WINN, P.J., RELIGA, T.L., BATTEY, J.N., BANERJEE, A., WADE, R.C. 2004. Determinants of functionality in the ubiquitin conjugating enzyme family. *Structure*, 12, 1563–74.

WITTE, M. M. & SCOTT, R. E. 1997. The proliferation potential protein-related (P2P-R) gene with domains encoding heterogeneous nuclear ribonucleoprotein association and Rb1 binding shows repressed expression during terminal differentiation. *Proc Natl Acad Sci USA*, 94, 1212-1217.

XIA, Y., PAO, G.M., CHEN, H.W., VERMA, I.M., HUNTER, T. 2003. Enhancement of BRCA1 E3 ubiquitin ligase activity through direct interaction with the BARD1 protein. *J. Biol Chem*, 278, 5255–5263.

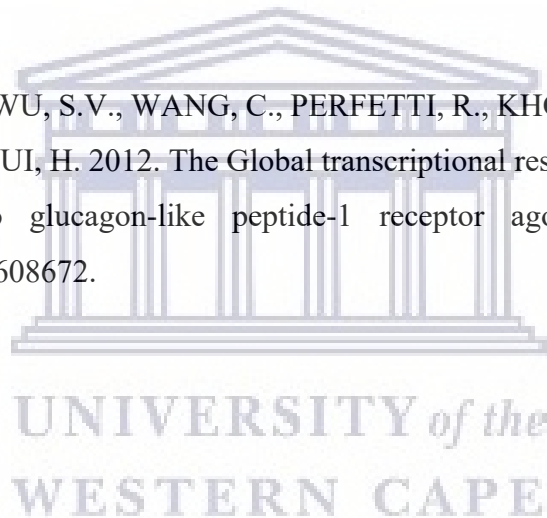
YEH, E, T, H., GONG, L. & KAMITANI, T. (2000). Ubiquitin-like proteins: new wines in new bottles, *Gene*, 248, 1-14.

YUNJE, C., FORINA, S., JEFFREY, P.D., PAVLETICH, N.O., 1994. Crystal structure of p53 tumour suppressor-DNA complex: understanding tumorigenic mutations. *Science* 265, 346-355.

YOSHITAKE, Y., NAKATSURA, T., MONJI, M., SENJU, S., MATSUYOSHI, H., TSUKAMOTO, H., HOSAKA, S., KOMORI, H., FUKUMA, D., IKUTA, Y., KATAGIRI, T., FURUKAWA, Y., HIROMI, I., SHINOHARA, M., NAKAMURA, Y. & NISHIMURA, Y. 2004. Proliferation Potential-Related Protein, an ideal esophageal cancer antigen for immunotherapy, identified using complementary DNA microarray analysis. *Clinical Cancer Research*, 10, 6437–48.

YOUNG, P., DEVERAUX, Q., BEAL, R.E., PICKART, C.M., RECHSTEINER, M. 1998. Characterization of two polyubiquitin sites in the 26S protease subunit 5a. *J Biol Chem*, 273, 5461–5467.

ZHAO, X., TANG, Y.G., WU, S.V., WANG, C., PERFETTI, R., KHOURY, N., CAI, D., HE, F., SU, X., GO, V.L.W., HUI, H. 2012. The Global transcriptional response of isolated human islets of Langerhans to glucagon-like peptide-1 receptor agonist liraglutide. *ISRN Endocrinology*, article ID 608672.



APPENDICES

APPENDIX I

The work reported in this appendix represents the original focus of my research.-Although not pursued to conclusion, the project did result in the successful generation of FLAG-tagged expression constructs for DWNN-GG and DWNN-IP, which may prove useful in future research. It is therefore appropriate that their construction be fully reported in this thesis, albeit only in an appendix. Furthermore, the new constructs were designed in such a way that the multiple cloning cassette of pGEX-6P was not altered, with the result that any cDNA in a pGEX-6P vector could be sub-cloned directly into the new vector, thereby incorporating a FLAG-tag between the GST tag and the target protein.

Introduction

The background to this investigation is presented in §1.8.3. Briefly, the ubiquitin-like fold of the DWNN domain, combined with the presence of a di-glycine motif at the equivalent structural position as found in ubiquitin, suggested that the domain may become covalently attached to other proteins in a process we have called DWNNylation (Pugh *et al.*, 2006). Preliminary results obtained in our laboratory suggested that incubation of the bacterially expressed DWNN domain, terminated immediately after the di-glycine motif, with mammalian cell lysates resulted in a ladder of higher molecular weight bands which may correspond to DWNNylated species. If this is the case, then it is to be expected that removal of the di-glycine motif from the C-terminus of the DWNN domain should eliminate this effect.

The objective was therefore to clone and express two different forms of the DWNN domain in *E. coli* and incubate them with mammalian cell lysates. The first construct, FLAG-DWNN-GG, terminated with the di-glycine motif, whereas the other form, FLAG-DWNN-PI, lacks the di-glycine motif and should therefore serve as a negative control. *In vitro* DWNNylation assays were conducted and immune-detection of the resultant complexes was carried out using anti-FLAG antibody specific for the FLAG tag incorporated into these proteins.

Generation of pGEX-FLAG-DWNN-GG and pGEX-FLAG-DWNN-PI

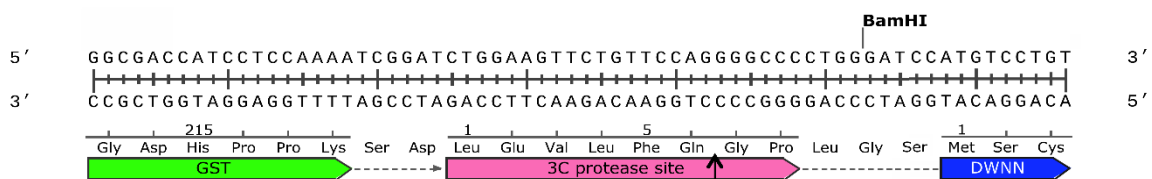
The pGEX-DWNN13 expression vector, coding for isoform 3 of RBBP6 and incorporating an N-terminal GST-tag, was already available in the laboratory. The first objective was to amplify

DWNN-GG, terminating immediately following the di-glycine motif incorporating a FLAG tag at the N-terminus. Since most of the GST-fusion constructs expressed in our laboratory have been inserted between the BamHI and XhoI sites of the pGEX-6P-2 vector, our strategy was to insert the FLAG tag in such a way that existing constructs could be sub-cloned directly out of pGEX-6P-2 into our “pGEX-FLAG” vector using BamHI and XhoI restriction enzymes, following excision of DWNN-GG.

To do so, the forward primer was designed to incorporate a BglIII site upstream of the FLAG sequence, followed by the BamHI site and the start of the DWNN domain. The amplicon would then be digested with BglIII and XhoI and inserted into pGEX-6P-2, following digestion with BamHI and XhoI. Since BglIII and BamHI are [isoschizomers](#), the cloning site would be destroyed, leaving the BamHI and XhoI sites flanking DWNN-GG, with an upstream FLAG-tag separated from DWNN-GG by the spacer residues Gly-Ala-Gly-Ser.

Primers pGEX-FLAG-DWNN-GG-F and pGEX-FLAG-DWNN-GG-R can be found in Table A. In the forward primer, the BglIII site is indicated in yellow, the FLAG tag in magenta and the BamHI site in cyan. In the reverse primer, the XhoI site is indicated in green and the pair of stop codons in red; the six nucleotides coding for the GlyGly motif are indicated with italics. The regions which anneal to the template are underlined. The same forward primer was used to make the FLAG-DWNN-PI construct, along with the pGEX-DWNN-PI-R reverse primer (see Table A), which was already available in the laboratory; note that the 6 nucleotides coding for the GlyGly motif are not present.

A



B

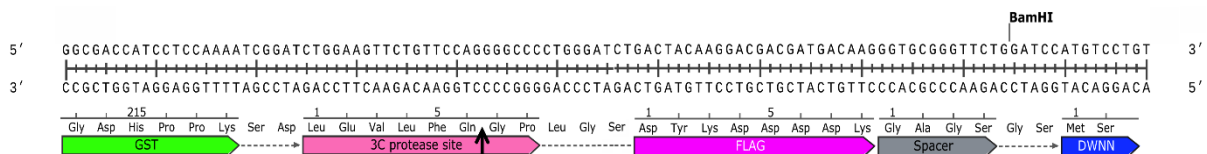


Figure A.1: Scheme for generation of construct expressing GST- FLAG-DWNN-GG/PI.The linker between GST and the DWNN domain prior to (A) and following (B) insertion of cDNA coding the FLAG-tag (indicated in magenta).

Table A: Sequence specific oligonucleotides for the addition of FLAG-tag (DYKDDDK) to the DWNN constructs. The primers were designed to incorporate the XhoI (green) and BglII (yellow) restriction sites. The FLAG-tag is indicated in purple, the BamHI site in cyan and stop codons in red.

Primer name	Sequence	Tm (°C)
pGEX-FLAG-DWNN-GG-F	5'- GAGGCGAGATCTGACTACAAGGACGACGAT GACAAGGGTGC GGGTTCTGGATCCATGTCC TGTGTGCA -3'	62
pGEX-FLAG-DWNN-GG-R	5'- GAGGCGCTCGAGTCATCAACCTCCAATAGG AATTCTTCTAA -3'	62
pGEX-DWNN-PI-R	5'- GAGGCGCTCGAGTTAAATAGGAATTCTTCT ACAATTACA -3'	62



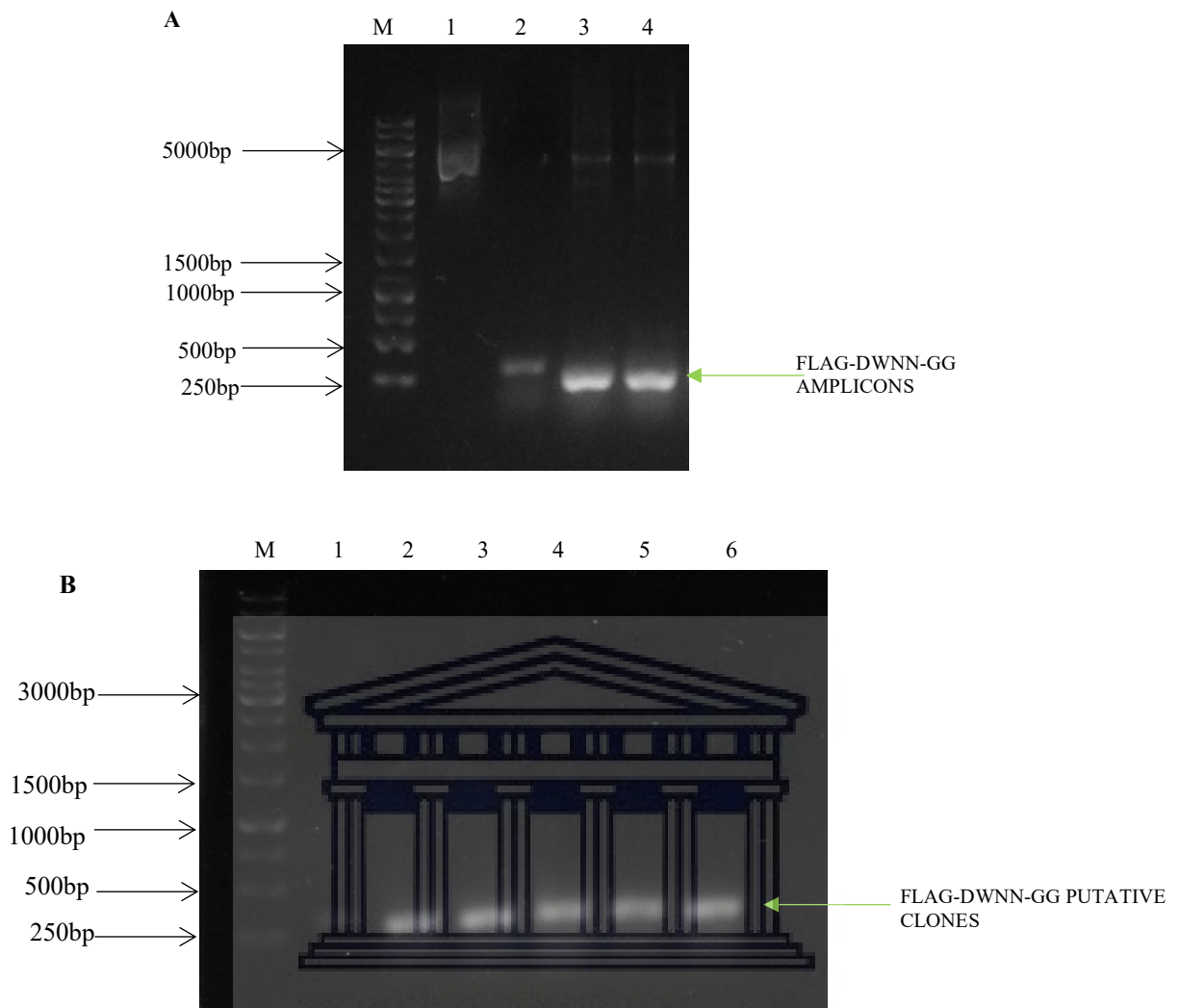


Figure A.2: Cloning of FLAG-DWNN-GG into pGEX-6P-2 (A) The FLAG-DWNN-GG fragment was amplified from pGEX-6P-2-DWNN-GG. Lanes 3 and 4 confirm amplification of DWNN-GG with a size of approximately 250bp. The amplicon was double-digested and cloned into pGEX-6P-2. (B) A PCR-screen to confirm the presence of DWNN-GG after molecular cloning. A fragment consistent with the size of DWNN-GG (237 bp) is amplified in lanes 2-6.

PCR amplifications for FLAG-DWNN-GG and FLAG-DWNN-PI were carried out as described in Section 2.3.2 and the corresponding amplicons resolved on 1% agarose gels as described in Section 2.3.5. Figure A.2 (A) and Fig A.3(A) show successful amplification of FLAG-DWNN-GG and FLAG-DWNN-PI respectively, at an approximate sizes of 240 bp in lanes 3 and 4. The PCR product was purified using a GeneJet gel purification Kit (GE Healthcare), digested with BglII and XhoI and inserted into pGEX-6P-2, following digestion with BamHI and XhoI, as described above. Putative clones were selected from experimental plates and overnight cultures were prepared for plasmid DNA isolation. Plasmid DNA from the

presumptive positive clones were isolated and subjected to PCR screening. Figure A.2 (B) and Fig A.3 (B), lanes 2-6, show successful amplification of fragments corresponding to the expected size of 237 bp for FLAG-DWNN-GG and FLAG-DWNN-PI respectively.

Sequences were confirmed by direct sequencing (Inqaba Biotechnical Industries) and found to be 100 % in agreement with the expected sequences. As expected, the new constructs includes the sequence upstream of DWNN:

SEQUENCE VERIFICATION OF FLAG-DWNN-GG CLONED INTO pGEX-6-P2 vector

ctggaagtctgtccaggggccctgggatctgactacaaggacgacgatgacaagggtgctggatccatgtcctgtgtgc
attat

LEVLFGPLGSDYKDDDDK GAGSGS MSCVHY

The sequence indicated in grey represents the 3C protease cleavage site, that in magenta the FLAG tag, and that in yellow the beginning of the DWNN domain. The nucleotides indicated in cyan are the BamHI site and those in green are the result of ligating the BglII site into the BamHI site; they are no longer cleavable by either BamHI or BglII.

Query	1	ATGTCCTGTGTGCATTATAAATTTTCCTCTAAACTCAACTATGATACCGTCACCTTTGAT	60
Sbjct	109	ATGTCCTGTGTGCATTATAAATTTTCCTCTAAACTCAACTATGATACCGTCACCTTTGAT	168
Query	61	GGGCTCCACATCTCCCTCTGCGACTTAAAGAAGCAGATTATGGGGAGAGAGAAGCTGAAA	120
Sbjct	169	GGGCTCCACATCTCCCTCTGCGACTTAAAGAAGCAGATTATGGGGAGAGAGAAGCTGAAA	228
Query	121	GCTGCCGACTGCGACCTGCAGATCACCAATGCGCAGACGAAAGAAGAATATACTGATGAT	180
Sbjct	229	GCTGCCGACTGCGACCTGCAGATCACCAATGCGCAGACGAAAGAAGAATATACTGATGAT	288
Query	181	AATGCTCTGATTCTAAGAATTCTTCTGTAATTGTTAGAAGAATTCCTATTGGAGGT	237
Sbjct	289	AATGCTCTGATTCTAAGAATTCTTCTGTAATTGTTAGAAGAATTCCTATTGGAGGT	345

Query denotes the expected sequence and subject denotes the experimental sequence to be determined.

SEQUENCE VERIFICATION OF FLAG-DWNN-PI CLONED INTO pGEX-6-P2 vector

```
Query 1 ATGCCTGTGTGCATTATAAATTTTCCTCTAAACTCAACTATGATACCGTCACCTTTGAT 60
|
Sbjct 112 ATGCCTGTGTGCATTATAAATTTTCCTCTAAACTCAACTATGATACCGTCACCTTTGAT 171

Query 61 GGGCTCCACATCTCCCTCTGCGACTTAAAGAAGCAGATTATGGGGAGAGAGAAGCTGAAA 120
|
Sbjct 172 GGGCTCCACATCTCCCTCTGCGACTTAAAGAAGCAGATTATGGGGAGAGAGAAGCTGAAA 231

Query 121 GCTGCCGACTGCGACCTGCAGATCACCAATGCGCAGACGAAAGAAGAATATACTGATGAT 180
|
Sbjct 232 GCTGCCGACTGCGACCTGCAGATCACCAATGCGCAGACGAAAGAAGAATATACTGATGAT 291

Query 181 AATGCTCTGATTCCCTAAGAATTCTTCTGTAATTGTTAGAAGAATTCCTATTTGATGA 237
|
Sbjct 292 AATGCTCTGATTCCCTAAGAATTCTTCTGTAATTGTTAGAAGAATTCCTATTTGATGA 348
```

Query denotes the expected sequence and sbjct denotes the experimental sequence to be determined.



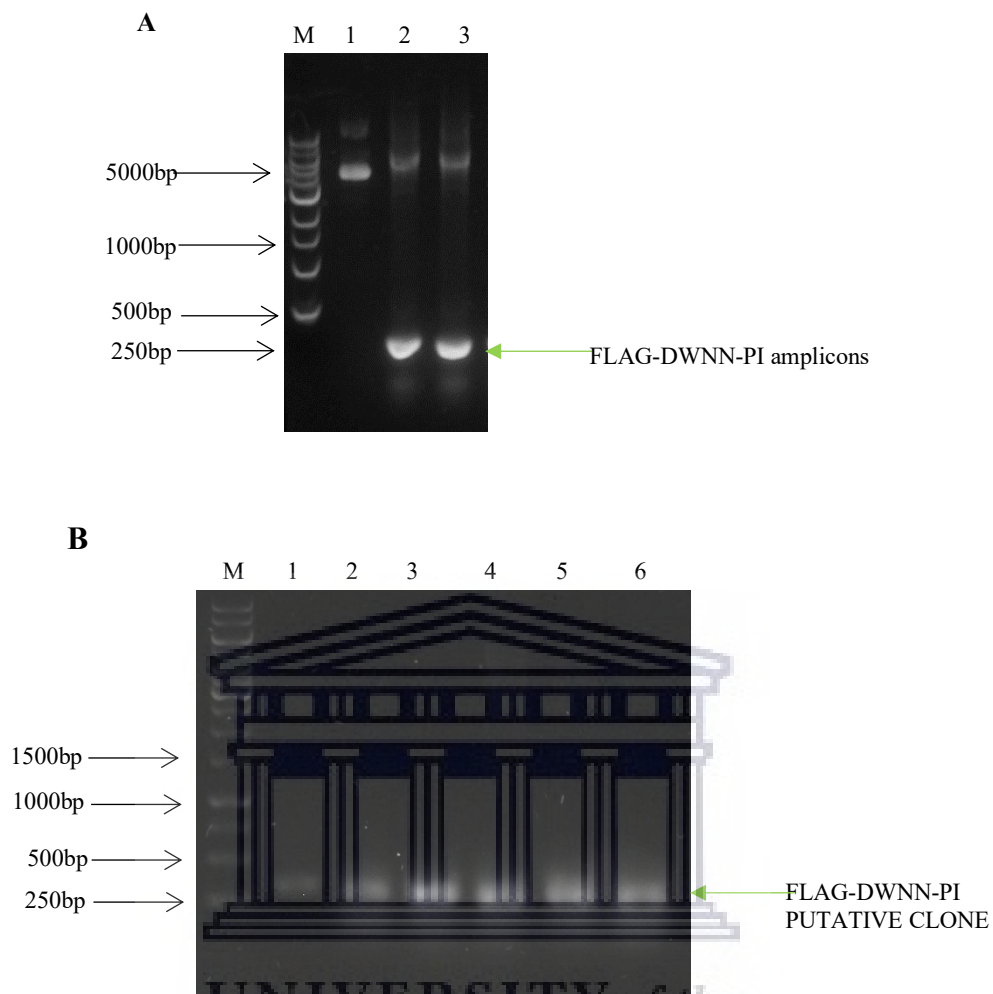


Figure A.3: Cloning of FLAG-DWNN-PI into pGEX-6P-2 (A) The FLAG-DWNN-PI fragment was amplified from pGEX-6P-2-DWNN13. Lanes 2 and 3 confirm amplification of DWNN-PI with a size of approximately 250 bp. The amplicon was double digested and cloned into pGEX-6P-2. (B) An agarose gel confirming the presence of DWNN-PI after molecular cloning. Lanes 2, 3, 4, 5 and 6 shows the presence of DWNN-PI in the plasmid after screening using PCR.

Recombinant expression of FLAG-DWNN-GG and FLAG-DWNN-PI

Expression of GST-FLAG-DWNN-GG and GST-FLAG-DWNN-PI was carried out in *E. coli* Codon+ cells at 37°C using an IPTG concentration of 0.5mM, as described in Section 2.4.1. Following cell lysis, the fusion (GST-tagged) protein was separated from *E.coli* bacterial proteins using glutathione affinity chromatography, as described in Section 2.4.2.

Figure A.4 (A) indicates the successful elution of a band corresponding to GST-FLAG-DWNN-GG in lanes 6-9 with an approximate molecular weight of 35 kDa. The band corresponding to GST-FLAG-DWNN-GG can also be seen in the flow through (lanes 3 and 4), which indicates that the size of the column was insufficient to retain all of the protein. GST-FLAG-DWNN-GG fractions were pooled and concentrated after which it was dialysed using dialysis buffer as described in Section 2.4.2.3 to remove excess salts and small molecules. A fraction of the GST-FLAG-DWNN-GG fusion protein was aliquoted and glycerol was added to a final concentration of 10 % and stored at -20 °C for future use in GST-pull-down assays.

The remaining GST-FLAG-DWNN-GG was cleaved with 3C protease and dialysed as described in Section 2.4.2.3 to remove free glutathione within the sample. Cleaved samples were returned to the glutathione agarose column in order to separate the GST from FLAG-DWNN-GG., as shown in Figure A.4 (B) Lane 1 shows the protein before cleavage. Lanes 2 and 3 show what flowed directly through the column, which contain mainly the cleaved FLAG-DWNN-GG at a molecular weight consistent with 11 kDa. Lane 2 also contains small amounts of GST and 3C protease. Lanes 6-9 contain the bulk of the GST, which was retained by the column-Samples containing FLAG-DWNN-GG were pooled and concentrated and glycerol added to a final concentration of 10 % and stored at -20 °C for future use.

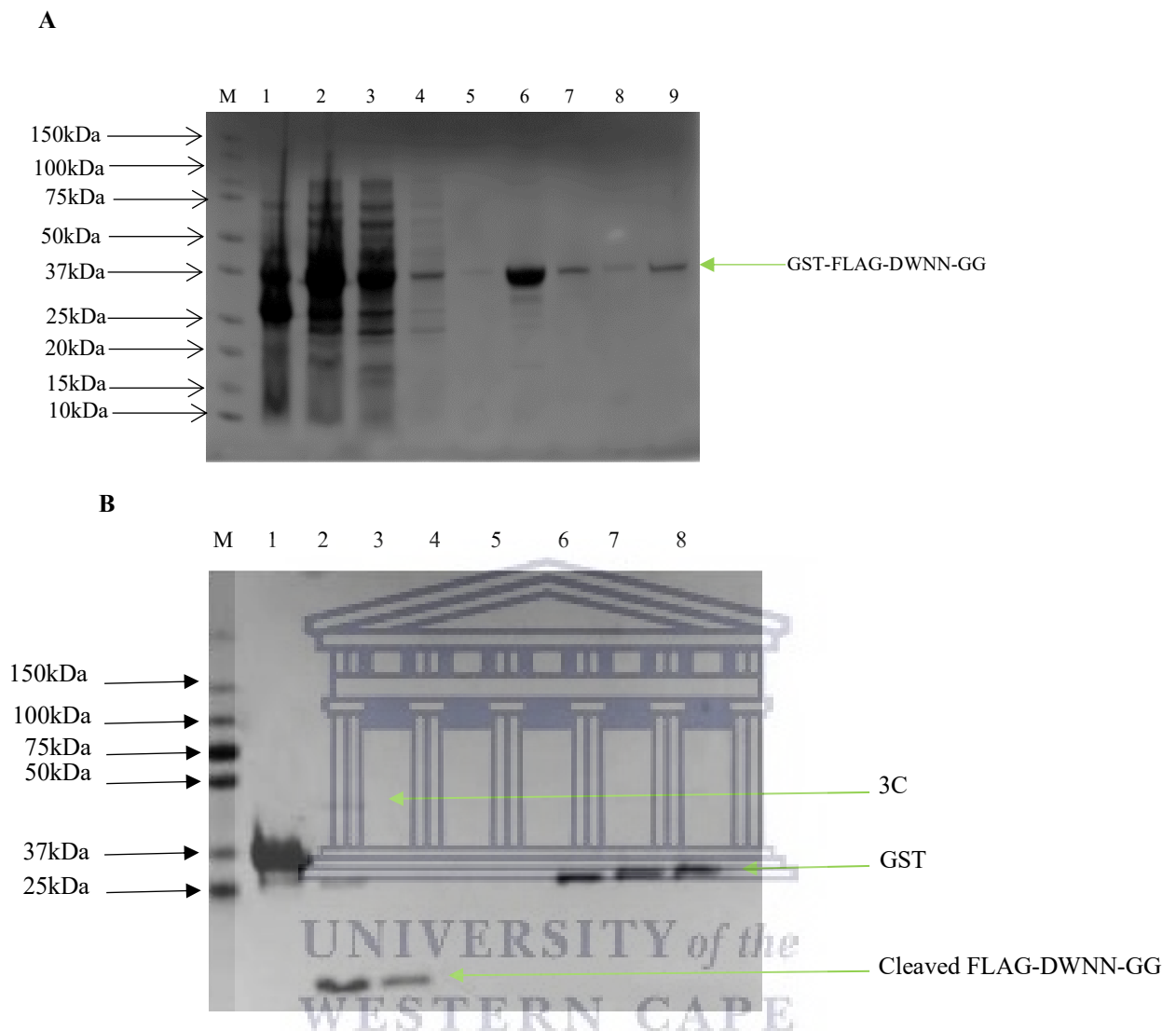


Figure A.4: Recombinant Expression and Purification of pGEX-FLAG-DWNN-GG. (A) Lane M indicates the molecular weight marker. Lane 1 indicates the insoluble protein (pellet), Lane 2 indicates the lysate (soluble protein), lane 3 indicates the flow through, lanes 4 and 5 indicate washes 1 and 3 respectively, lanes 6 to 9 indicates the fractions eluted from the glutathione agarose column. (B) Purification of FLAG-DWNN-GG following cleavage with 3C protease. Lane M indicates the marker, Lane 1, indicates the protein before cleavage with 3C protease, lane 2 is the flow through, lanes 3, 4 and 5 are washes 1, 2 and 3 respectively and lanes 6-9 are the fractions eluted from the glutathione agarose column.

Similar results were obtained for FLAG-DWNN-PI. Figure A.5 shows successful elution of GST-FLAG-DWNN-PI in lanes 6-9 with an approximate molecular weight of 35 kDa. GST-FLAG-DWNN-PI was cleaved using 3C protease and GST purified away from FLAG-DWNN-PI using a second round of glutathione affinity purification as described above. Figure A.5A

shows successful elution of GST-FLAG-DWNN-PI in lanes 6-9 with an approximate molecular weight of 35 kDa. Figure A.5B shows successful elution of cleaved FLAG-DWNN-PI in lanes 4 and 5 with an approximate molecular weight of 10 kDa.

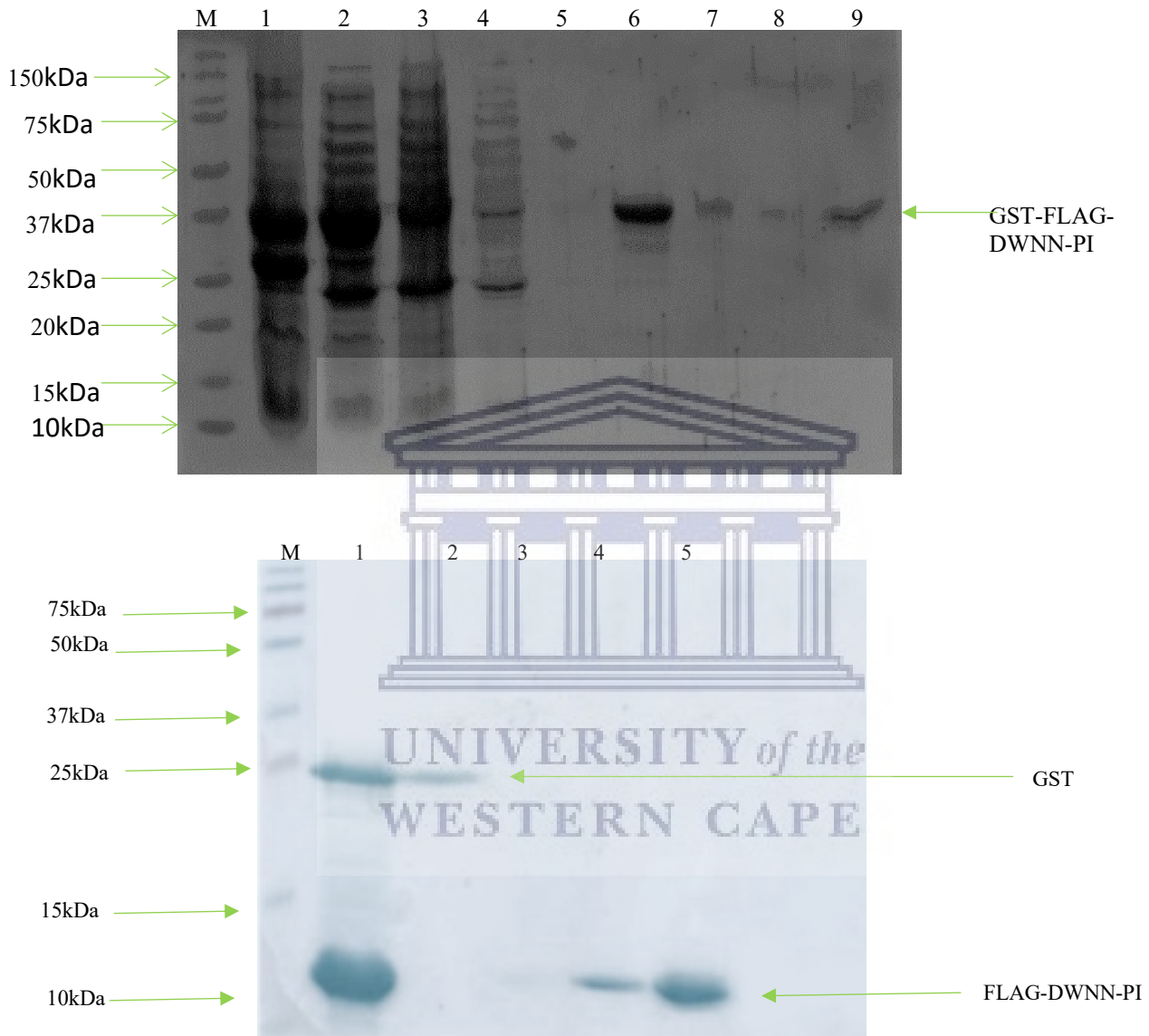


Figure A.5: Recombinant Expression and Purification of pGEX-FLAG-DWNN-PI. (A) Lane M indicates the molecular weight marker. Lane 1 indicates the insoluble protein (pellet), Lane 2 indicates the lysate (soluble protein), lane 3 indicates the flow through, lanes 4 and 5 indicate washes 1 and 3 respectively, lanes 6 to 9 indicates the fractions eluted from the glutathione agarose column. (B) Purification of FLAG-DWNN-PI following cleavage with 3C protease. Lane M indicates the marker, Lane 1, indicates the protein after cleavage with 3C protease, lane 2 is the flow through, lane 3 wash and lanes 4 and 5 are the fractions eluted from the glutathione agarose column.

Preliminary western blots were performed which showed that the FLAG-tag was successfully detected on the western blots using anti-FLAG antibodies which could prove useful in future research conducted within the laboratory.

APPENDIX II

SEQUENCE VERIFICATION OF R2 CLONED INTO pGEX-6P-2 vector

```

Query 5      GGATCTGG-AGTTCTGTTCCAGGGGCCCTGGGATCCGACCCGATCAACTACATGAAAAA 63
            |||
Sbjct 914    GGATCTGGAAGTTCTGTTCCAGGGGCCCTGGGATCCGACCCGATCAACTACATGAAAAA 973

Query 64     ACCGCTGGGTCCGCCCGCCGCGAGCTATACCTGCTTTCGTTGTGGCAAACCGGGTCACTA 123
            |||
Sbjct 974     ACCGCTGGGTCCGCCCGCCGCGAGCTATACCTGCTTTCGTTGTGGCAAACCGGGTCACTA 1033

Query 124    CATCAAAAACGTGCCGACGAATGGCGATAAAAACTTGAATCTGGTCCGCGTATTAAAAA 183
            |||
Sbjct 1034    CATCAAAAACGTGCCGACGAATGGCGATAAAAACTTGAATCTGGTCCGCGTATTAAAAA 1093

Query 184    ATCTACCGGCATCCCGCGCTCCTTCATGATGGAAGTGAAAGATCCGAATATGAAAGGCGC 243
            |||
Sbjct 1094    ATCTACCGGCATCCCGCGCTCCTTCATGATGGAAGTGAAAGATCCGAATATGAAAGGCGC 1153

Query 244    AATGCTGACCAACACGGGTAAATATGCTATTCCGACCATCGATGCTGAAGCGTACGCCAT 303
            |||
Sbjct 1154    AATGCTGACCAACACGGGTAAATATGCTATTCCGACCATCGATGCTGAAGCGTACGCCAT 1213

Query 304    TGGTaaaaaagaaaaaCCGCCGTTCTGCCGGAAGAACCGTCATCGAGCTCTGAAGAAGA 363
            |||
Sbjct 1214    TGGTAAAAAAGAAAAACCGGCCGTTCTGCCGGAAGAACCGTCATCGAGCTCTGAAGAAGA 1273

Query 364    TGACCCGATCCCGGATGAACTGCTGTGCCTGATTTGTAAAGATATCATGACGGACGCAGT 423
            |||
Sbjct 1274    TGACCCGATCCCGGATGAACTGCTGTGCCTGATTTGTAAAGATATCATGACGGACGCAGT 1333

Query 424    GGTATTCCGTGCTGTGGTAATTCATATTGCGATGAATGTATCCGCACCGCCCTGCTGGA 483
            |||
Sbjct 1334    GGTATTCCGTGCTGTGGTAATTCATATTGCGATGAATGTATCCGCACCGCCCTGCTGGA 1393

Query 484    ATCGGACGAACATACCTGCCCGACGTGTCACCAAAATGATGTTAGTCCGGACGCACTGAT 543
            |||
Sbjct 1394    ATCGGACGAACATACCTGCCCGACGTGTCACCAAAATGATGTTAGTCCGGACGCACTGAT 1453

Query 544    TGCTAACAAATTTCTGCGCCAGGCTGTCAATAACTTCAAAAACGAAACGGGCTACACGAA 603
            |||
Sbjct 1454    TGCTAACAAATTTCTGCGCCAGGCTGTCAATAACTTCAAAAACGAAACGGGCTACACGAA 1513

Query 604    ACGTCTGCGTAAACAACAcatcatcatcatcatTAATAA CTCGAGCGGCCGCATCGTGA 663
            |||
Sbjct 1514    ACGTCTGCGTAAACAACATCATCATCATCATTAATAA CTCGAGCGGCCGCATCGTGA 1573

Query 664    CTGACTGACGATCTGCCTCGCGCGTTTCGGTGATGACGGTGAAAACCTCTGACAC 718
            |||
Sbjct 1574    CTGACTGACGATCTGCCTCGCGCGTTTCGGTGATGACGGTGAAAACCTCTGACAC 1628
    
```

The beginning of R2 is indicated in purple, the His tag in turquoise and the BamHI and XhoI restriction sites are indicated in green and red respectively.

Query	5227	TTCCTGCATAGCGGTACGGCGAAATCGGTTACCTGCACGTATTCTCCGGCACTGAATAAA	5286
Sbjct	186	TTCCTGCATAGCGGTACGGCGAAATCGGTTACCTGCACKTATTCTCCGGCACTGAATAAA	245
Query	5287	CTGTTTTGCCAGCTGGCTAAAACCTGTCCGGTCAACTGTGGGTCGATAGCACCCCGCCG	5346
Sbjct	246	CTGTTTTGCCAGCTGGCTAAAACCTGTCCGGTCAACTGTGGGTCGATAGCACCCCGCCG	305
Query	5347	CCGGGTACGCGTGTCCGTGCAATGGCTATTTACAAACAGTCTCAACACATGACGGAAGTG	5406
Sbjct	306	CCGGGTACGCGTGTCCGTGCAATGGCTATTTACAAACAGTCTCAACACATGACGGAAGTG	365
Query	5407	GTTTCGTCGCTGCCCCGATCACGAACGCTGTAGCGATTCTGACGGTCTGGCCCCGCCGAG	5466
Sbjct	366	GTTTCGTCGCTGCCCCGATCACGAACGCTGTAGCGATTCTGACGGTCTGGCCCCGCCGAG	425
Query	5467	CACCTGATCCGCGTGAAGGTAACCTGCGTGCAGAAATATCTGGATGACCGCAATACCTTT	5526
Sbjct	426	CAYCTGATCCGCGTGAAGGTAACCTGCGTGCAGAAATATCTGGATGACCGCAATACCTTT	485
Query	5527	CGTCATTCAGTCGTGGTTCCGTACGAACCGC-CGGAAGTGGGCTCGGATTGTACCACGAT	5585
Sbjct	486	CGTCATTCAGTCGTGGTTCCGTACGAACCGCMCGGAAGTGGGCTCGGATTGTACCACGAT	545
Query	5586	TCACTATAACTACATGTGC-TATTCCTCATGTATGGGCGGTATGAACCGTCGCCGAT-C	5643
Sbjct	546	TCACTATAACTACATGTGGYTATTTCCTCATGTATGGGCGGTATGAACCGTCKCCCGATYC	605
Query	5644	CTGACC-A-TTATCACGCTGGAAGATTCGAGCGGCAACCTGCTGGGTCGCGATAGTTTCG	5701
Sbjct	606	CTGACCCATTTATCWCCTGGAAGATTCGAGCGGCAACCTGYTGGGTCGCGATAGTTTCS	665
Query	5702	-AAGTCCGTGTGTGCGCATGTCCGGTTCGTGACC-GTCGCACCGAA-GAAG-AAAACC-T	5756
Sbjct	666	AAAGTCCGTGTGTGCGCATGTCCGGKTCGWACCCGTCGCACCSAAAAGAAAACCCCT	725
Query	5757	GCGTAAG-AAAGG-CGAA 5772	
Sbjct	726	GCGTAAGWAAAGGGCGAA 743	

AvrII site is indicated in green and the FLAG tag in purple.

SEQUENCE VERIFICATION OF p53DBD CLONED INTO pET28 vector

Query	5024	TTCCCTCTAGAAATAATTTTGTTTAACTTTAAGAAGGAGATATAACCATGGGCAGCAGCC	5083
Sbjct	2	TTCCCTCTAGAAATAATTTTGTTTAACTTTAAGAAGGAGATATAACCATGGGCAGCAGCC	61
Query	5084	atcatcatcatcatcaCAGCAGCGGCTGGTGCCGCGGGCAGCCATGACTACAAGGACG	5143
Sbjct	62	ATCATCATCATCATCACAGCAGCGGCTGGTGCCGCGGGCAGCCATGACTACAAGGACG	121
Query	5144	ACGATGACAAGGGTGC GGTTCTCCTAGGTCTAGTGTGCCGAGCCAGAAAACCTATCAAG	5203
Sbjct	122	ACGATGACAAGGGTGC GGTTCTCCTAGGTCTAGTGTGCCGAGCCAGAAAACCTATCAAG	181

```

Query 5204 GCTCTTACGGTTTTTCGTCTGGGCTTCCTGCATAGCGGTACGGCGAAATCGGTTACCTGCA 5263
          |||
Sbjct 182 GCTCTTACGGTTTTTCGTCTGGGCTTCCTGCATAGCGGTACGGCGAAATCGGTTACCTGCA 241

Query 5264 CGTATTCTCCGGCACTGAATAAACTGTTTTGCCAGCTGGCTAAAACCTGTCCGGTTCAAC 5323
          |||
Sbjct 242 CGTATTCTCCGGCACTGAATAAACTGTTTTGCCAGCTGGCTAAAACCTGTCCGGTTCAAC 301

Query 5324 TGTGGGTCGATAGCACCCCGCCCGGGTACGCGTGTCCGTGCAATGGCTATTTACAAAC 5383
          |||
Sbjct 302 TGTGGGTCGATAGCACCCCGCCCGGGTACGCGTGTCCGTGCAATGGCTATTTACAAAC 361

Query 5384 AGTCTCAACACATGACGGAAGTGGTTCGTGCTGCCGCATCACGAACGCTGTAGCGATT 5443
          |||
Sbjct 362 AGTCTCAACACATGACGGAAGTGGTTCGTGCTGCCGCATCACGAACGCTGTAGCGATT 421

Query 5444 CTGACGGTCTGGCCCCGCCGAGCACCTGATCCGCGTGGAAGGTAACCTGCGTGCGGAAT 5503
          |||
Sbjct 422 CTGACGGTCTGGCCCCGCCGAGCACCTGATCCGCGTGGAAGGTAACCTGCGTGCGGAAT 481

Query 5504 ATCTGGATGACCGCAATACCTTTTCGTTCATTAGTCGTGGTTCCGTACGAACCGCCGGAAG 5563
          |||
Sbjct 482 ATCTGGATGACCGCAATACCTTTTCGTTCATTAGTCGTGGTTCCGTACGAACCGCCGGAAG 541

Query 5564 TGGGCTCGGATTGTACCACGATTCACTATAACTACATGTGCTATTCCCTCATGTATGGGCG 5623
          |||
Sbjct 542 TGGGCTCGGATTGTACCACGATTCACTATAACTACATGTGCTATTCCCTCATGTATGGGCG 601

Query 5624 GTATGAACCGTCGCCCCGATCCTGACCATTATCACGCTGGAAGATTGAGCGGCAACCTGC 5683
          |||
Sbjct 602 GTATGAACCGTCGCCCCGATCCTGACCATTATCACGCTGGAAGATTGAGCGGCAACCTGC 661

Query 5684 TGGGTCGCGATAGTTTCGAAGTCCGTGTGTGCGCATGTCCGGTCTGACCGTCGCACCG 5743
          |||
Sbjct 662 TGGGTCGCGATAGTTTCGAAGTCCGTGTGTGCGCATGTCCGGTCTGACCGTCGCACCG 721

Query 5744 AAGAAGAATGACTCGAGcaccaccaccaccaccacTGAGATCCGGCTGCTAACAAAGCCC 5803
          |||
Sbjct 722 AAGAAGAATGACTCGAGCACCACCACCACCACCTGAGATCCGGCTGCTAACAAAGCCC 781

Query 5804 GAAAGGAAGCTGAGTTGGCTGCTGCCACCGCTGAGCAAT-AACTAGCAT 5851
          |||
Sbjct 782 GAAAGGAAGCTGAGTTGGCTGCTGCCACCGCTGAGCAAWAACTAGCAT 830

```

The AvrII and XhoI restriction sites are indicated in purple and green respectively, and the FLAG tag in yellow.

SEQUENCE VERIFICATION OF p53C CLONED INTO pET28 vector

```

Query 5024 TTCCCCTCTAGAAATAATTTTGTTTAACTTTAAGAAGGAGATATACCATGGGCAGCAGCC 5083
          |||
Sbjct 2 TTCCCCTCTAGAAATAATTTTGTTTAACTTTAAGAAGGAGATATACCATGGGCAGCAGCC 61

Query 5084 atcatcatcatcatcaCAGCAGCGGCTGGTGCCGCGCGGCAGCCATGACTACAAGGACG 5143
          |||
Sbjct 62 ATCATCATCATCATCACAGCAGCGGCTGGTGCCGCGCGGCAGCCATGACTACAAGGACG 121

```

```

Query 5144 ACGATGACAAGGGTGCGGGTTCT CCTAGG AACCTGCGTAAGAAAGGCGAACCGCATCACG 5203
          |||
Sbjct 122 ACGATGACAAGGGTGCGGGTTCT CCTAGG AACCTGCGTAAGAAAGGCGAACCGCATCACG 181

Query 5204 AACTGCCGCCGGGTAGCACCAAACGTGCACTGCCGAACAATACGTCTAGTTCCCCGCAGC 5263
          |||
Sbjct 182 AACTGCCGCCGGGTAGCACCAAACGTGCACTGCCGAACAATACGTCTAGTTCCCCGCAGC 241

Query 5264 CGAAGAAAAAACCGCTGGATGGCGAATATTTTACCCTGCAAATCCGTGGTCGCGAACGTT 5323
          |||
Sbjct 242 CGAAGAAAAAACCGCTGGATGGCGAATATTTTACCCTGCAAATCCGTGGTCGCGAACGTT 301

Query 5324 TTGAAATGTTCCGCGAACTGAACGAAGCGCTGGAAGTGAAGATGCGCAGGCCGGCAAAG 5383
          |||
Sbjct 302 TTGAAATGTTCCGCGAACTGAACGAAGCGCTGGAAGTGAAGATGCGCAGGCCGGCAAAG 361

Query 5384 AACCGGGCGGTAGTCGTGCCATTTCATCGCACCTGAAAAGCAAGAAAGGCCAGAGCACGA 5443
          |||
Sbjct 362 AACCGGGCGGTAGTCGTGCCATTTCATCGCACCTGAAAAGCAAGAAAGGCCAGAGCACGA 421

Query 5444 GCCGCCATAAAAACTGATGTTCAAACGGAAGGCCCGGACAGCGACTGAGGATCCGAAT 5503
          |||
Sbjct 422 GCCGCCATAAAAACTGATGTTCAAACGGAAGGCCCGGACAGCGACTGAGGATCCGAAT 481

Query 5504 TCGAGCTCCGTCGACAAGCTTGCGGCCGCA CTCGAG caccaccaccaccaccacTGAGAT 5563
          |||
Sbjct 482 TCGAGCTCCGTCGACAAGCTTGCGGCCGCA CTCGAG CACCACCACCACCACCACACTGAGAT 541

Query 5564 CCGGCTGCTAACAAAGCCCGAAAGGAAGCTGAGTTGGCTGCTGCCACCGCTGAGCAATAA 5623
          |||
Sbjct 542 CCGGCTGCTAACAAAGCCCGAAAGGAAGCTGAGTTGGCTGCTGCCACCGCTGAGCAATAA 601

```

The AvrII and XhoI restriction sites are indicated in green and purple respectively.

APPENDIX III

List of reagents and suppliers

40 % 37:1 acrylamide: bis-acrylamide	Promega
Absolute ethanol	Merck
Acetone	Merck
Antibodies	Genscript
Acetic acid	Merck
Agarose	Separation
Ammonium persulphate	Biorad
Ampicillin	Melford
Antibodies	Santa Cruz
Bromophenol Blue	Merck
Bovine Serum Albumin	Roche
Casein	Sigma
Clarity™ Western ECL substrate	BioRAD
Coomassie Blue R-250	Sigma
Dithiothreitol (DTT)	Melford
Ethylene Diamine Tetra Acetic acid (EDTA)	Merck
GeneJet Gel extraction kit	Thermo Scientific
GeneJet maxi-prep kit	Thermo Scientific
GeneJet plasmid mini-prep kit	Thermo Scientific
Glacial acetic acid	Merck
Glycerol	Merck



Glycine	Merck
Imidazole	Sigma
Isopropyl β -D-1-thiogalactopyranoside (IPTG)	Sigma
Isopropanol	Merck
Kanamycin sulphate	Sigma
Lysozyme	Roche
Luria Broth	Merck
Magnesium chloride	Merck
Methanol	Merck
MG132 (proteasome inhibitor)	Sigma
N,N,N',N'-Tetra methylene-diamine	Sigma
Nickel sepharose	Sigma
Nuclease free water	Qiagen
Nutrient Agar	Merck
Polyethylene glycol 4000	Merck
Protease inhibitor cocktail	Roche
Reduced-L-glutathione (GSH)	Sigma
PCR Reagents	NEB
Restriction Enzymes	NEB/ThermoFisher Scientific
Snakeskin® Dialysis tubing	Separations
Sodium Chloride	Merck
Sodium Dodecyl Sulfate	Merck
T4 DNA Ligase	Thermo Scientific



Tris [hydroxymethyl] aminomethane	Merck
Tween-20	Merck
Triton X-100	Merck
Zinc sulphate	Merck

General stock solutions, buffers, and media

10X PBS (1 L)

Dissolved 80 g NaCl, 2 g KCl, 14.4 g Na₂HPO₄ and 4.8 g KH₂PO₄ in 600 ml distilled water. pH was adjusted to 7.4 using NaOH, volume adjusted to 1L and stock autoclaved. Stock was stored at room temp and diluted to 1L as needed.

10X Running Buffer (1 L)

Dissolved 30.2 g Tris, 144.1 g Glycine, and 20 g SDS in 600 ml distilled water until dissolved and adjusted to 1 L final volume. Stock was stored at room temp and diluted to 1L as needed.

10X Transfer Buffer (1 L)

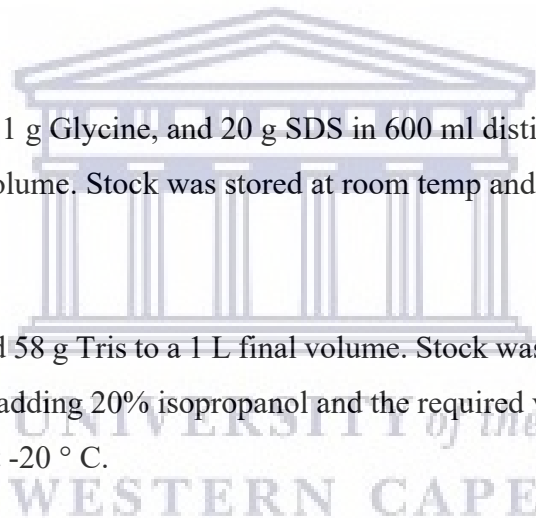
Dissolved 29 g Glycine and 58 g Tris to a 1 L final volume. Stock was stored at room temp and diluted to 1x as needed by adding 20% isopropanol and the required volume of distilled water. 1X working stock stored at -20 ° C.

2X SDS PAGE sample buffer (100 ml)

10ml 1.5 M Tris pH 6.8, 6 ml 20% SDS, 30ml 100% glycerol and 1ml/ml bromophenol blue was mixed and the volume adjusted to a final volume of 100ml with distilled water. Sample buffer stock was stored at room temperature. Stock was diluted to make a working stock as needed. 200 mM β-mercaptoethanol was added to 800 μl 2x Sample buffer before use.

50X TAE (1 L)

242 g Tris was dissolved in 500 ml distilled water. Added 100ml 0.5 M EDTA (pH 8.0) and 57.1 ml Glacial acetic acid to the 500 ml Tris. Adjusted the volume to 1 L and stored at room temperature. Stock was diluted to make a working stock as needed.



Ammonium Persulfate (10 % APS)

Dissolved 10 % (w/v) APS in distilled water. 10 % APS stored at -20 °C

Ampicillin (100 mg/ml)

Ampicillin was dissolved in distilled water to a final concentration of 100 mg/ml, filter sterilized and stored at -20 °C.

Binding Buffer

1 mM DTT, 5%BSA adjusted to required volume with 1xPBS

Cell lysis buffer

0.5% Triton X-100, Complete™ EDTA-free protease inhibitor cocktail, 5 mM β-mercaptoethanol, 50 mM Tris, pH 8.0, 150 mM NaCl, 5 % (v/v) glycerol, 100 μM ZnSO₄, 100 μg/ml lysozyme in 1XPBS.

Coomassie stain

Add 0.25 g Coomassie Blue-R-250, 10 % acetic acid and 40 % ethanol in required volume of distilled water.

Chloramphenicol

Chloramphenicol was dissolved in ethanol to a final concentration of 34 mg/ml, filter sterilized and stored at -20 °C.

Cleavage Buffer

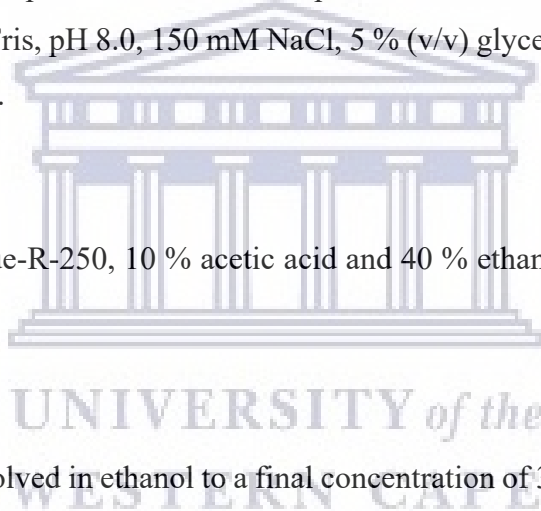
50 mM Tris, pH 8.0, 20 mM NaCl, and 1 mM DTT made up to required volume with distilled water.

Dithiothreitol (DTT)

1M DTT stock was prepared in 10 mM sodium acetate (pH 5.2), filter sterilized and stored at -20 °C.

Destain

40 % (v/v) ethanol , 10 % (v/v) acetic acid made up to the required volume with distilled water.



Isopropyl β -D-1-thiogalactopyranosid (IPTG)

1M IPTG made up in distilled water, filter sterilized and stored at -20 °C.

Kanamycin (30 mg/ml)

Kanamycin was dissolved in distilled water to a final concentration of 30 mg/ml, filter sterilized and stored at -20 °C.

Cleansing Buffer 1

1 M boric acid, 0.5 M NaCl, adjusted to pH 8.5 and made up to required volume with distilled water.

Cleansing Buffer 2: 1 M acetate and 0.5 M NaCl, adjusted to pH 4.5 and made up to required volume with distilled water.

Luria Bertani Broth (LB)

25g of Luria Bertani Broth dissolved in 1 L distilled water and autoclaved.

LB Agar

10 g/L Tryptone, 5 g/l yeast extract , 5 g/l NaCl and 10 g/l agar in required volume of distilled water.

Mg.ATP (0.1 M)

0.01g Mg.ATP dissolved in required volume of distilled water.

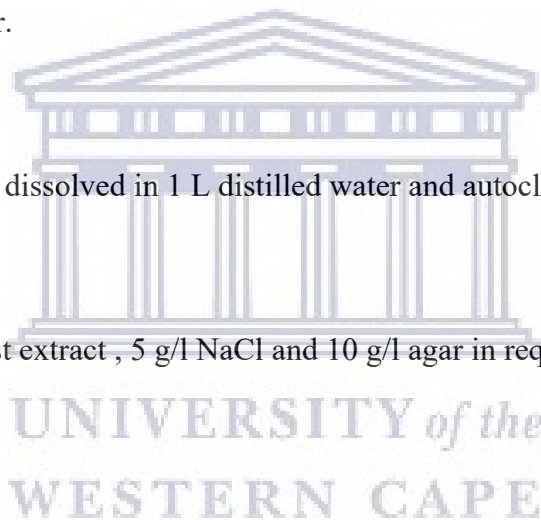
Phosphate buffered saline-Tween-20 (PBST)

1x PBS containing 0.1 % (v/v) Tween 20 made up to required volume with distilled water.

Protein Elution Buffer

GST-tagged proteins- 20 mM reduced glutathione in 1x PBS and used immediately

6His tagged proteins – 100-400 mM Imidazole made up in 1XPBS



Protein Wash Buffer

GST-tagged protein- 1x PBS, 1 mM β -mercaptoethanol

6His tagged proteins – 20 mM imidazole, 1XPBS

Resolving Buffer

1.5 M Tris-HCl adjusted to pH 8.8 with HCl

Stacking Buffer

0.5 M Tris- HCl adjusted to pH 6.8 with HCl

TFB1

30 mM Potassium acetate, 50 mM $MnCl_2$, 0.1 M KCl, 10 mM $CaCl_2$ and 15 % glycerol. Volume adjusted to required volume with distilled water, filter sterilised and stored at 4 °C until use.

TFB2

9 mM Na-MOPS, 50 mM $CaCl_2$, 10 mM KCL and 15 % glycerol. Volume adjusted to required volume with distilled water, filter sterilised and stored at 4 °C until use.

TYM Broth

2 % peptone, 0.5 % yeast extract, 0.1 M NaCl, 0.2 % glucose and 10 mM $MgCl_2$ Volume was adjusted to the required final volume with distilled water. TYM broth was autoclaved and stored at room temperature

Zinc Sulphate

0.1 M $ZnSO_4$ made up in distilled water